1. INTRODUCTION

This document describes the activities carried out in 2004 in the frame of the Contract of Associated Laboratory on Plasma Physics and Engineering, signed on November 23rd 2001 between "Instituto Superior Técnico" (IST) and "Fundação para a Ciência e a Tecnologia" (FCT). These activities are inserted in two thematic areas:

- Controlled Nuclear Fusion;
- Technologies of Plasmas and High-Power Lasers,

and have been performed by staff of two Research Units of IST:

- Centro de Fusão Nuclear (CFN);
- Centro de Física dos Plasmas (CFP).

The CFN research staff has been organized in four scientific groups:

- Group of Experimental Physics (Head: Carlos Varandas);
- Group of Microwave Diagnostics (Head: Maria Emilia Manso);
- Group of Theory and Modelling (Head: Fernando Serra);
- Group of Control and Data Acquisition (Head: Jorge Sousa)

which carried out in 2004 the following projects[1]:

- Tokamak ISTTOK (Figure 1.1);
- Participation in the Collective Use of the JET Facilities by the EFDA Associates;
- Participation in the ASDEX-UPGRADE Programme;
- Participation in the TJ-II Programme;
- Participation in the MAST Programme;
- Participation in the TCV Programme;
- Participation in the ITER Project (Figure 1.2);
- Other Activities on Theory and Modeling;
- Other Activities on Control, Data Acquisition and Signal Processing.

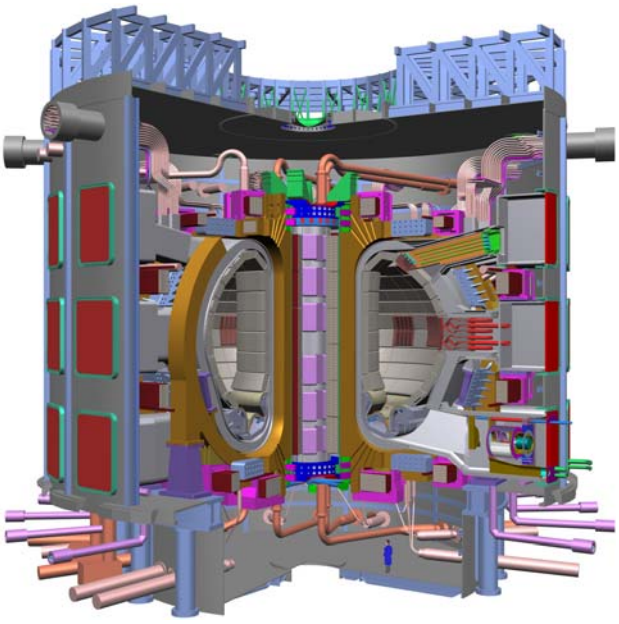

Figure 1.2 – The tokamak ITER

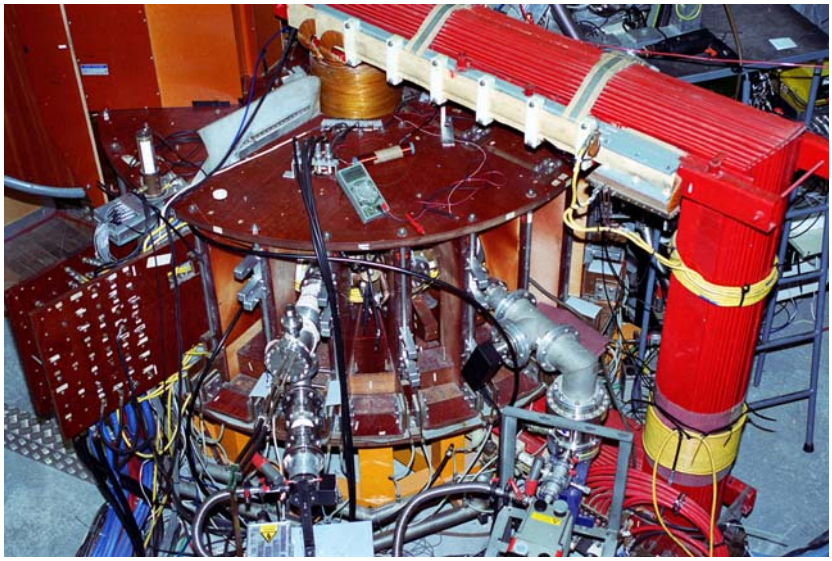

Figure 1.1 – The tokamak ISTTOK

[1] In the frame of the Contract of Association between the "European Atomic Energy Community" (EURATOM) and IST.

The CFP research staff has been organized in three scientific groups:

- Group of Lasers and Plasmas (Head: José Tito Mendonça);
- Group of Space Plasmas (Head: Armando Brinca);
- Group of Gas Discharges and Gaseous Electronics (Head: Carlos Matos Ferreira).

which performed activities in the following research lines:

- Ultra high power, ultra-short lasers[2] (Figure 1.3);
- Theory and simulation on extreme plasma physics[2];
- Studies on complex and space plasmas;
- Space plasma physics
- Environmental Plasma Engineering (Figure 1.4);
- Modelling of plasma reactors.

The research and development activities carried out in the frame of these projects are described in detail in chapters 2 to 13, which also present the main scientific and technical results. Chapter 14 describes other activities and chapter 15 contains the list of publications.

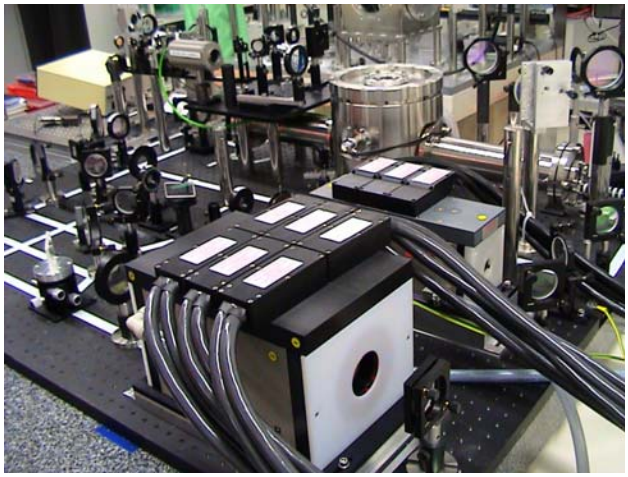

Figure 1.3 – Ultra-short laser system

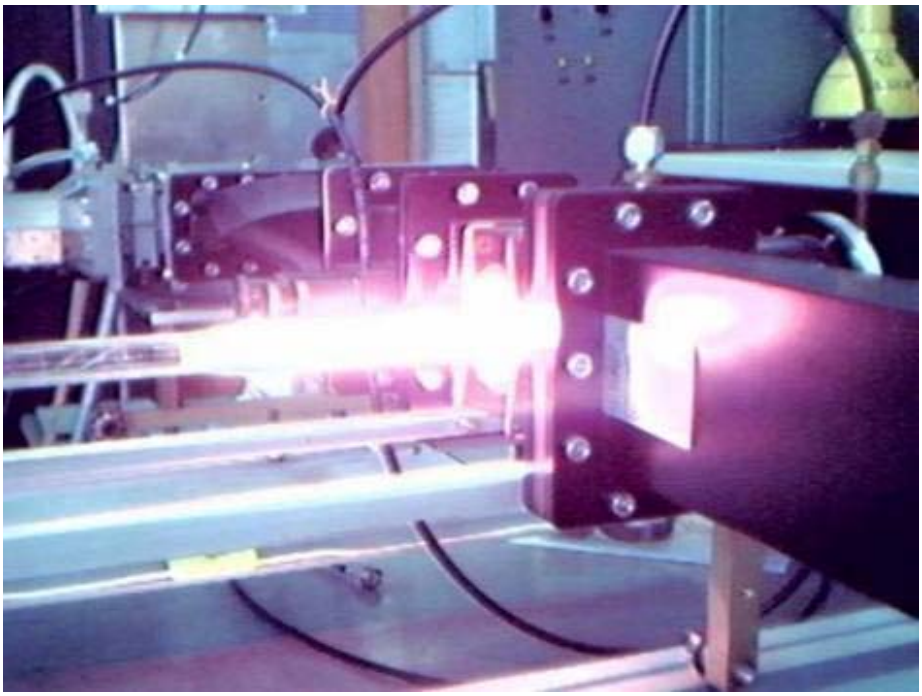

Figure 1.4 – Surface wave sustained discharge

[2] In the frame of the Contract of Association EURATOM/IST.

2. TOKAMAK ISTTOK

H. Fernandes, C. Silva and C.A.F. Varandas (Heads), M.P. Alonso, B.B. Carvalho, I. Carvalho, P. Carvalho, R. Coelho, J. Ferreira, H. Figueiredo, J. Fortunato, R. Gomes, I. Nedzelskij, A. Neto, T. Pereira, V. Plyusnin, A. Soares, Y. Tashev, D. Valcárcel.

2.1. INTRODUCTION

ISTTOK is a small-size (R=46 cm, a=8.5 cm), large-aspect-ratio, low magnetic field (0.46 T) limiter tokamak with an iron core transformer (flux swing of 0.22 Vs), equipped with a distributed VME control and data acquisition system. Its low temperature (150 eV) low density ($8x10^{18}$ m^{-3}) plasmas are diagnosed by electric and magnetic probes, a microwave interferometer, a heavy ion beam diagnostic, a Thomson Scattering system and spectroscopic diagnostics.

The main objectives of this project are: (i) the development of new diagnostic and control and data acquisition systems; (ii) testing of new operation scenarios (liquid metal limiter and alternating plasma current); (iii) study of the influence of external applied signals on the plasma confinement and stability; and (iv) education and training on tokamak physics and engineering.

This project included in 2004 work in the following research lines:

- Testing of the liquid metal limiter concept;
- Diagnostics;
- Control and data acquisition;
- Plasma physics studies.

2.2. TESTING OF THE LIQUID METAL LIMITER CONCEPT

IST/CFN has proceeded with the collaboration with the Association EURATOM/University of Latvia on the testing of the liquid metal limiter concept.

The liquid metal loop experimental rig has been commissioned in the ISTTOK Laboratory. Tests of this experimental apparatus have begun. A controlled heating system, using a Dallas DS80-C400 microprocessor with Ethernet connection and Java based technology, has been designed, implemented and tested, intended to ensure a 60 ºC stable temperature in the main liquid metal loop. A device to introduce oxide-free Gallium in the main loop for compatibility with UHV operation has been implemented and tested (Figure 2.1). The Gallium cleaning system has been tested. A heating backup system designed to keep Ga in the lower part of the loop always above the melting point has been implemented. A free expansion tank, where Gallium could be stored for long periods, has been designed, implemented and tested (Figure 2.2).

One Portuguese Researcher has participated in Riga in an experimental campaign, aiming at testing a new fast frame camera and studying the jet stability with several diameter nozzles (1.5, 1.8, 2.1 and 2.4 mm).

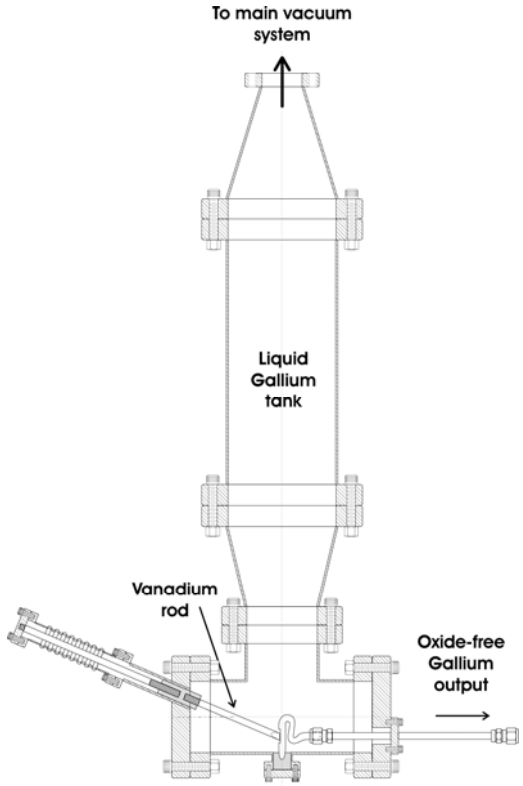

Figure 2.1 - System designed to introduce oxide-free Gallium in the main reservoir.

2.3. DIAGNOSTICS

2.3.1. Introduction

A new diagnostic for magnetohydrodynamic (MHD) studies has been implemented using signals from a set of 12 equally spaced Mirnov coils. A new Gundestrup probe for flow measurements has been developed, giving particular attention to the materials used in its construction. The time-of-flight technique for plasma potential measurements by the heavy ion beam diagnostic with a multiple cell array detector has been optimized. The possibility of using this diagnostic for zonal flows studies has been theoretically evaluated. The design of a soft X-ray tomography diagnostic based on commercial CCD cameras has started. The emissive electrode used in biasing experiments has been optimized, aiming at easy replacement of the emitter material and operation for longer periods.

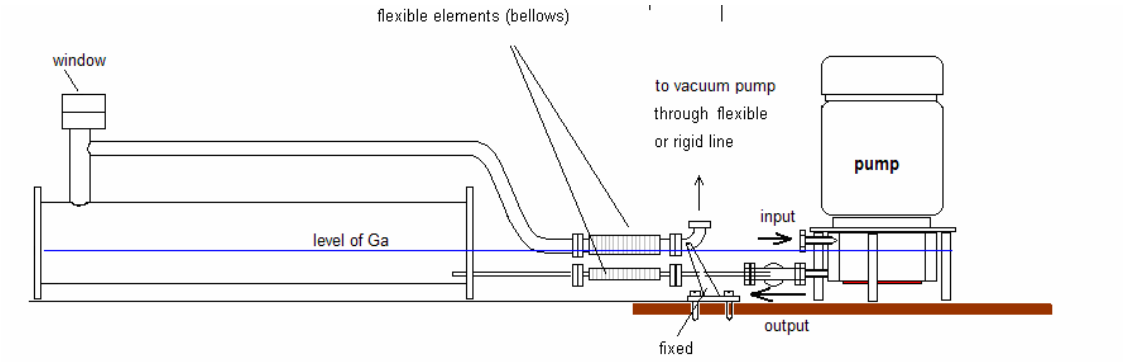

Figure 2.2 - Gallium store tank

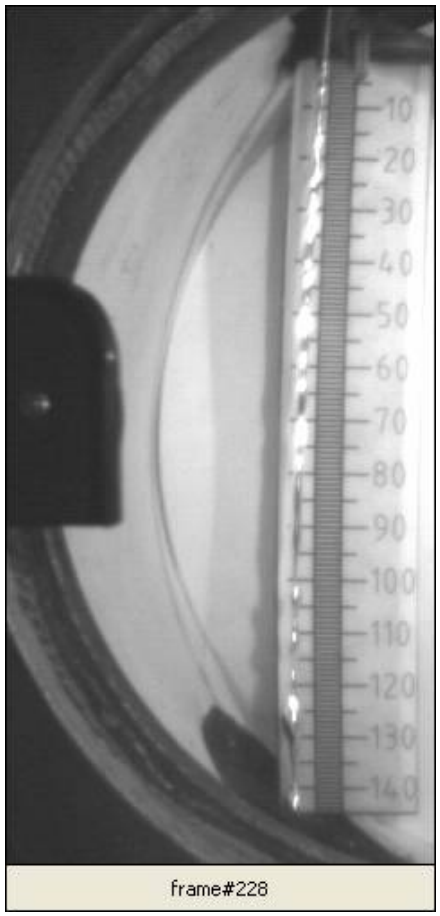

Figure 2.3 - Jet image obtained with the fast frame camera

2.3.2 Diagnostic for MHD studies

This diagnostic uses signals from a set of twelve equally spaced Mirnov coils, originally designed for plasma shape and position equilibrium determination (Figure 2.4). The data acquisition and processing system is based on a locally-developed galvanic isolated, 8 channel, fast PCI transient recorder module, with a 2 MSPS sampling rate, 14 bit resolution and a total memory of 256 MWords. This module includes a Digital Signal Processor (DSP) and a Field Programmable Gate Array (FPGA), allowing real-time determination of MHD modes using advanced identification algorithms, in a sub-millisecond cycle time.

Preliminary data analysis indicates the presence of rotating modes with dominant m=3 poloidal mode number with frequencies of the order of 100 kHz (about 480 times smaller than characteristic toroidal Alfven time).

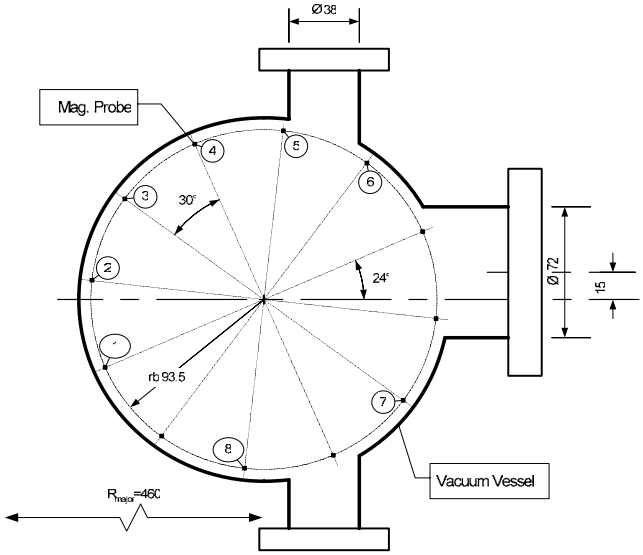

Figure 2.4 - Schematic drawing of the ISTTOK poloidal layout, showing magnetic probe positions.

2.3.3. Gundestrup probe

A new Gundestrup probe has been developed, giving particular attention to the materials used in its construction, aiming at its operation in fusion plasmas. Copper and quartz have been replaced respectively by molybdenum and boron nitride.

The probe has been successfully operated in a large number of ISTTOK discharges without perturbing the plasma behavior. Furthermore, no significant damage in the probe has been found after its removal from the machine, proving that the new probe design is adequate to be used in the edge of tokamak plasmas.

2.3.4. Plasma potential measurements by heavy ion beam diagnostic with time-of-flight energy analyzer

A 4-channel time-of-flight energy analyzer (TOFEA) is being developed for plasma potential profile measurements with the heavy ion beam diagnostic (HIBD). Figure 2.5 presents the picture and schematic illustration of the diagnostic. It is placed inside an auxiliary vacuum chamber attached to a ISTTOK horizontal diagnostic port, and consists of three main parts: (i) a modified multi-channel array detector (MCAD) with TOFEA input slits; (ii) a control module with deflecting cylindrical electrostatic plates and a set of planar alignment electrostatic plates; and (iii) a TOF-path module with "start" and "stop" detectors.

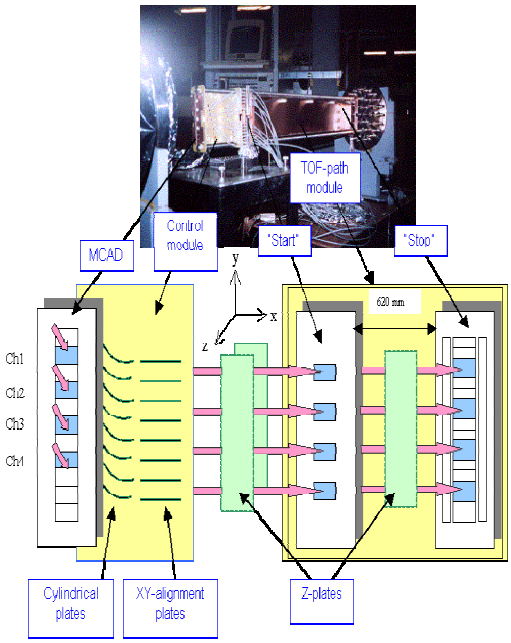

Figure 2.5 - Picture and schematic drawing of the four-channel TOFEA.

One channel of the data acquisition system (DAS) (Figure 2.6) consists of conditioning electronics and a time-to-amplitude converter (TAC). The DAS is used in successive acquisitions of both "start" and "stop" signals, when they are discriminated inside the time-of-flight of the beam pulse along the TOF-path.

Figure 2.7 presents the plasma potential measured in the central region of the ISTTOK plasma by the HIBD and at plasma periphery by electric probes. Although the sign of the core plasma potential agrees with the neoclassical predictions, its absolute value is approximately 1.5-2 times higher (Φ_{neo} ~ - (120-200) V.

The sensitivity of plasma potential measurements by TOFEA has been checked in experiments with limiter biasing.

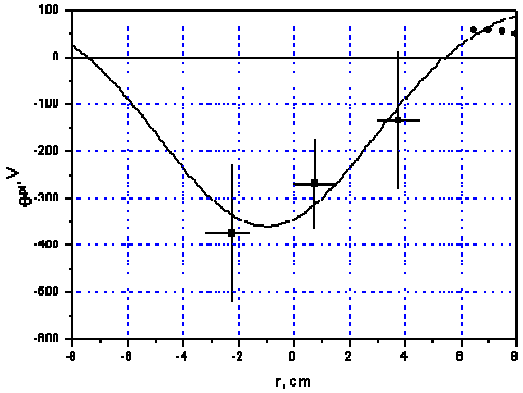

Figure 2.7 - Profile of the plasma potential measured by the TOFEA

2.4. CONTROL AND DATA ACQUISITION

2.4.1. Main activities

Software for shared remote data consulting and analysis has started to be developed, aiming at replacing the existing applications based on DOS and allowing data viewing and analysis by any authorized user, from any personal computer, anywhere in the world. The upgrade of the ISTTOK data acquisition system from the former "dbf" files-based system to an Open Source RDBMS PostgreSQL database has begun, by creating a PostgreSQL data mirror in a Linux server, replicating the original data structure and copying the pulse data on a

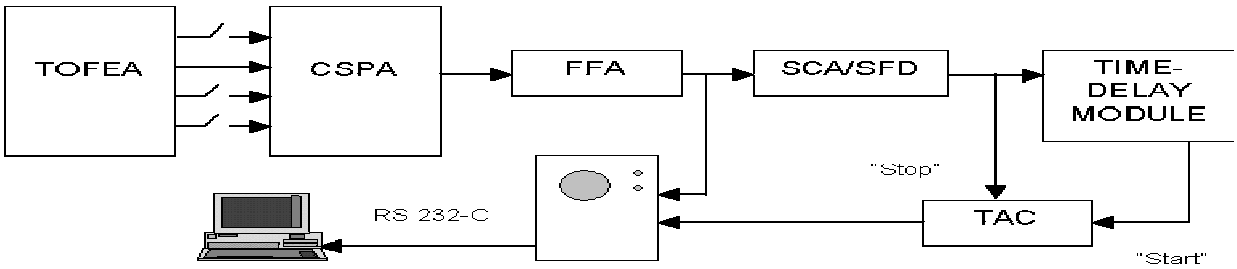

Figure 2.6 – Block diagram of the TOFEA data acquisition system

daily basis to the new relational database, using script codes written in "Python". A modular USB controller for low speed (8 kbytes/s) data acquisition has been developed. The system consists of a small printed circuit board that incorporates 8 I/O lines, 8 open collector lines for power control (500 mA each), I2C bus, as well as 4 analog lines (12 bit of maximum resolution). A library of functions in C language has been also developed to be used with this interface, which allows a quick and simple implementation in slow control and data acquisition systems. A cooperative multi-user program has started to be developed in Java to control and launch the ISTTOK discharges, replacing the present DOS shot launcher program.

2.4.2. Software for shared remote data consulting and analysis "QueryTOK"

A platform, based on standards like CORBA, XML and JAVA, has been developed allowing accessing to data and its analysis in a straight forth way. Several users may be connected simultaneously to the platform and whenever a user launches his configuration query the resulting data is broadcasted to all users, allowing simultaneous analysis and discussion of results between users (Figure 2.8).

Each user has a collection of profiles where he may store the parameters, equations and macros that he usually requests from the database. These profiles can be stored locally or directly in the database and may be shared between users.

The software is plugin-based, allowing addition of new data viewers and data calculation algorithms without the need of rewriting any code. Data is stored in a SQL database and calculations are made locally or by remote computers, which run an application-server routine waiting for a remote procedure call for heavy calculus computation. The application-server routine can be designed on any analysis code built on MatLab, Octave, IDL and others.

The entire platform is fully internationalized. Current available languages are Portuguese and English. The addition of a new language is trivial due to the use of JAVA standard internationalization mechanisms through the insertion of new bundles into the distribution. A built-in chat is also available for users to discuss hardware configuration and data analysis.

The platform is distributed using the JAVA Web-start technology, which greatly simplifies the installation process and version renewing.

2.5. PLASMA PHYSICS STUDIES

Following previous studies on the influence of emissive electrode biasing on the plasma confinement and stability, experiments have been made in 2004 aiming at a better characterization of the modifications introduced by the electrostatic polarization at the plasma edge The evolution of the radial electric field (E_r) profile has been measured. Figure 2.9 presents the radial profiles of the floating potential and radial electric filed, measured by the rake probe. As the biasing is applied, a large electric field is observed for both polarities, reaching a value of around ±12 kV/m in the region near the limiter, associated with a strong E_r shear. Therefore, the velocity shear may be responsible for the observed particle confinement improvement. This is corroborated by probe measurements, which show a decrease of the turbulent particle transport when the bias is applied.

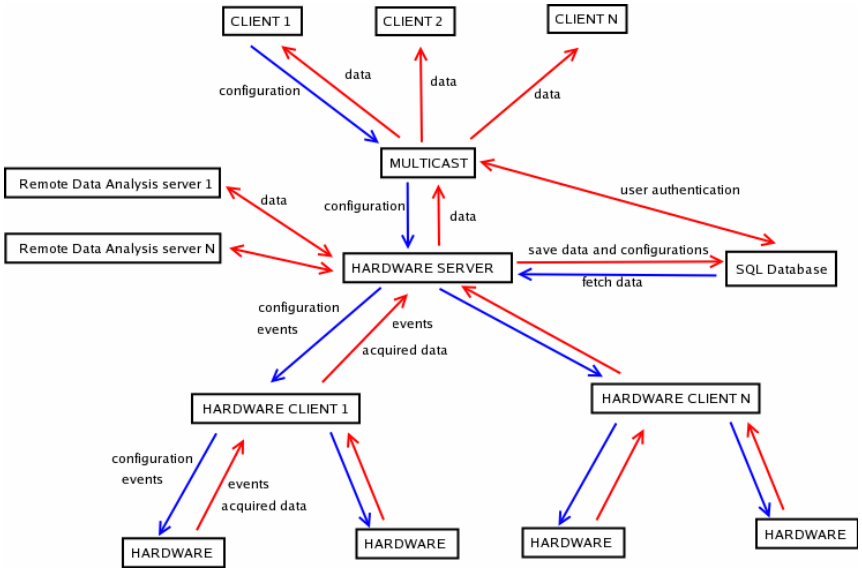

Figure 2.8 - General platform overview showing data flow between the logical entities.

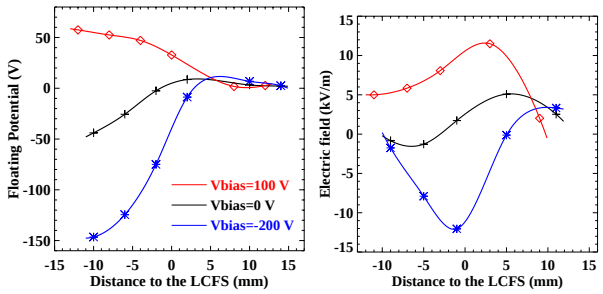

Figure 2.9 - Floating potential and radial electric field radial profiles for positive (V_{bias}=100 V) and negative (V_{bias}=-200 V) emissive electrode biasing. Profiles with no applied voltage are also shown for comparison.

Although the radial electric field induced by emissive electrode biasing is of the same magnitude for both polarities (~12 kV/m), a significant improvement in particle confinement is only observed for negative biasing. In order to understand this different behavior, edge turbulent transport is being investigated. The edge plasma parameters, and in particular the edge density, are characterized by intermittent events (low frequency, large amplitude oscillations). The behaviour of density fluctuations is clearly modified by emissive electrode biasing, being the large-scale transport events reduced for both polarities (Figure 2.10). The different behavior of the particle confinement for positive and negative biasing is possibly related with the large amplitude fluctuations with roughly Gaussian distribution induced by positive biasing. Furthermore, emissive electrode biasing as opposite effects on the low frequency edge fluctuations; at negative bias a reduction is observed for frequency below ~70 kHz, while for positive bias the fluctuations increase in this frequency range.

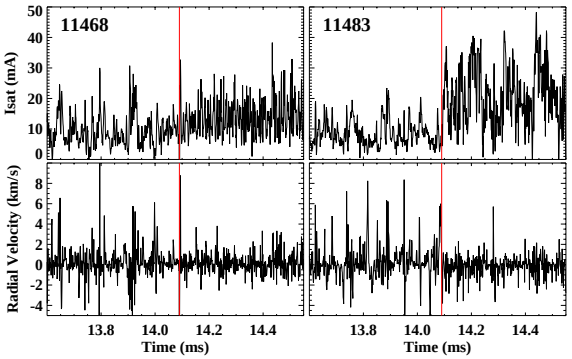

Figure 2.10 - I_{sat} and the effective radial velocity in expanded time scale. The red line indicates the biasing time.

3. PARTICIPATION IN THE USE OF THE JET FACILITIES BY THE EFDA ASSOCIATES

F. Serra (Head), D. Alves, P. Belo, D. Borba, R. Coelho, S. Cortes, N. Cruz, L. Cupido, L. Fattorini, A. Figueiredo, B. Gonçalves, S. Hacquin, M.E. Manso, L. Meneses, F. Nabais, M.F. Nave, I. Nedzelski, I. Nunes, V. Plyusnin, T. Ribeiro, F. Salzedas, C. Silva, J. Sousa, C. Varandas, P. Varela.

3.1. INTRODUCTION

The Association EURATOM/IST has proceeded with its participation in the collective use of the JET[1] Facilities, in the frame of the "European Fusion Development Agreement" (EFDA), through the "JET Operation Contract" and the "JET Implementing Agreement".

This chapter presents the main activities carried out during this year in the areas of:

- Operation;
- Scientific exploitation;
- Performance enhancements;
- Management.

3.2. OPERATION

Three members of the IST/CFN staff have been involved in the JET operation: Drs. Sebastien Hacquin and Isabel Nunes have participated in the JET Operation Team, through Secondment Agreements with the Association EURATOM/UKAEA, working respectively in the "Electron Kinetics Group" and "Operation Group"; Mr. Luis Meneses has provided technical support to the operation and maintenance of the KG8 correlation reflectometer.

3.3. SCIENTIFIC EXPLOITATION

3.3.1. Introduction

The participation in the JET 2004 Work Programme had contributions from fifteen scientists to the experimental campaigns C13 and C14 at the JET site (Table 3.1).

The work has been focused on code developments, leading to the following studies and/or tasks in plasma physics and/or engineering mainly related with Task Forces M, D and E: (i) Study of the sawtooth stability in plasmas with counter-NBI; (ii) Expansion of the JET sawtooth database; (iii) Validation of q-profiles in JET optimised shear discharges; (iv) Documentation of JET diagnostics for analysis of fluctuations; (v) Stability domains for the internal kink mode; (vi) Limiter H-mode studies in JET; (vii) Evidence of fast ion redistribution during fishbones from TAE in JET deuterium plasmas; (VIII) Transport studies in Tritium plasmas; (ix) Time–frequency analysis of non-stationary fusion plasma signals by comparison between the Choi–Williams distribution and wavelets; (x) Disruptions and runaway electrons in JET; (xi) Effects of large magnetic islands on particle confinement trace-Tritium studies (TRANSP modelling); (xii) Cross-correlation between parallel and radial fluctuating velocities; (xiii) Design of a new reciprocating probe head; (xiv) Studies of MHD and turbulence based on microwave reflectometry results.

Name	Competence	Number of days
Duarte Borba	TFL, MHDAE	47
M. Filomena Nave	TSL, SL, MHDAE	52
Paula Belo	IEMHDA, CATS	47
Fernando Nabais	FPE	47
Vladislav Plyusnin	MHDME	33
Carlos Silva	KY3	19
Isabel Nunes	KG8b	26
Jorge Ferreira	PTM	26
Igor Nedzelski	KY3	26
Luis Meneses	KG8b	12
Ricardo Galvão	MHDAE	32
Sebastien Hacquin	JOC	20

Table 3.1 – IST/CFN staff envolved in the JET experimental campaigns

3.3.2. Study of the sawtooth stability in plasmas with counter-NBI

During a recent reversed toroidal field (B_T) campaign at JET, experiments were performed to investigate the effect on sawteeth of NBI-driven toroidal plasma rotation counter to the direction of the toroidal plasma current ($I_{p)}$ and B_T. A power scan at constant density has permitted comparison of the reverse B_T domain with previous experiments with forward field and hence co-rotation. Unlike observations with co-NBI heating where the sawtooth period increases with power, with counter-NBI the sawtooth period was found to decrease to a minimum value (about 1/3 of Ohmic sawtooth periods) at 4 MW (Figure 3.1). The possible reasons why the sawtooth period is shorter with counter-NBI are under investigation. In earlier JET experiments with reversed B_T and I_p plasmas this was attributed to changes in the q-profile due to neutral beam current drive (NBCD). Modification in the core current density due to NBCD, j_{CD}, was calculated with the PENCIL code. j_{CD} was larger with counter-injection and increased with the input power (Figure 3.2). PENCIL calculations show that the fast ions pressure increased with power for both the usual and the reversed B_T cases. The lack of correlation between the observed sawtooth period and fast ion pressure in the counter-NBI case indicates that the

[1] JET is an European tokamak, operated and scientifically exploited in the frame of the European Fusion Development Agreement (EFDA).

contribution from the fast particle component cannot explain the observed sawtooth period dependence on P_{NBI}. On the other hand, kinetic effects from trapped thermal ions qualitatively explain the sawtooth observations. The effect of sheared flow on these kinetic effects modifies the stability threshold of the internal kink mode in such a way that the critical beta for instability is much lower for small or reversed toroidal rotation, as observed in the discharges with reversed B_T and I_P.

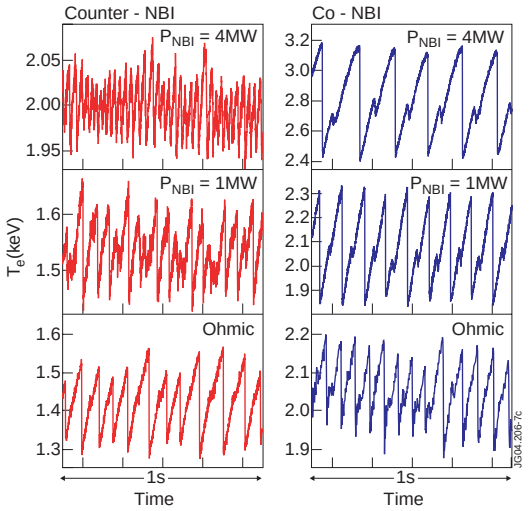

Figure 3.1 – Central electron temperature traces showing the different sawtooth behaviour for different input powers observed with co and counter NBI.

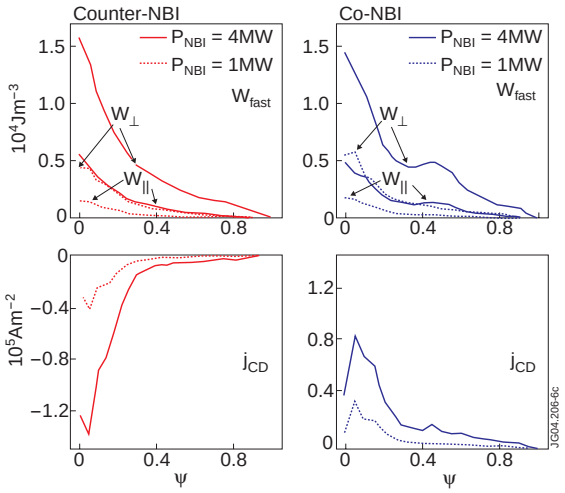

Figure 3.2 – (a) and (b) Profiles of fast ion energy density $W_{//fast}$ and $W_{\perp fast}$ calculated with the PENCIL code (finite orbit width effects neglected); (c) and (d) Profiles of driven current density ($j_{CD}/j_0 \leq 10\%$ for co- and counter-NBI).

3.3.3. Expansion of the JET Sawtooth Database

A sawtooth database, initiated during campaigns C1-C4 for the study of sawtooth observations in NBI heated discharges, has been expanded. The database now contains information on ICRH discharges including recent experiments on grassy sawteeth and some He plasmas. In addition, data from several TFE pedestal and divertor experiments performed during the reversed toroidal field campaign have been included. The database contains average plasma and heating parameters, as well as specific sawtooth characteristics.

Figure 3.3 shows a comparison of the sawtooth period versus the central electron temperature obtained for NBI heating with the usual JET B_T and I_p polarity (co-NBI) and with reversed B_T and I_p (counter-NBI). For co-NBI, the sawtooth period scales with $T_e^{1.7}$. This is not found for counter-NBI. The comparison confirms that sawtooth periods are generally smaller with counter-NBI for similar central T_e. Therefore tokamak operation with counter-NBI is an effective way to control the sawtooth period in H-mode as well as in L-mode plasmas. Figure 3.4 presents a plot of the sawtooth period versus the central electron temperature for NBI as well as ICRH discharges in the normal B_T and I_P operation. The open triangle symbols correspond to an interesting low density regime with ICRH that shows small sawteeth, referred to as the "grassy" sawtooth. Although auxiliary heating has been associated with sawtooth stabilization leading to large sawtooth periods, these figures clearly show that with either ICRH or with NBI heating there are regimes of operation where sawtooth periods shorter than in Ohmic plasmas can be obtained.

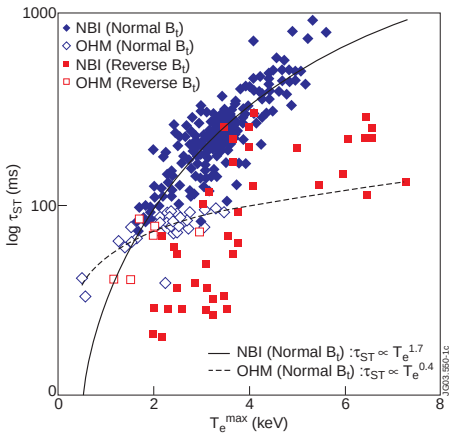

Figure 3.3 – A comparison of sawtooth periods with co-NBI (in solid blue kytes) and counter-NBI (red solid squares).

3.3.4. Validation of q-profiles in JET optimised shear discharges

A comparison of q-values obtained MHD analysis and q-profiles determined from EFIT with MSE measurements was performed for a set of discharges from the Trace Tritium Experiment (TTE). Alfvén Eigenmode (AE) cascades with frequencies ranging from 100-250 kHz can be identified with spectrograms from microwave signals in interferometry mode, as well as from magnetic signals.

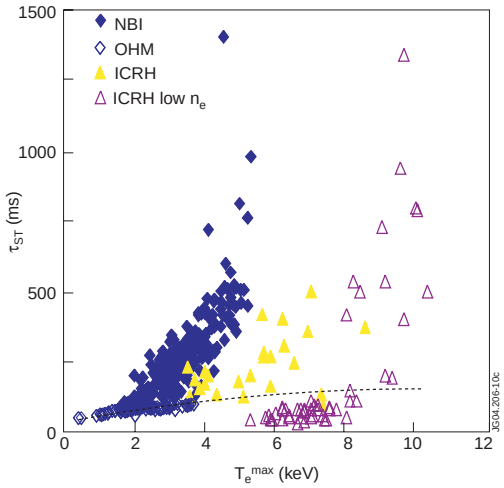

Figure 3.4 – A comparison of sawtooth periods in low-density ICRH pulses (open symbols) with observations in high density ICRH plasmas (solid yellow triangles) and NBI heated plasmas (blue solid kites).

In the case of reversed shear plasmas, the Alfvén cascades are used to determine the minimum of the safety factor (q_{min}).

The frequency pattern of the AE cascades reflects the time evolution of the Alfvén continuum at the location of q_{min} which is linked to the frequency of the eigenmode located at that surface. Measurements performed using the reflectometer diagnostic were able to detect eigenmodes with high toroidal mode numbers allowing more accurate determination of the (q_{min}) than with the magnetic diagnostic.

Figure 3.5 presents an example of q profile validation for a TTE discharge using MHD mode analysis. For the time shown, the AE analysis revealed a non-integer q_{min}~2.7-2.8. A snake with mode number m=3, n=1 indicated the presence of a integer q=3 surface. Figure 3.5 shows EFIT reconstructions of the q-profile with different fitting constraints. The EFIT reconstruction with magnetic data only (curve 1) is monotonic. Only the MSE data detects the current hole, however, the equilibrium reconstruction with MSE constrains shows a very large uncertainty in the plasma core. Clearly the MHD analysis is an important guide in selecting the optimum curvature of the fitted profiles.

3.3.5. Documentation of JET diagnostics for analysis of fluctuations

A set of fast magnetic pick-up coils was designed for high frequency MHD activity studies (up to 500 kHz). determination. A new data collection system (named KC1M) has been commissioned in 2004, allowing the magnetic signals to be recorded at 2 MHz for up to 32 s in each pulse. The system will be be enlarged to 32 magnetic MHD signals and 32 other selectable fast diagnostic signals in 2005. The ECE, SXR and O-mode reflectometer diagnostic measurements permit the identification of low amplitude, core MHD modes not measured by the external magnetic pick-up coils.

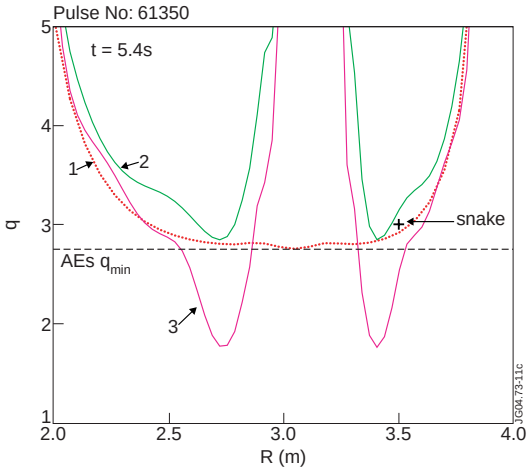

Figure 3.5 - q profile from EFIT with different boundary conditions: (1) magnetics only, (2) and (3) with magnetics and MSE data, fitting MSE data approximately (2) or very closely (3). Indicated in the figure is the estimated q_{min} from AE cascade analysis and the radius of q=3 obtained from the snake.

3.3.6. Stability domains for the internal kink mode

Fishbone and sawtooth activity are caused by different branches of the solution of the dispersion relation for the internal kink mode. The activity of these instabilities is governed mainly by three parameters, the growth rate of the ideal internal kink mode, $\gamma_I = -\omega_A \delta W_{MHD}$, the diamagnetic frequency ω_{*i} and the fast ions beta β_h. Following trends in the space of parameters ($\gamma_I, \omega_{*i}, \beta_h$), changes on sawtooth or fishbone activity occur when lines separating different stability regions for the internal kink mode are crossed.

To determine the stability domains for each instability in the space of parameters it is necessary to solve the marginal equation corresponding to the dispersion relation for the internal kink mode. The marginal equation produces two solutions if the ideal growth rate is below a maximum value $\gamma_I=\gamma_M$. The diagram containing these solutions in the space of parameters is presented in Figure 3.6 (red lines). It includes a (horizontal brown) line $\gamma_I = \omega_{*_i}/2$ that indicates when the kink branch is stabilized by diamagnetic effects and to complete the stability regions, lines traducing resistive effects (at low values of γ_I) and finite orbit width effects (at large values of β_h) were also added to the diagram.

3.3.6.1. Fishbones cycle

Low-frequency (diamagnetic) fishbones are usually observed for low values of the fast ions beta while high-frequency (precessional) fishbones are observed only for high values of β_h. For intermediate values of β_h no fishbones are observed since it falls in the stable triangle of Figure 3.6. In recent experiments carried out with low-density plasmas, a new type of fishbones was observed.

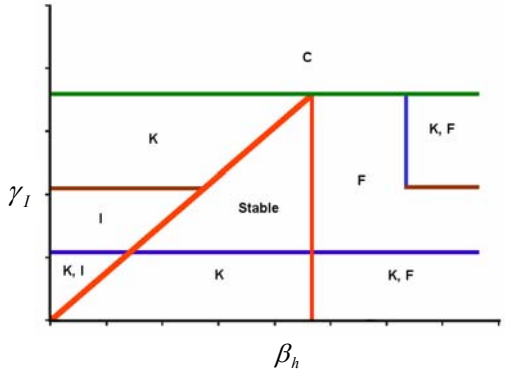

Figure 3.6 - Stability regions for the different branches of the internal kink mode in the space of parameters (the diamagnetic frequency determines the location of the red and brown lines). In the regions labelled with K, I and F the kink, ion and fishbone branches responsible for respectively sawteeth, low-frequency fishbones and high-frequency fishbones are unstables. For $\gamma_I > \gamma_M$ the low-frequency and high-frequency branches coalesce (region labelled with C).

These fishbones ranged all the way from high frequencies to low frequencies having characteristics of both diamagnetic and precessional fishbones, reason why were called hybrid fishbones. The fishbone behaviour was also observed to evolve during a sawteeth free period from high-frequency fishbones to low-frequency fishbones (Figure 3.7). Each hybrid fishbone corresponds to a single burst (Figure 3.8).

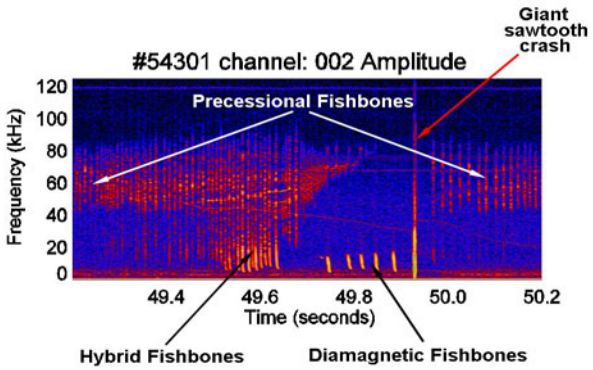

Figure 3.7 - Spectrogram of MHD activity for pulse #54301 showing the evolution of fishbone behaviour between sawtooth crashes.

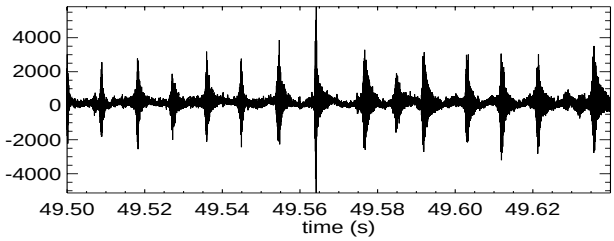

Figure 3.8 – Bursts of hybrid fishbones

At some point, hybrid fishbones begin chirping down only for a small range of frequencies becoming precessional fishbones and at the same time diamagnetic fishbones appear in the low frequencies. A new stage is reached where low amplitude bursts of both types of fishbones can be observed simultaneously. This occurs just before t=49.8 s. The precessional fishbones progressively disappear until only diamagnetic fishbones remain. A monster sawtooth crash occurs just after t=49.91 s and the fishbone activity is suppressed, but after a short time (t=50.0 s) precessional fishbones reappear.

3.3.6.2. Hybrid fishbones generating mechanism

The mechanism that produces this newly observed type of fishbones can be explained using the variational formalism.

The diamagnetic frequency (ω_{*i}) is mainly determined by the radial gradient of the background ions' pressure, so this means that when sawteeth are stabilized by fast ion effects, both γ_I and ω_{*i} increase. The effect of this increase in ω_{*i} over the stability diagram of Figure 3.9 is that the brown line ($\gamma_I = \omega_{*i}/2$) drifts upward and at the same time the green line ($\gamma_I = \gamma_M$) drifts downward. In these experiments the condition $\gamma_I < \omega_{*i}/2$ was reached first but the system remains in the same region of Figure 3.9 and only precessional fishbones are still observed.

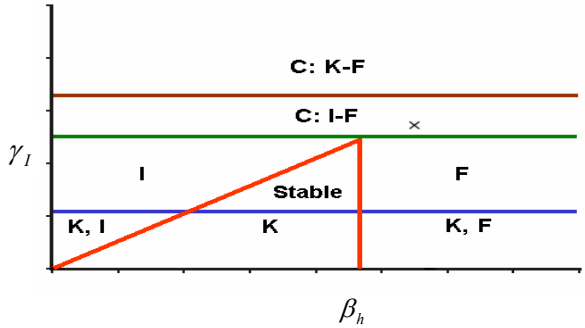

Figure 3.9 - Stability regions for the internal kink mode. In the regions labelled with K, I and F the kink, ion and fishbone branches are unstable. In the regions labelled with C:I-F and C:K-F the ion-fishbone and kink fishbone modes are unstable. The cross represents the state of the plasma when hybrid fishbones are observed.

After that, ω_{*i} continues to increase and at some point the condition $\gamma_I > \gamma_M$ is also reached. When this happens, the fishbone branch coalesces with the ion branch and a new region in the stability diagram is accessed (Figure 3.10).

The ion-fishbone branch is always unstable and, for a given value of ω_{*i}, behaves like the fishbone branch for high values of β_h and like the ion branch for lower values of β_h. If β_h is high enough when a fishbone burst is triggered, it begins as a precessional burst. During the burst fast particles are expelled from the plasma core and β_h decreases significantly. Thus, it is possible that β_h reaches values small enough for the mode behaviour change to that of a diamagnetic fishbone (Figure 3.10).

The result is that the fishbone that started as a precessional fishbone, accesses a new source of energy related to the bulk ions, that allows the amplitude of the oscillations to grow again, now with the characteristics of a diamagnetic fishbone with much slower oscillations in $\tilde{\dot{B}}_\theta$ (Figure 3.11). This mechanism produces hybrid fishbones which can only be observed when the coalescent ion-fishbone mode is unstable.

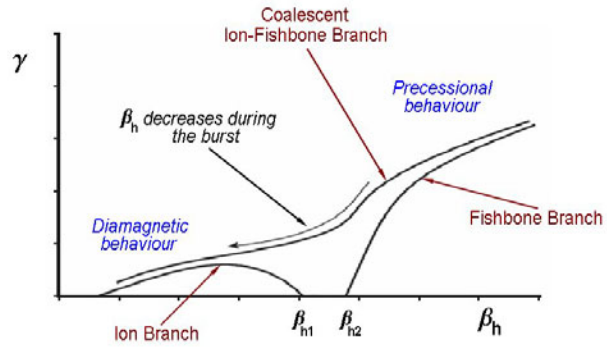

Figure 3.10 - Schematic diagram of the solution of the dispersion relation including diamagnetic and fast ion effects. The smaller arrow indicates the evolution of the mode behaviour during a hybrid burst, as fast ions are expelled from the plasma core and β_h decreases.

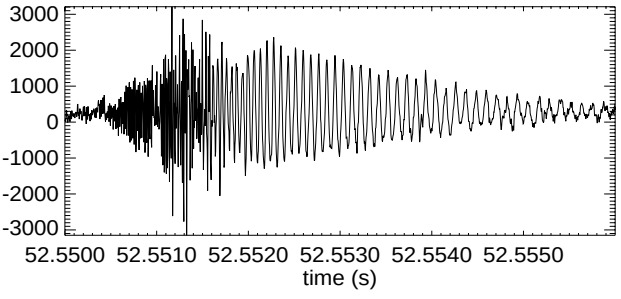

Figure 3.11 - Temporal evolution of $\tilde{\dot{B}}_\theta$ for the hybrid fishbone in pulse #54300.

3.3.7. Limiter H-mode studies in JET

Confinement transitions with the characteristics of H-mode were observed in JET inner wall limited plasmas in experiments performed at magnetic field of 0.8 T and at a current of 0.9 MA, using 5 MW of auxiliary heating power. The NBI heating is switched on for a period of 3 seconds (Figure 3.12), which is sufficient to achieve quasi steady state, given that both the overall energy confinement time and the beam slowing down time in these discharges are less than 200 ms. During this period several abrupt transitions in confinement are observed, which are characterised by a significant decrease in the H-alpha emission (Figure 3.13). However, limiter H-modes in JET are short lived (<20ms) and they are terminated by a burst of magnetic fluctuations with very similar characteristics to those of ELMs. The onset of the good confinement period is caused by a reduction in micro-turbulent transport very close to the plasma edge. On the other hand the termination of the period of good confinement has a clear magnetic signature, most likely caused by an edge instability driven by the steep pressure or current profiles.

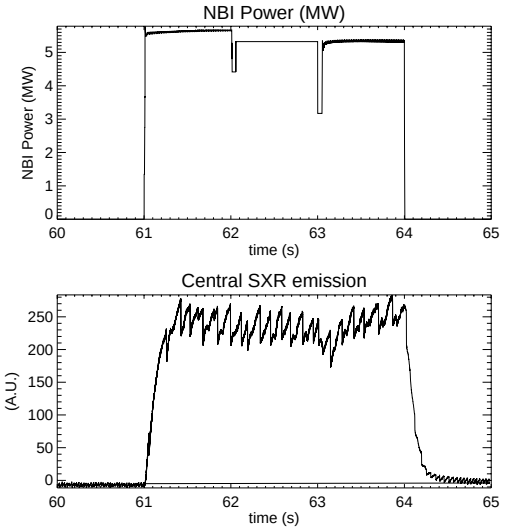

Figure 3.12 - Time evolution of NBI power for the limiter discharge #60908 and the central soft x-rays emission showing the Sawtooth.

3.3.8. Evidence of fast ion redistribution during fishbones from TAE in JET deuterium plasmas

TAEs were found to be unstable in JET limiter plasmas with B_t = 0.8 T and I_p = 0.9 MA. TAEs and large amplitude fishbones were destabilised by 5 MW of NBI. TAEs with toroidal mode numbers n=4, 5 and 6 were seen in the absence of fishbones, while n=2 and 3 TAEs appear in the presence of fishbones (Figures 3.14 and 3.15). This observation is consistent with a fishbone localised mainly inside q=1 redistributing fast ions and providing a steeper dp_{beam}/dr outside q=1. A steeper dp_{beam}/dr outside q=1 destabilises TAEs with lower n.

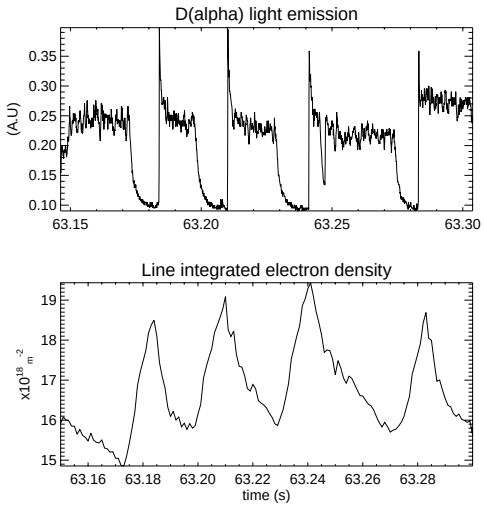

Figure 3.13 - D-alpha light emission and edge density (microwave interferometer) evolution during the H-mode transitions.

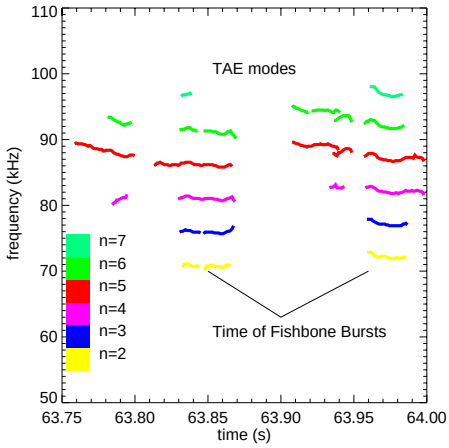

Figure 3.14 - TAE mode spectrum with different toroidal mode numbers (n), during the fishbone bursts.

3.3.9. Tritium transport studies

3.3.9.1. Modelling Tritium penetration

In recent JET campaigns, "trace" tritium gas puff was used in high performance discharges, to study the transport of a hydrogen isotope particle in high performance ELMy H-mode plasmas.

To model the trace tritium penetration, a 1.5D transport code JETTO was used. Tritium, being a minority species, is considered as low Z impurity for the neo-classical transport. NCLASS code was used for the neo-classical diffusion and convective velocity. For the anomalous particle diffusion the empirical model Bohm/GyroBohm was considered. For the anomalous convective velocity two theory motivated models are used in JETTO. This velocity is dependent on the magnetic shear or/and temperature gradient/Tritium boundary values.

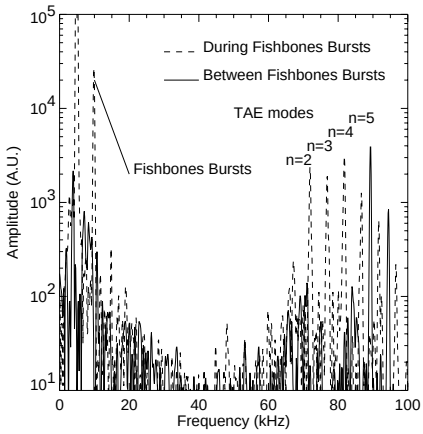

Figure 3.15 - TAE mode spectrum with different toroidal mode numbers (n), during the fishbone bursts and in between the fishbone bursts.

To observe the effect of the influx of tritons to its penetration to the plasma core, two different time dependent tritium density boundary conditions were used at the last closed flux surface: (i) a constant value of $n_T(a) = 5\times10^{15}$ m^3; (ii) varying from $n_T(a) = 5\times10^{15}$ m^{-3} up to $n_T(a) = 3\times10^{18}$ m^{-3}. During the tritium puff this boundary was decreased to its initial value 500 ms after the puff. In these simulations the plasma has been considered to be completely neo-classic without any anomalous contribution.

Figure 3.16 shows the results from the simulation. It is clear that the time between the starting of the gas puffing and the time that the neutron yield reaches its maximum, at the edge and the core channels, is longer for the simulation with non-constant boundary tritium density. The difference in the level of the reaction rate is also obvious for the case with a higher boundary density. The higher the tritium densities at the last closed flux surface, the lower is the out flux of particles (or even reverses the sign of the particle flux from positive to negative), keeping the tritium particles in the plasma core for a longer time.

The recycling (or reflection) coefficient R^{TT} is the least known parameter, which depends on the status of the wall and target plates. The best we can do is to study how sensitive is the result of our simulation with respect to a variation between $0 \le R^{TT} \le 0.9$ that is, R=0.0, R=0.5 and R=0.9. Figure 3.17 presents an increase of the neutron yield in all the plasma with the recycling and a smoothing of the initial ramp. The recycling change the tritium penetration by longer time to peak of the neutron yield and longer decaying time after it reaches its maximum. This is because there is a larger number of tritium particles that return back to the plasma, in other words the tritium stay longer inside of the plasma core. R = 0.5 leads the closet result to the experimental data.

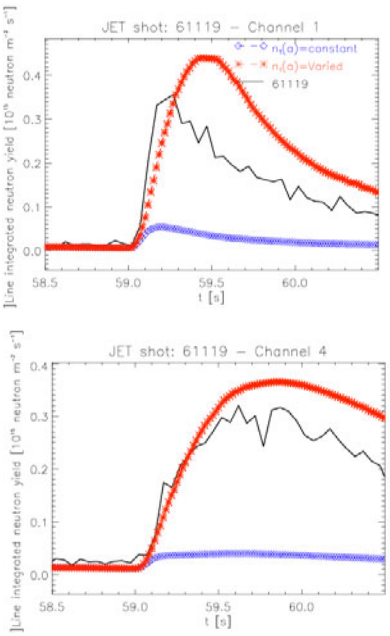

Figure 3.16 - Neutron yields horizontal camera for the edge channel (channel 1) and in the core channel (channel 4) for the two different time evolution of the tritium density at the last closed flux surface: a constant value of $n_T(a) = 5\times10^{15}$ m^{-3} (in blue) and varied boundary with the maximum value of $n_T(a) = 3\times10^{16}$ m^{-3} (in red), the experimental neutron yield for the pulse no. 61119 (in black).

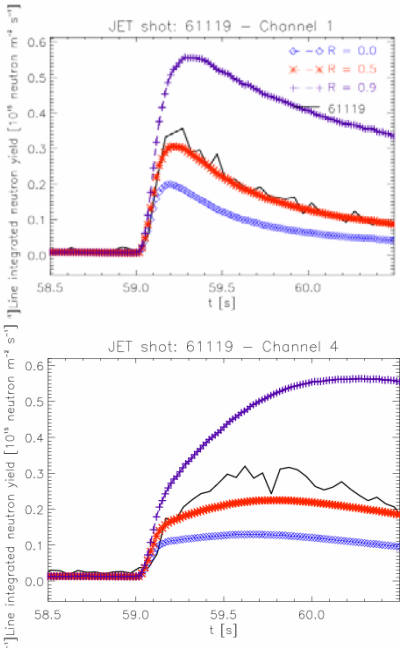

Figure 3.17 - Neutron yields horizontal camera for the edge channel (channel 1) and in the core channel (channel 4) for the three different recycling values: R = 0.0 (in blue), R = 0.5 (in red) and R = 0.9 (in purple).

3.3.9.2. Transport

(i) The ETB

In recent work with impurities it was shown that the neo-classical convective velocity for impurities changes sign from positive to negative when the edge deuterium density falls below the critical value. To take this effect into account, three different boundary values for the deuterium density have been prescribed. The neo-classical diffusion does not change significantly within the ETB for the different simulations. On the other hand the neo-classical convective velocity changes dramatically with the density gradient. The velocity is positive for the lower density gradient and it becomes negative for the higher density gradients.

(ii) The core

Three different tritium diffusion profiles neo-classical and two with additional anomalous contribution with different values of the anomalous multipliers of $c_T = 0.5$ and $c_T = 1.0$ were used to study the influence of the anomalous diffusion in the tritium penetration. It was found in the time to peak of the integrated neutron yield. The biggest difference was observed in the core channel. The time difference between the neo-classical diffusion and the highest level of the anomalous diffusion was around $\Delta t \cong 200$ ms. The neutron yield decay after it reaches the maximum is also faster for the highest diffusion.

(iii)Power deposition.

It was found that the higher is the plasma density the closer the tritium transport is to the neoclassical values. Nevertheless the tritium transport for pulses with ICRH had a higher anomalous contribution than the ones with NBI only. For example, in two consecutive JET pulses #61119 described above (Figure 3.17) and #61118 with 10.5 MW of NBI and 2.5 MW ICRH. The latter pulse had a higher density and lower temperatures but the best values of the anomalous transport coefficients for the particle diffusion and convective velocity were $c_T = 1.0$ and $c_{Tq} = 1.7$ comparatively, with #61119 that was $c_T = 0.5$ and $c_{Tq} = 0.0$. In these simulations only the NBI power deposition was considered. But simulations with the PION code demonstrated that the power is not going all to the electrons but mainly to the ions due to synergy effects. The results for different power deposition profiles are plotted in Figure 3.18 and it clearly indicates that the influence of ICRH should be taken into account, even when the power is low.

3.3.10. Neoclassic Tearing Modes (NTM) in hybrid regime

3.3.10.1. Triggering processes

In JET hybrid scenarios (HS) three types of triggering for the (3,2) NTM were observed: (i) as a (3,2) tearing mode

that started during the L-mode phase; (ii) during H-mode and in the presence of (1,1) modes; (iii) spontaneously during H-mode. During the L-mode, the collisionality regime is in the Pfirsch-Schlüter. In this regime the boostrap current is small and so the (3,2) mode can only be current driven and it is therefore probably triggered when the stability parameter Δ' is positive. The (3,2) mode becomes a NTM after the L to H-mode transition when the bootstrap current is significant. For the spontaneous NTMs, the (3,2) island growth rate was exponential, similar to those observed in low β_N plasmas where the onset coincides with the first sawtooth crash after the L to H transition.

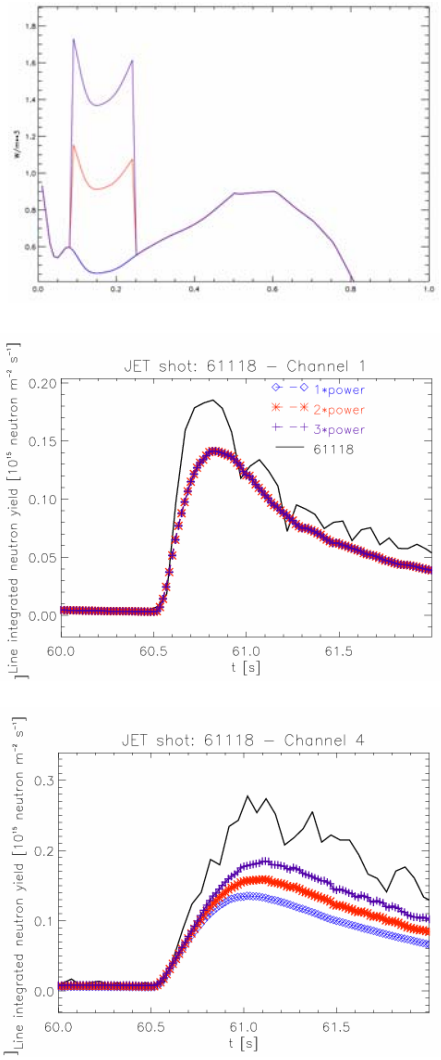

Figure 3.18 - a) Power deposition profile used in the simulations; b) the respective results and the experimental neutron yield for the pulse no. 61118.

The total number of pulses in the HS database was 48. In half of them neither the fishbone nor the sawtooth were observed and for these pulses q(0) > 1 was assumed. In all these pulses a (3,2) NTM was triggered. In the pulses, in which the (3,2) NTM was triggered spontaneously the shear is small at q = 1.5. In the other half of the pulses from the HS database (Figure 3.19), the q(0) ≤ 1 was assumed when, at least the fishbone instabilities were observed. In 12 of these pulses the (3,2) NTM was not observed but the sawtooth and the fishbone instabilities were present.

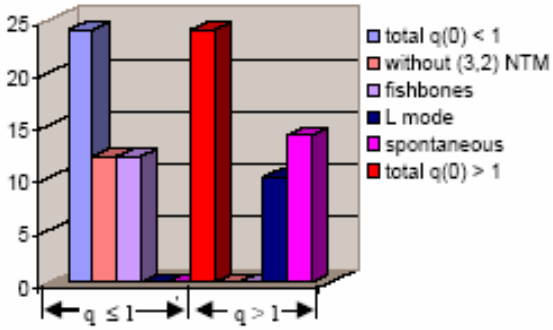

Figure 3.19 - Number of JET pulses in the hybrid scenario database for different types of (3,2) triggering

(ii) Energy confinement

In positive shear plasmas a reduction typically of 10-20 % in energy content is observed after the (3,2) NTM onset. The decrease in energy confinement is much lower for HS pulses (≤ 5%) the increase of confinement degradation with β_N is also lower. A possible explanation is the island width that is in average around 2 to 6 cm.

The island width is proportional to the square root of the magnetic perturbation for a constant shear and radius of the resonance surface. The island width is not only perturbed by the ELMs but also by the (4,3) NTM. Figure 3.20 shows that after the disappearance of (4,3) NTM, the (3,2) NTM grows to a saturated width and the core ion temperature decreases more than the core electron temperature.

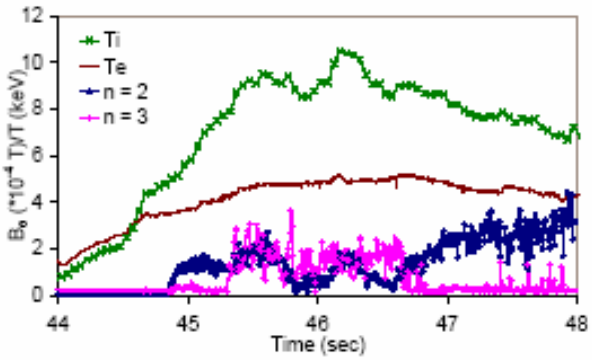

Figure 3.20 - Mode amplitude for the (3,2) NTM (blue), the amplitude of the (4,3) NTM for comparison (pink); electron temperature at R = 3.2 (brown); ion temperature at R = 3.14 (green) for the pulse # 60926.

3.3.11. Time–frequency analysis of nonstationary fusion plasma signals: comparison between the Choi –Williams distribution and wavelets

Recently, the Choi–Williams distribution has been effectively used to analyze nonstationary phenomena in fusion plasmas for which the spectrogram did not produce the best possible result. In principle, the Choi–Williams distribution is superior to wavelets, as it can yield excellent time–frequency resolution. Here, the advantages of using the Choi–Williams are shown using real fusion plasma signals. The comparison is for phenomena in JET, such as sawtooth (ST) crashes and neoclassical tearing modes (NTM) in discharges with ion cyclotron resonant heating (ICRH), and Alfvén cascades. In Figure 3.21, a ST crash appears as a broadband event at 60.6095 s, along with several modes including the (m =3, n =2) NTM at 5 kHz. In such a discharge with low β_N and ICRH, NTM may start with, or after the ST crash. So, good time–resolution is required. The time resolution of the spectrogram is not quite satisfactory, the region around the ST crash appearing blurred. The dependency of the time resolution of the scalogram on frequency is evident. In this case, for which good time resolution is important at all frequencies, the scalogram actually gives a worse representation than the spectrogram. The Choi–Williams distribution represents the modes and the ST crash with better time resolution than the spectrogram and the scalogram, although higher frequency modes appear somewhat masked by artifacts.

Using the Choi–Williams distribution is advantageous if the spectrogram fails to produce acceptable results, as long as the signal structure is not too complex, that is, with too many modes too close together in the time–frequency plane, so that artifacts can be adequately reduced. Wavelets, on the other hand, although sometimes improving upon the spectrogram, are unable to render sharp time–frequency representations as those produced by the Choi–Williams distribution.

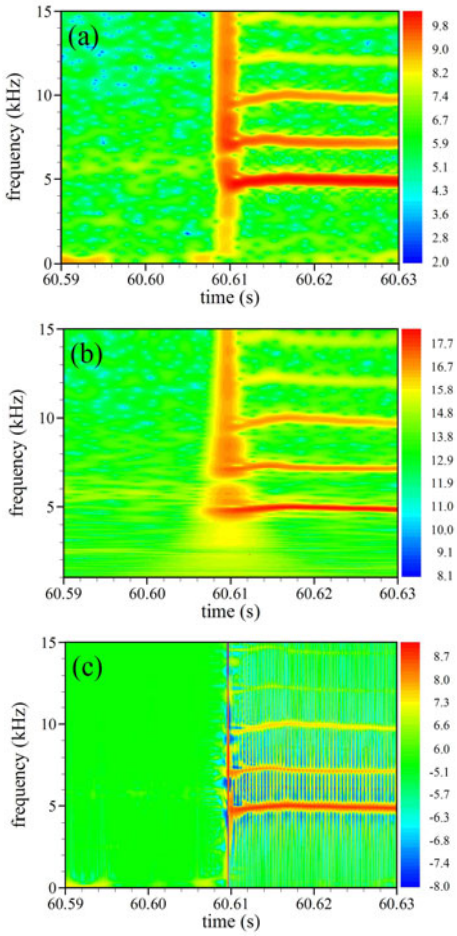

Figure 3.21 - Analysis of a magnetic pickup coil signal (JET pulse 50668), using (a) the spectrogram, (b) the scalogram, and (c) the Choi–Williams distribution.

3.3.12. Disruptions and runaway electrons in JET

Experiments and concurrent numerical modelling provided further contributions to the model for disruption generated runaway electrons (REs) in large tokamaks.

Limiter configuration with low elongated plasmas in JET enabled more stable behaviour of the runaway beams during and after disruptions resulting in long-lived runaway current plateaux (Figure 3.22). Interacting with cold post-disruption plasma RE beam produces detectable soft X-ray radiation providing information on evolution of runaway current-carrying channel in time and space. This data has been used in numerical modelling of the runaway process during disruptions.

A set of equations for the electron momenta (normalized to $m_e c$) together with evolution of runaway electron density has been solved at the initial conditions being inferred from the experimental data (plasma current, density, etc).

Experimental values of τ (characteristic current decay time) are concentrated in a range between 10 and 20 ms over a wide variation of the pre-disruption plasma currents. Calculations yield the values of post-disruption electron temperature $T_e \cong$ 10-15 eV at given plasma inductance $L_p \cong 4.5 \cdot 10^{-6}$ H. With these T_e values the numerical modelling provided close agreement between evolutions of the measured plasma current in disruption #63117 and total calculated current, which consists of two fractions: calculated runaway current (I_{RE}) and exponentially decayed resistive part (Figure 3.23(a)). Numerical simulations also show that the secondary avalanching process causes the dominating part of the disruption generated runaway electrons (Figure 3.23(b)). Depending on the initial conditions the current densities being inferred from calculated n_{RE} can achieve values up to $j_{RE} \cong 1$ MA/m^2.

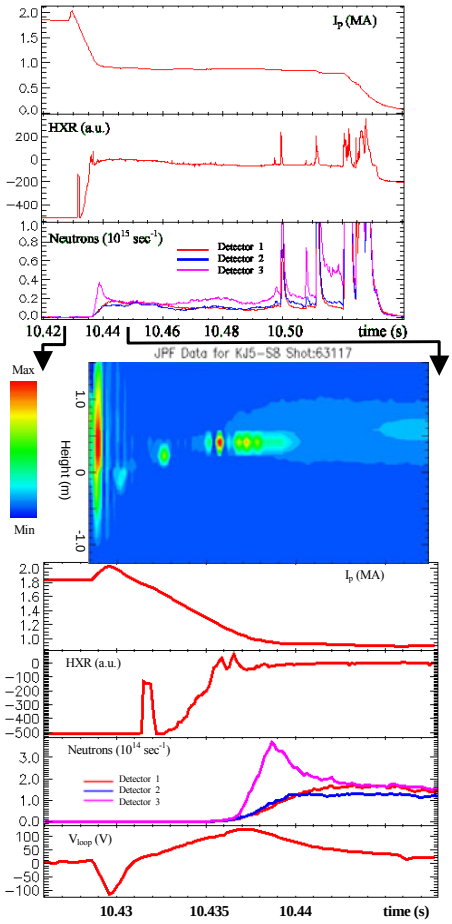

Figure 3.22 - Long-lived runaway electron beam generated at disruption #63117. Plasma currents (I_p), photo-neutron emission (Neutrons), Hard X-ray (HXR) and loop voltage (V_{loop}) signals are compared to the evolution of the soft X-ray emission (in arbitrary units).

The evolution of the test runaway electron in a momentum space and temporal evolution of RE density have been modelled in assumption that cross-section of RE current-carrying channel might have different size during current quench phase. Increase of RE current (as a result of larger beam cross-section) at other equal initial plasma and runaway generation parameters decreases the maximal RE densities and energies. Note, that close correspondence of the modelled and measured currents in Figure 3.23(a) has been obtained if the evolution of the cross-section size of RE current-carrying channel (as estimated from soft X-ray measurements) has been taken into account.

3.3.13. Effects of large magnetic islands on particle confinement trace-tritium studies–TRANSP modelling

The recent JET trace tritium campaign allowed us to study the effects of large magnetic islands induced by neo-classical tearing modes (NTMs) on tritium (T) particle transport. These kind of discharges are generally correlated

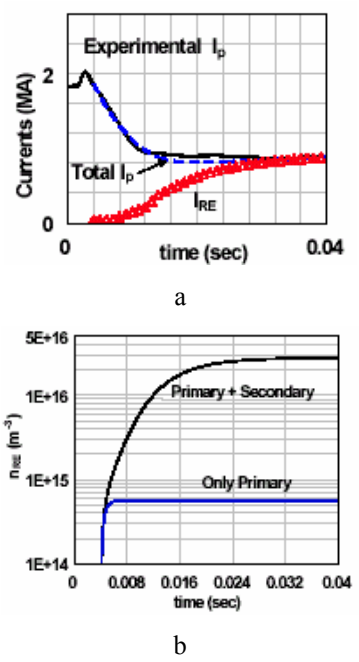

Figure 3.23 - Comparison of the measured plasma current to the calculated total current (RE current+plasma resistive current) at exponential decay of the resistive plasma current with characteristic time 0.01 sec (a). Calculated runaway electron density for primary only and for primary+avalanching mechanisms of runaway electron generation (b).

with an energy confinement degradation which could be related to the flattening the pressure around the magnetic islands. To quantify these effects transport studies were initiated using the suggested method proposed by the Task Force DT (TF-DT). Simulations with TRANSP were carried to estimate the two-dimensional profile of the neutron emissivity and the transport coefficients for neutrals, which are, then, used by the TF-DT to run the transport analysis package UTC. This code computes the T transport diffusion coefficient D_T and the relative pinch velocity V_T/D_T that best fits the experimental observation of the 2.5 MeV (D-D) and 14 MeV (D-T) neutron emission along 19 lines of sight.

Two trace tritium pulses, with and without NTMs have been modeled. Figures 3.24 and 3.25 show two-dimensional profiles of the 14 MeV neutron emissivities obtained by TRANSP for a given test T density profile. Similar simulations were done for each discharge for a set of 20 different T density profiles which are then used by UTC as a function basis for the T density. From the neutron emissivities given by TRANSP as a function of these T density profiles and the observable neutron emission, UTC estimates D_T and V_T/D_T profiles. Preliminary results suggest that the presence of magnetic islands can increase the T diffusion (D_T) in the plasma enclosed by the island and could reduce the T pinch velocity in the vicinity of the island (Figure 3.26).

However, since the majority of the 14 MeV neutron emission come from collisions between thermal T and D-beam, a more rigorous study requires further modeling because the effects of the magnetic island on the fast NBI ions were not yet taken into account.

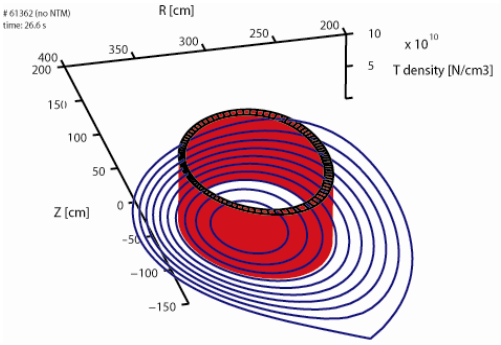

Figure 3.24 - 14 MeV neutron emissivity contours for the pulse #61362 (no NTM) using the given T density profile

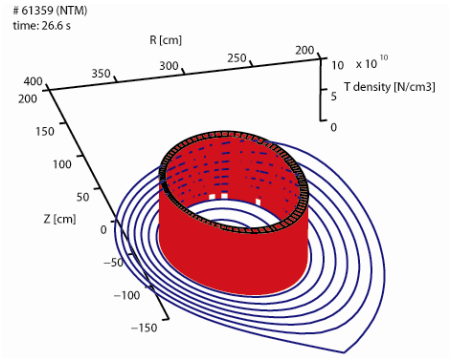

Figure 3.25 - 14 MeV neutron emissivity contours for the pulse #61359 (with NTM) using the given T density profile

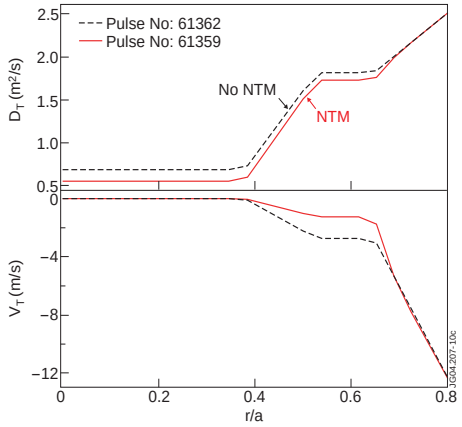

Figure 3.26 – UTC transport results for D_T and V_T for pulses #61362 (no NTM, black) and #61359 (with NTM, red)

3.3.14. On the cross-correlation between parallel and radial fluctuating velocities

The possible role of turbulence on the momentum re-distribution mechanisms in the plasma boundary region of tokamak plasmas was studied. Plasma profiles in the JET boundary plasma have been obtained using a fast reciprocating probe system that consists of arrays of Langmuir probes allowing the simultaneous investigation of the radial structure of fluctuations and parallel Mach numbers.

The contribution of the Reynolds stress term, $d<\tilde{v}_r\tilde{M}_{||}>/dr$, $\tilde{v}_r$ and $\tilde{M}_{||}$ being the fluctuating (ExB) radial velocity and the fluctuating parallel Mach number respectively, provides the mechanism to convert the turbulent scales (high frequency fluctuations) into a mean parallel flow. A comparison between the parallel flow profiles between forward and reversed field discharges is presented in Figure 3.27. In the forward field direction, (ion $B\times\vec{\nabla}B$ drift direction down towards the divertor), a strong parallel flow is measured at the top of the machine in the direction from the outer to the inner divertor. For reversed field, the measured flow is smaller but approximately symmetric with respect to a symmetry axis given by a positive offset. Figure 3.28 shows radial profiles of $<\tilde{v}_r\tilde{M}_{||}>$ obtained in forward and reversed field in the proximity of the LCFS in JET. In the plasma region where the floating potential becomes more negative (which turns out to be very close to the region where the perpendicular velocity shear is developed) there is evidence of significant radial gradients. It should be noted that the quadratic term of fluctuating velocities changes sign when the magnetic field is reversed.

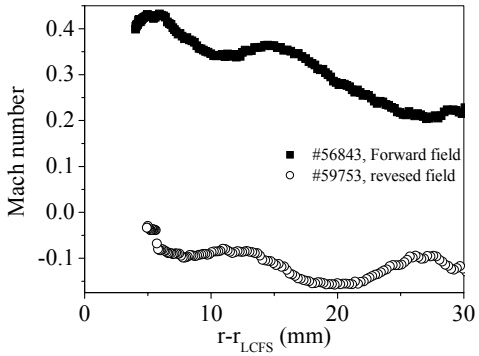

Figure 3.27 - Comparison of Mach number profiles between a forward and reversed toroidal field discharges in JET.

An estimate of the importance of turbulence in the evolution equation of the parallel flow requires a comparison of $d<\tilde{v}_r\tilde{M}_{||}>/dr$ with the magnitude of the parallel flows damped / driven by different mechanisms. The radial derivative of $<\tilde{v}_r\tilde{M}_{||}>$ was computed near the shear layer being its value in excess of $5\text{x}10^3$ s^{-1} both in

forward and reversed field in the JET tokamak. This result implies that, in the framework of our limited data base, the transport related momentum source ($n_e m_i \, d < \tilde{v}_r \tilde{v}_{\parallel} > / dr$) will be in the range of 1 – 5 N/m^3 in the JET boundary region, comparable with previous analysis of force balance which indicate a momentum source at the level of 10 N/m^3. Therefore, in the plasma edge, the Reynolds stress seems capable of sustaining a non- negligible parallel velocity.

This mechanism might be an ingredient to explain recent observations in Alcator C-mod showing that the toroidal momentum propagates in from the plasma edge, without any external source involvement. This mechanism can be particularly relevant during the L-H transition where the level of turbulence is mainly reduced near the edge. Then, radial gradients in the level of turbulence might develop, allowing a momentum redistribution (driven by internal-turbulent forces).

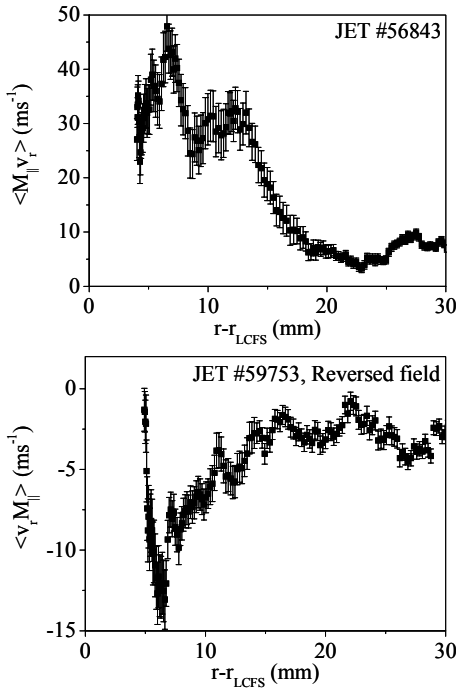

Figure 3.28 - Radial profiles of the cross-correlation between parallel and radial fluctuating velocities in JET L-mode plasmas near the LCFS in forward and reverse field discharges

3.3.15. Design of a new reciprocating probe head

A new reciprocating probe head has been designed to study momentum transport (Figure 3.29). The probe will be rather compact allowing the simultaneous measurement of the parallel flow at two radially separated positions, the radial and poloidal velocities and the fluctuations induced particle flux.

Concerning physics goals for the probe, the emphasis will be on the momentum re-distribution mechanisms driven by turbulence. Both the poloidal and parallel components of the momentum can be measured as well as the energy transfer between turbulence and parallel flows. The probe will also allow the continuation of the investigation in the dynamical relation between transport, radial electric fields, parallel flows and gradients.

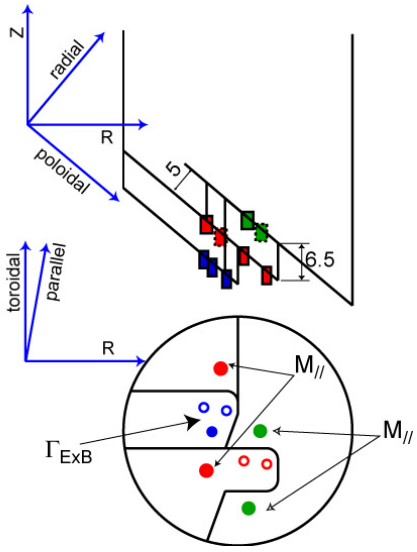

Figure 3.29 – Schematic illustration of the new turbulent transport probe head

3.3.16. Exploitation of the microwave reflectometry systems

3.3.16.1. ELMs studies

A study of the ELM activity using an X-mode correlation reflectometer (KG8b diagnostic) has been carried out. The 76-78 GHz channels (which generally probe the plasma edge region) are quite sensitive to the ELM activity (Figure 3.30). A drop of the signal amplitude as well as a significant increase of the fluctuations of the signal phase is observed during the ELMs. This result highlights that the loss of confinement during the ELMs is coupled with an increase of the turbulence. This is confirmed by the correlation reflectometry measurements on the bottom of the figure, which point out a significant drop of the correlation between the phases of two reflected signals at close frequencies, during the ELMs.

3.3.16.2. Turbulence studies

Spectral broadening induced by parametric instability in lower hybrid current drive experiments have been studied. Reflectometry measurements from the KG8b diagnostic showed an enhancement of the density fluctuation spectrum in the plasma edge region during the phase of injection of LHCD power. After the LHCD is switched on, a broadening of the spectrum of the reflected signal is observed (Figure 3.31).

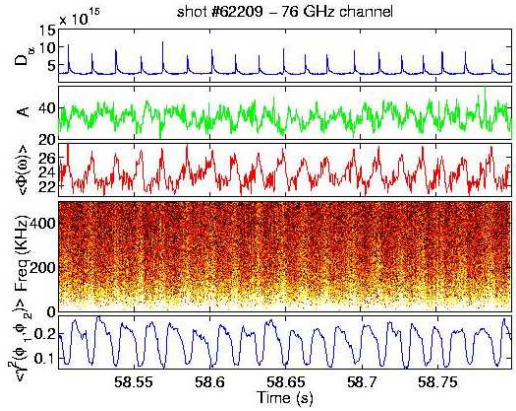

Figure 3.30 – Effects of type I ELMs on the X-mode correlation reflectometer data. From the top to the bottom: (a) Emission D_α displaying the ELM occurrence; (b) Amplitude of the reflected signal; (c) Averaged level of phase fluctuations of the reflected signal; (d) Spectrogram of the reflected signal phase; (e) Correlation between the reflected signal phases at two close frequencies (76 and 76.9 GHz)

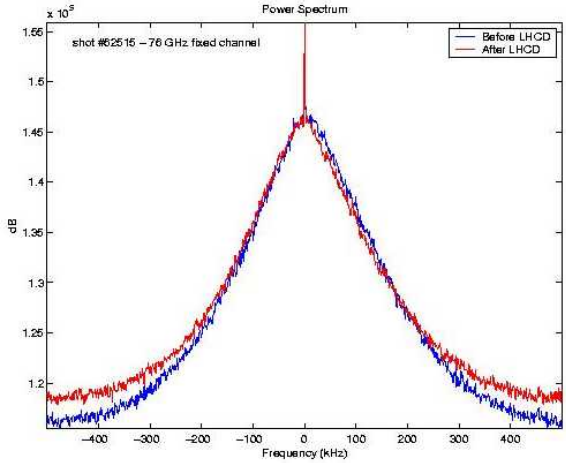

Figure 3.31 – Effect of the LHCD heating on a reflectometry signal of fixed frequency 76 GHz probing the plasma edge region.

The link between turbulence and plasma rotation is being investigated. A significant reduction of the turbulence was noticed when the cut-off layer of the reflectometry probing signal explores the ITB region associated with large negative poloidal velocity v_θ of plasma rotation. The spectrogram obtained from a sliding FFT of a reflected signal displays a reduction of signal fluctuations when the cut-off layer moves inner in the plasma where the ITB forms (Figure 3.32).

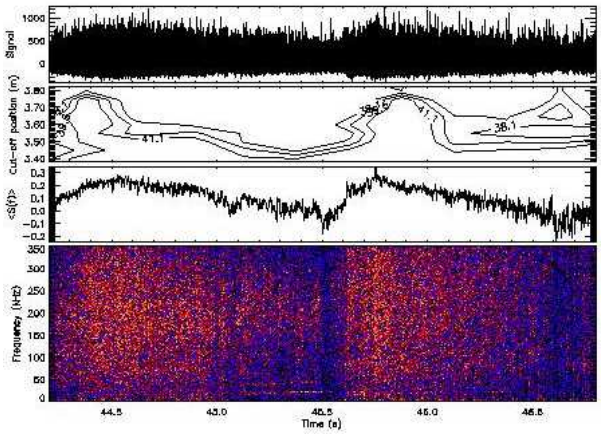

Figure 3.32 – Reduction of plasma turbulence in the ITB region observed from a reflectometry signal at fixed frequency 39.6 GHz. From the top to the bottom: (a) Raw reflected signal (b) Radial position of the cut-off layer (c) Averaged level of the reflected signal fluctuations (d) Spectrogram of the reflected signal.

3.4. PERFORMANCE ENHANCEMENTS

3.4.1. Introduction

IST/CFN was responsible in 2004 for four tasks of the JET Enhanced Performance Project:

- Mw Access-Project Management and Implementation;
- MPR-Project Design and Procurement Activities[2];
- TOF-Project Design and Procurement Activities[2];
- RTP-Development Real-time Test Facility.

Concerning the *Mw access – Project: management and implementation,* Dr. Luis Cupido has assured the coordination of the project, including the supervision of the commercial contracts. Test and measurement activities of the antenna cluster have been also carried out (Figure 3.33).

Figure 3.33 – MWA antennas delivered to JET in September 2004.

[2] Work in collaboration with the Association EURATOM/SKN

Regarding the *development real-time test facility*, transition from the initial design based on a System-On-Chip approach to a PC based system has been made. The schematic and layout design of the waveform generator (WG) PCI module prototype have been performed. One WG prototype board has been assembled and tested. Four final WG modules have been commissioned and tested. Firmware codes have been written for the development of the programmable logic devices, including the design, simulation and test of a CIC interpolator filter and sharpening FIR filter, both programmable in real-time. The low-level Digital Signal Processor (DSP) software has been implemented. A code for interfacing with the ATM real-time network has been developed. A complete PC based system with four waveform generator modules has been assembled. The Linux based control software, the Application Programming Interface (API) and the MDSPlus interface software have been developed.

Concerning the *MPR-Project: design and procurement activities* and the *TOF-Project: design and procurement activities,* two prototypes of the time digitizer (TD) module have been assembled and tested (Figure 3.34). A Matlab® data analysis program for automatic detection of functional and performance errors on TR has been developed. Six plus two spare TR boards as well as three TD boards have been assembled and tested at IST and sent to the Swedish EURATOM Association for integration on the MPRu and TOFOR diagnostics. The modules control and test software both for the Windows and Linux OS have been completed. Software and hardware manuals have been finished. IST/CFN staff has collaborate with VR on the integration of the modules in the diagnostics.

3.4.2. Real-time test facility

The test-bench system provides an analogue or digital replica of signals stored in a database, to generate stimulus for real-time control and data acquisition tools under test.

The on-site developed system (Figure 3.35), incorporating four DAC PCI modules, provides 32 analogue channels and one ATM link with the following main characteristics: (i) 32 analogue output channels with 16 bits resolution at up to 50 MSPS sampling rate; (ii) ±10 V output range on 600 Ω output impedance; (iii) 2 GByte of real-time signal storage capacity; (iv) includes four TMS320C6415 DSPs and four XC2V1500 FPGAs for real-time signal processing; (v) one full-duplex ATM optical port with 155 Mbps of transfer rate.

The software developed for the test-bench allows the integration with the JET MDSplus signal database server as well as with the Web server based Level-1 control interface with JET CODAS.

Figure 3.35 - Test-bench system.

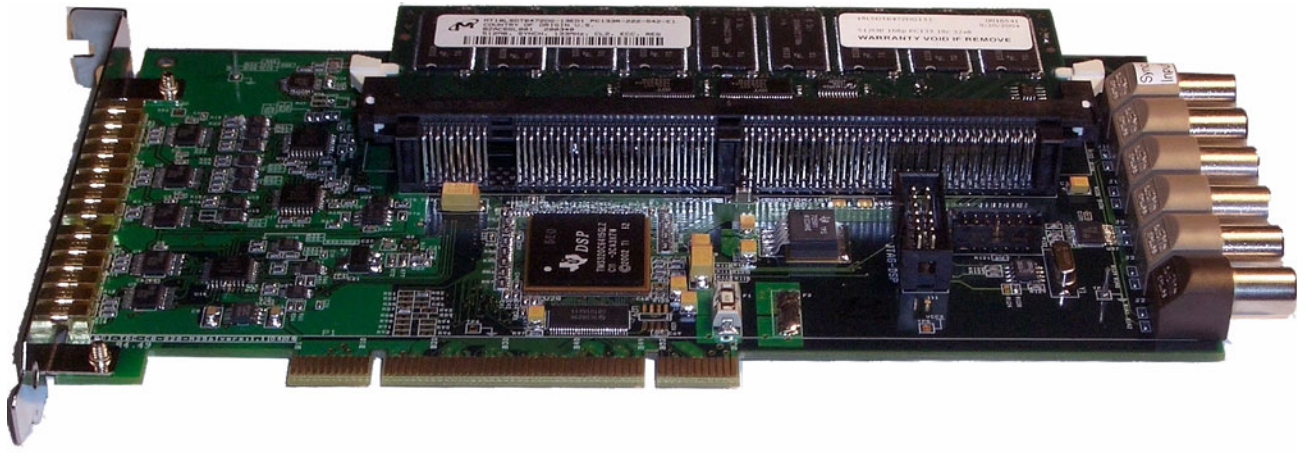

Figure 3.34 - Time digitizer module.

4. PARTICIPATION IN THE ASDEX UPGRADE PROGRAMME[1]

M.E. Manso and F. Serra (Heads), D. Borba, R. Coelho, L. Cupido, L. Fattorini, R. Galvão, S. Graça, L. Meneses, I. Nunes, V. Plyusnin, T. Ribeiro, F. Salzedas, J. Santos, A. Silva, F. Silva, P. Varela.

4.1. INTRODUCTION

The Portuguese participation in the ASDEX Upgrade[2] (AUG) programme has been mainly focused in two research lines:

- Microwave reflectometry;
- MHD, turbulence and transport.

4.2. MICROWAVE REFLECTOMETRY

4.2.1. Introduction

This research line included in 2004 activities on microwave systems and electronics, control and data acquisition, data processing, diagnostic developments, modelling and plasma physics studies.

Concerning *microwave systems and electronics*, a new active frequency multiplier for the Q-band X-mode channel has been installed. A permanent marker switch has been implemented to provide dynamic calibration curves for all frequency sweeps every shot. All heterodyne channels have been tested and new IF filters with larger bandwidth have been installed for proper fast sweep operation. V-band X-mode channel was upgraded (new mixer and correction of default in antenna). Detailed dynamic frequency calibration circuit using a millimetre wave delay line (Figure 4.1) has been developed, to provide together with frequency markers a very accurate frequency calibration (Figure 4.2). A new in-vessel directional coupler at the Ka-band HFS channel has been installed, replacing the one damage by ECHR operation. New thermal and plasma protection for the waveguides (at LFS access port) were installed to avoid Halo currents in the waveguides. A vacuum window misalignment in the W-band LFS has been repaired.

Regarding *control and data acquisition*, control software of broadband channels has been optimized. It was modified after the installation of a new RS232 control boards to improve hardware control. New functionalities have been added to the broadband section: (i) new channels have been implemented to measure calibration signals; (ii) a logfile has been introduced to control eventual hardware faults; and (iii) software has been developed to switch on/off remotely each microwave source. Control software for a new "hopping" frequency system is being developed.

Concerning *data processing*, the burst mode data analysis for automatic density profile evaluation was validated with a 2D FDTD code. Software tools for automatic evaluation of the very edge ne-profile with X-mode have been developed.

Regarding *diagnostic developments*, a software tool to simulate O/X mode reflectometry has been developed. Results show that toroidal magnetic ripple plays a crucial role in X-mode reflectometry. A correction of the position of first plasma layer (derived from the first X-mode cutoff frequency) of about 1 cm was estimated. The reliability and accuracy of plasma position measurements has been assessed with a dedicated numerical workbench.

Concerning *modelling*, unidirectional transparent signal injection in electromagnetic codes has been modelled.

Physics studies on the impact of type I and type III ELMs on the plasma edge density, MHD and turbulence were carried out in 2004.

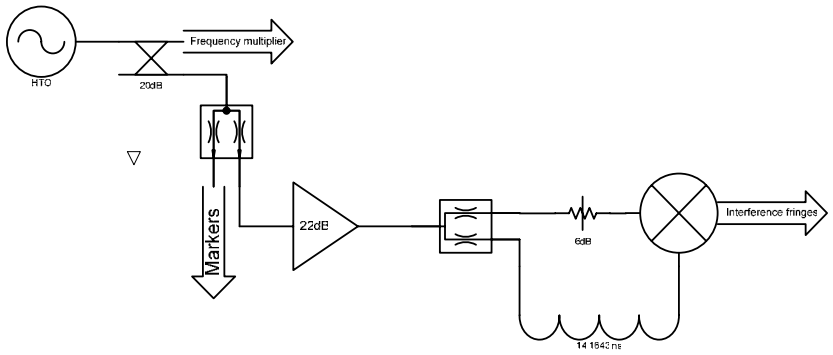

Figure 4.1 – Circuit for detailed dynamic frequency calibration using a millimetre wave delay line

[1] Work carried out in collaboration with the ASDEX-Upgrade Team. Contact Person: G. Conway.

[2] ASDEX-Upgrade is a tokamak of the Association EURATOM/IPP

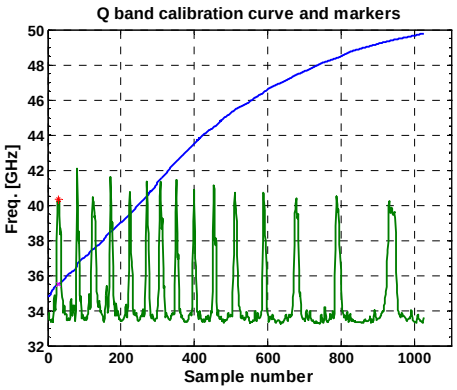

Figure 4.2 – Dynamic frequency calibration curve

4.2.2. Numerical studies for plasma position

In order to test the robustness of position measurements to plasma turbulence, **d**ensity perturbations were added to the n_e-profiles:

$$\delta n_e(r) = \sum_{i=1}^{n} a_i \cos(\ i\Delta k\,.r + \varphi_i) \qquad (4.1)$$

where a_i and φ_i are, respectively, amplitude and phase of the density fluctuations with a wave number $k=i\Delta k$.

Three levels of density fluctuations were investigated: rms amplitudes of 1.5%, 3%, and 5% of a density ($\hat{}n_{sep}=2x10^{19}$ m$^{-3}\approx$ *25%* n_{e_med}) slightly above the corrected separatrix density found for this profile. The rms position errors at densities n_e *=1, 1.62* and $3x10^{19}$ m^{-3} were less than 5 mm for single sweep profiles while in burst mode analysis (grouping of several sweep samples) were significantly reduced err_{rms}*<1-2* mm (Figure 4.4). Errors also diminish for higher densities (n_e = $3x10^{19}$ m^{-3}, err_{rms}*<1* mm) with burst mode analysis.

Three initial positions were simulated: the standard limiter, limiter-3 cm, and limiter+3 cm. Figure 4.3 shows the position errors at densities n_e=1.6 and 3x10^{19}m^{-3} for simulated profiles with 5% turbulence level using burst analysis (8 sweeps). The absolute errors are, in all cases, below 1 cm, and decrease for higher densities. In the LFS the errors are smaller than in the HFS due to the higher proximity to the limiter and to the steepness of the profiles.

4.2.3. Modelling[3]

A novel numerical signal injection technique has been developed allowing unidirectional injection of a wave in a wave-guiding structure, applicable to 2D finite-difference time-domain electromagnetic codes, both Maxwell and wave-equation. The reflected or backscattered waves (returned) are separated from the probing waves allowing direct access to the information on amplitude and phase of the returned wave (Figure 4.5). It also facilitates the signal processing used to extract the phase derivative (or group delay) when simulating radar systems.

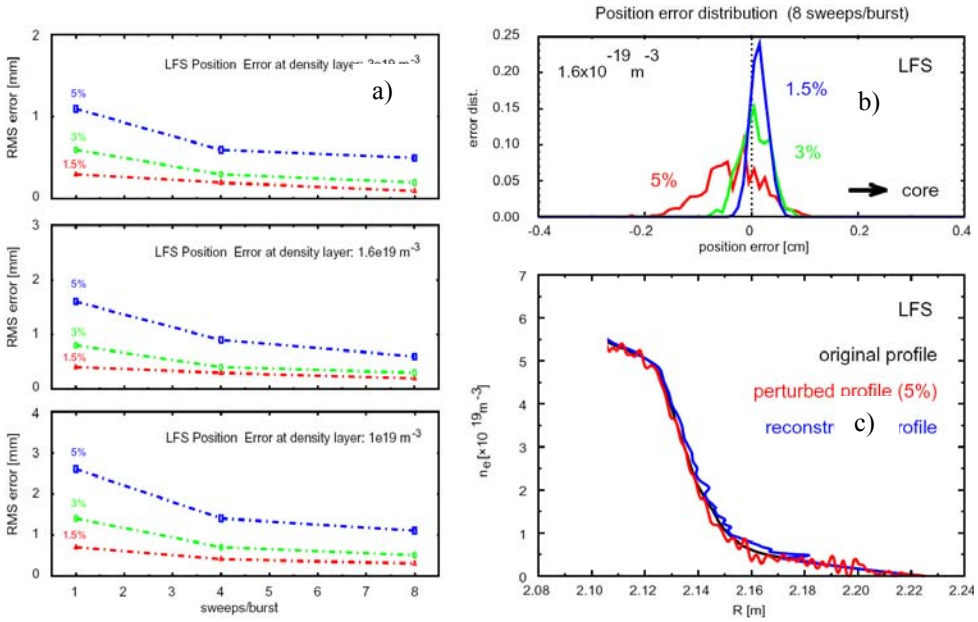

Figure 4.3 – Position error for density layers 1.0, 1.6 and 3.0x10^{19} m^{-3} of LFS H-mode profile. Left: position error versus the number of sweeps per burst. Three layers and three levels of simulated turbulence (1.5%, 3% and 5% of n_{sep}) are considered. On the top right, the position error distribution at density layer 1.6x10^{19} m^{-3} for 8 sweeps/burst and three levels of turbulence.

[3] Work carried out in collaboration with Dr. S. Heuraux (Universitè Poincaré, Nancy, France)

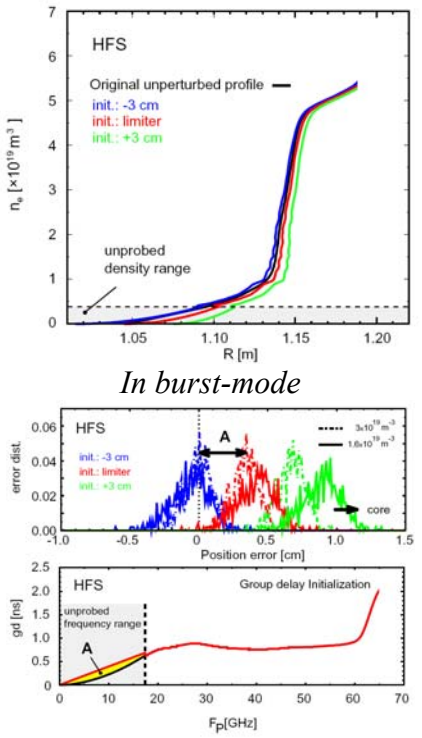

Figure 4.4 - Position error resulting from turbulence and initialization error. The original profile was initialized at three locations: the inner limiter (its original position) and 3 cm before and after the limiter. The non probed group delay was approximated linearly and its difference to the original is responsible for the shift (A) of the distribution. The distribution was calculated for density layers 1.6 and 3.0x10^{19} m^{-3} and 5% turbulence level.

4.2.4. Study of the impact of type I and type III ELMs on the plasma edge density profiles

From the analysis of the density profile evolution during an ELM event, three characteristic phases of the ELM can be defined: precursor, collapse and recovery both at the LFS and HFS. At the collapse phase, coincident with the period of enhanced MHD activity, the crash of the density profile is observed. After the collapse of the density, the pedestal-top has moved inwards while the density profile at the scrape-off layer (SOL) broadens defining a radial pivot point localized very close and inside the separatrix, (Figure 4.6) where $t = 0$ at the onset of the ELM.

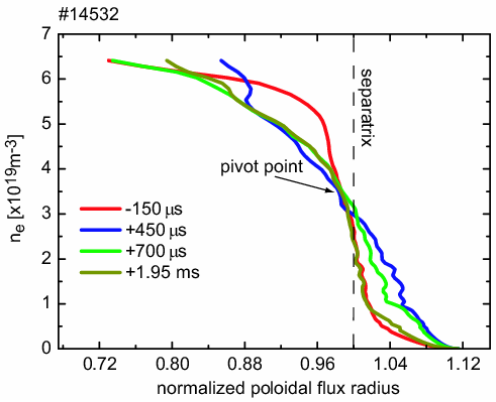

Figure 4.6 – Time evolution of the density profiles before and after an ELM event.

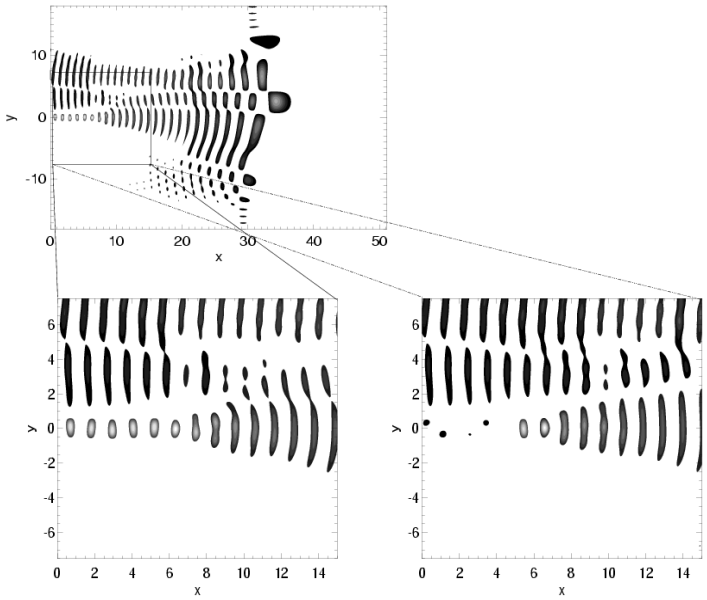

Figure 4.5 - the electric field structure close to an instant where the destructive interference occurs, is shown using an usual source (left) and an Unidirectional Transparent Source (UTS) (right). With an UTS the minute signal structures can be localized while they become completely masked when the UTS is not used.

The two plasma regions, inside and outside the pivot point, are observed to behave differently during the recovery phase. Inside, the recovery time decreases with the ELM frequency ($f_{ELM,}$) and is independent of the plasma parameters; outside, the recovery time is approximately constant, independently in particular of $f_{ELM,}$ (Figure 4.7).

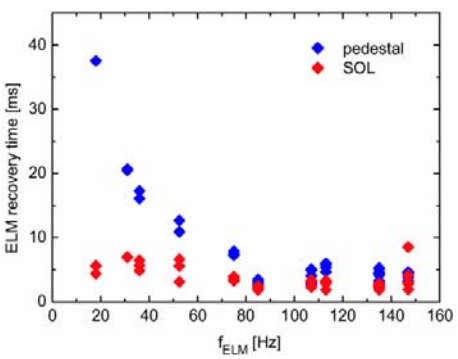

Figure 4.7 – Pedestal and SOL recovery time as a function of the ELM period.

The radial extent of the ELM perturbation, ELM affected depth (ELMAD), on the density profiles within the region of closed flux lines was determined by using the density profile before and after the ELM. ELMAD is given by the distance between the pivot point and the inner radial point (A and B, respectively, in Figure 4.8).

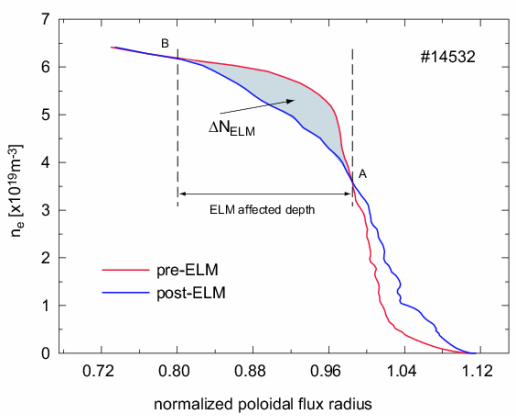

Figure 4.8 – The radial extent of the perturbation is given by the distance between the pivot point and the inner radial point where no change of the density reflected layer due to the ELM is observed (points A and B respectively). The region where the particles losses, ΔN_{ELM} are determined is also defined by these two points.

It is found that the ELMAD normalised to the plasma minor radius, at the LFS, decreases slightly with the pedestal density (normalised to the Greenwald density) (Figure 4.9(a)). The ELM perturbation affects the outermost 10-20 cm (20-40% of the plasma minor radius), as it is also observed at JET, DIII-D and JT-60U. In AUG it is found that the ELMAD is correlated with the ELM particle losses, ΔN_{ELM} and weakly dependent on the plasma parameters (Figure 4.9(b)).

The average radial velocity $<v_r>$ at which the density profiles collapse can be determined as the maximum radial displacement of a density layer over the time elapsed to reach this maximum. Figure 4.10 shows the absolute value of $<v_r>$ as a function of $\Delta r = r - r_{sep}$ where each curve represents one ELM; it increases for density layers situated farther away from the pivot point.

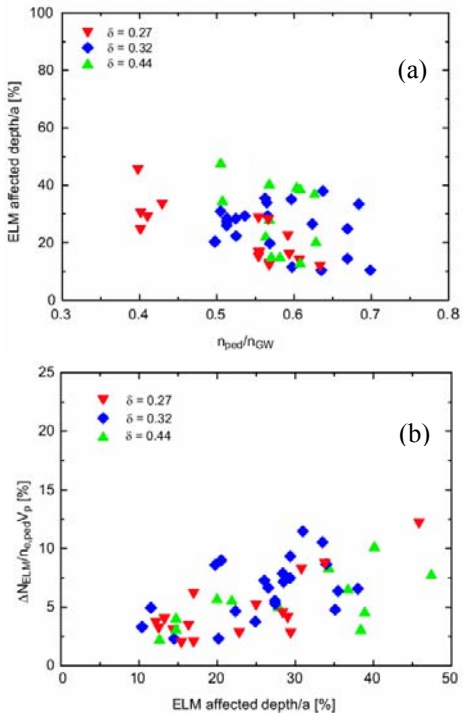

Figure 4.9 – (a) ELM affected depth normalised to the plasma minor radius as a function of the normalised pedestal density, ne,ped/nGW for the low-field side. A slight decrease of the ELM affected depth with density is observed. (b) ELM particle losses as a funcion of the ELM affected depth. A correlation between both is observed.

4.2.5. ELM frequency control by pellet injection and magnetic triggering

In AUG, full ELM control is achieved with the increase of the ELM frequency (f_{ELM}) by increasing the pellet frequency (f_{Pel}). Injection of small size cryogenic Deuterium pellets (at rates up to 83 Hz) imposed persisting ELM control without significant fuelling, well inside type-I ELM regime. ELM pace making was realized with the driving frequency ranging from 1.5 to 2.8 times the intrinsic ELM frequency (f^0_{ELM}). ELM frequency enhancement by pellet pace making causes much less confinement reduction. Moreover for pellet triggered ELMs the energy loss per ELM reduces with increasing f_{ELM} .

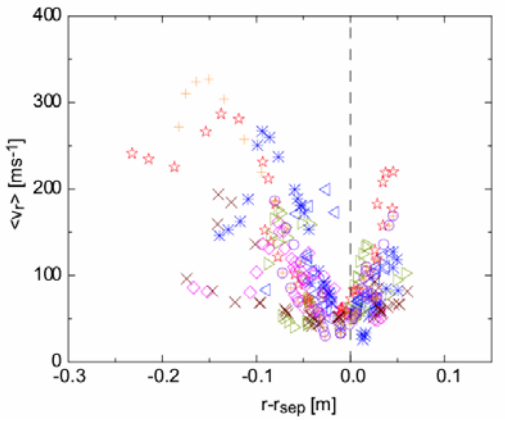

Figure 4.10 – Average radial velocity as a function of plasma position, where $r - r_{sep} = 0$ is the position of the separatrix. Each curve represents one ELM.

4.2.6. Dynamics of intrinsic and pellet triggered ELMs

FM-CW reflectometry diagnostic was used in broadband operation to study the evolution of density profiles with a very high temporal resolution during ELM phases (intrinsic and triggered ELMs). It was found that intrinsic and triggered ELMs have similar characteristics. With fixed frequency operation of the reflectometry system, the level of density fluctuations could be monitored. Adjusting the launching frequency to reflect from a plasma layer inside the steep gradient region (external transport barrier), an excellent monitor of the ELM instability was available. It was possible to characterize the turbulence footprints of intrinsic and pellet triggered ELMs, which show a very similar behavior. Thus, apart from the trigger mechanism both types of ELMs are obviously stamped by the same underlying physics and cannot be distinguished by their dynamics (Figure 4.11).

4.2.7. Magnetic triggering

An alternative technique to trigger ELMs was tested, based on a rapid vertical movement of the plasma column. The observed effect of locking the ELM time sequence with plasma oscillation is attributed to an edge current induction during the vertical movement in a spatially inhomogeneous single-null vacuum configuration. This method, used on TCV[4], has been adapted on AUG for type-I ELMy H-modes in the same discharges applied for the pellet approach (Figure 4.12). Shaking the plasma ("wobbling") showed an immediate impact on the ELM behavior and once steady state conditions are reestablished locking of the ELMs to the motion with a driving frequency (f_D) could be achieved. In first proof-of-principle experiments an operational range of f_D / f^0_{ELM} =0.75÷1.8 was obtained. Again, as in the pellet case, similar characteristics were found between intrinsic and triggered type-I ELMs (Figure 4.13).

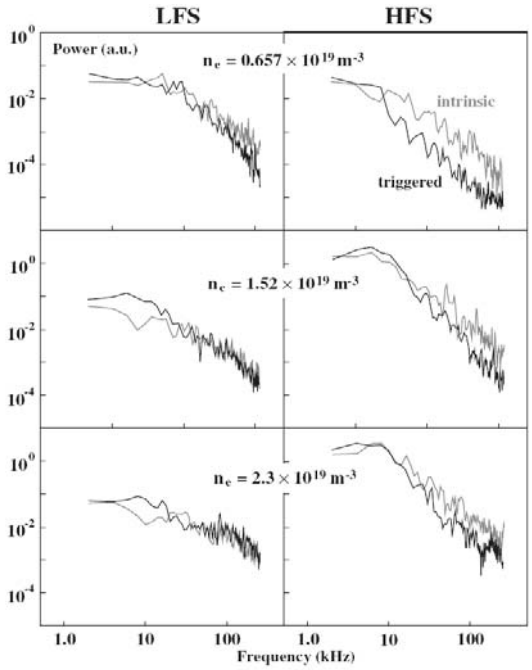

Figure 4.11 - Frequency power spectra obtained from reflectometry signals for reflected layer in the transport barrier region at different n_e values both for plasma HFS and LFS. Spectra derived from data in time windows, with duration 2.5 ms, including an intrinsic (grey) or pellet-triggered (black) ELM.

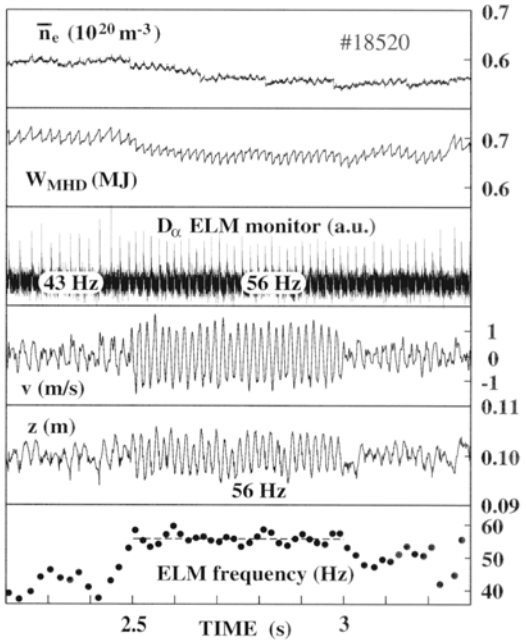

Figure 4.12 - Demonstration of magnetic ELM triggering in a type-I ELMy H-mode. The ELM frequency is raised and locks to the frequency of imposed vertical (position z, v=dz/dt) movement of the plasma column. During the driving phase (2.5-3.0 s) only a modest effect on particle and energy confinement is found.

[4] TCV is a tokamak of the Association EURATOM/Suisse Confederation

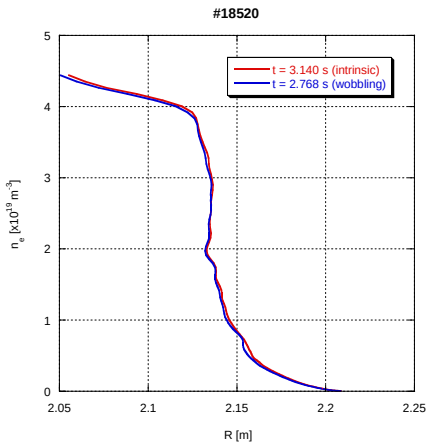

Figure 4.13 - LFS reflectometry density profiles: comparison between intrinsic and magnetic triggered ELM.

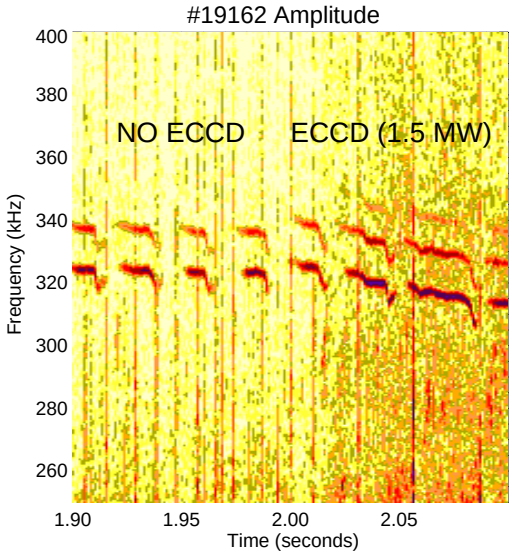

Figure 4.14 – Evolution of the AE frequency of the AE showing the effect of ECCD on the TAE amplitude

4.3. STUDIES ON MHD, TURBULENCE AND TRANSPORT

4.3.1. Effect of Electron Cyclotron Current Drive (ECCD) on Alfvén Eigenmodes on ASDEX Upgrade

Figure 4.14 presents the influence of ECCD on the TAE amplitude in a discharge with a constant level of ICRH power (5MW) and 1.5 MW of ECCD switched on at t=2.0 s. Without ECCD, two TAE modes are observed with frequencies around 300-350 kHz and the TAE are frequently interrupted by sawteeth. By applying ECCD the TAE amplitude increases, as measured by the Mirnov probes and the TAE survive most of the sawtooth period. A third mode can also be seen during the ECCD phase. Therefore, ECCD has a slight destabilizing effect on the TAE, probably caused by a different TAE damping, due to changes in the q-profile.

4.3.2. Code development for the analysis of turbulence and transport in the SOL of ASDEX Upgrade

The model behind the GEM3 code was extended to treat the locations where the magnetic field lines intersect the material limiter/divertor plates and the plasma faces those components. Debye sheath physics concepts were used to model such interactions. The results revealed the dominance of a convective cell mode ($k_{\parallel} = 0$) whenever the limiter was included, i.e., whenever the SOL boundary conditions were applied (Figure 4.15), in accordance with the experimental observations for the SOL region. The turbulent transport values were also found to increase as the large scale interchange dynamics became dominant, due to the absence of the adiabatic response of the electrons in the convective cell mode.

Conversely, with closed field lines boundary conditions, the field line connection in sheared magnetic field suppresses the convective cell mode, leaving the drift wave character typical of the plasma edge.

The effect of the AUG diverted geometry was investigated by performing turbulence simulations near the magnetic separatrix on a typical equilibrium magnetic field. In the region inside the magnetic separatrix, using closed flux surfaces boundary conditions, the results obtained revealed a reduction of the measured ExB turbulent transport (Figure 4.16).This result supports the scenario whereby the local magnetic shear facilitates the nonlinear decorrelation processes by twisting the turbulent perpendicular vortical structures, which are then torn apart to smaller scales. These results also stress the importance of using faithful descriptions of the tokamak geometry.

The joint effect of both the Debye sheath boundaries and the realistic geometry was also investigated. The results obtained in this case showed differences in the mode structure when the resolution of the computational grid was improved. This study revealed that the spatial scales resolution is a critically issue to cope with the poloidal dependence of the perpendicular metric components in ExB turbulence.

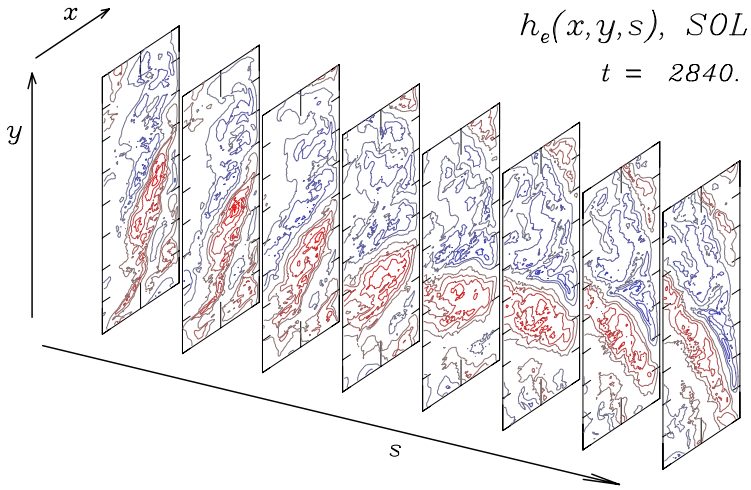

Figure 4.15 - Spatial morphology of the full computational domain of the nonadiabatic density ($\tilde{h}_e = \tilde{\phi} - \tilde{n}_e$) for the SOL situation (Debye sheath model), showing the largescale, field line following convective cell ($k_{\|} = 0$) "streamer" mode, now allowed by the geometry to exist

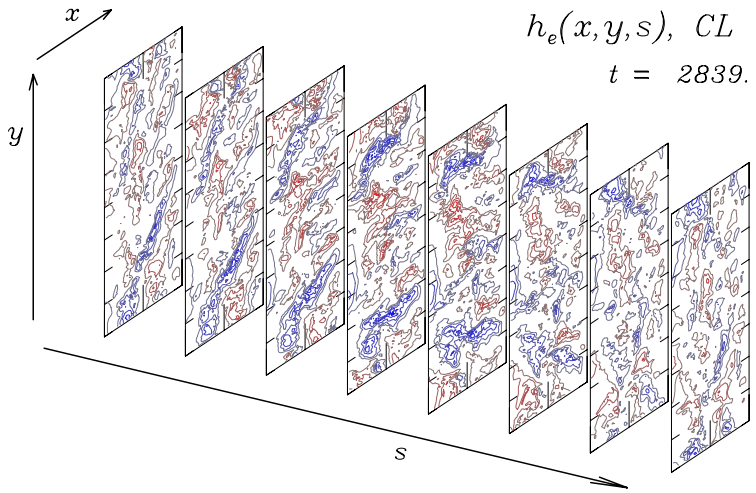

Figure 4.16 - Same as figure 1 for closed flux surfaces (CL). Note the absence of the k= 0 mode he k= 0 mode.

5. PARTICIPATION IN THE TJ-II PROGRAMME

C. Varandas, M. Manso (Heads), L. Cupido, B. Gonçalves, L. Meneses, I. Nedzelskij, L. Pereira, A. Silva, C. Silva, Y. Tashchev, P. Varela.

5.1. INTRODUCTION

The Portuguese participation in the TJ-II[1] programme has been mainly focused in three research areas:

- Microwave reflectometry;
- Edge plasma physics;
- Heavy ion beam diagnostic.

5.2. MICROWAVE REFLECTOMETRY[2]

5.2.1. Introduction

CFN has developed a fast frequency hopping reflectometer, operating in the Q-band (33-50 GHz), with wave propagation in X-mode. It can be tuned to any selected frequency, within a fraction of a ms, while keeping synchronized the local and radiofrequency oscillators, with the same stability of a fixed frequency system. This property enables to probe several plasma layers within a short time interval, to characterize the radial distribution of plasma turbulence.

In 2004 the hardware developed by CFN was delivered to Madrid and tested at CIEMAT. The reflectometer started to be routinely operated after the installation of vacuum windows and the development by CIEMAT of some control and acquisition software. Plasma physics studies based on the analysis of the experimental results have been initiated.

5.2.2. Description of the diagnostic

This reflectometer (Figure 5.1) incorporates: (i) a fast frequency synthesizer operating at 8-12.5 GHz multiplied into the millimeter-wave range 32-50 GHz; (ii) a harmonic mixer for heterodyne detection with sensitive phase and amplitude measurements; and (iii) low pass filters (not shown in Figure 5.1) to protect the system against the high RF power from the electron cyclotron heating system (f_{ECH}=53.2 GHz).

The system uses fundamental waveguide transmission line and separate antennas for launching and receiving the signals, viewing the plasma from the low field side. The antennas (Figure 5.2) are standard gain horn type with a 3dB beam width of about 20º and located in a toroidal position defined as φ = 85.3º where the plasma is not symmetric with respect to the equatorial plane of the device. To ensure an almost pure X-mode, 24º twists are included in the in-vessel transmission waveguides.

5.2.3 Experimental results

The reflectometer probes plasma densities from 0.3 to $1.5x10^{19}$ m^{-3}, almost the whole density range of the TJ-II plasmas heated by electron cyclotron waves (ECH). However, due to the shape of the ECH plasma density

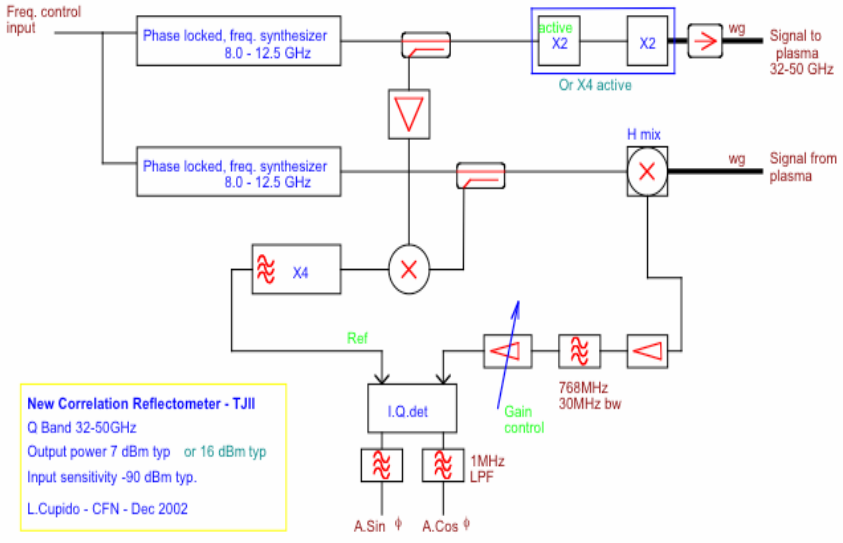

Figure 5.1 – Diagram of the fast hopping reflectometer installed in TJ-II

[1] TJ-II a stellarator of the Association EURATOM/CIEMAT
[2] Work carried out in collaboration with the TJ-II Team. Contact Person: J. Sanchez

profiles, they are flat (or even hollow) in the range $\rho < 0.6$, and due to the low radial gradient of the magnetic field, the radial range covered by the reflectometer is limited in most cases to $\rho \geq 0.6$.

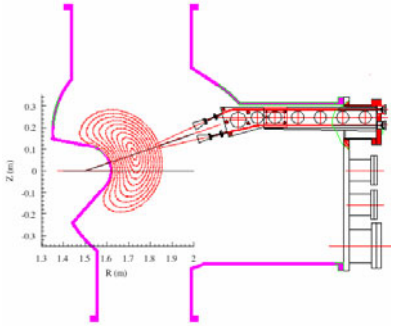

Figure 5.2 - Arrangement of the antennas and waveguides inside the vacuum vessel and magnetic surfaces of the standard magnetic configuration.

5.2.4. Plasma physics studies

It was previously found that above a critical plasma density, a perpendicular velocity shear layer develops spontaneously in the TJ-II plasma edge. Reflectometer measurements characterized the inversion in the perpendicular rotation velocity of the turbulence and its dependence on plasma conditions. Besides, reflectometry data indicate that a second velocity shear layer develops at inner radial locations and moves radially inwards when the plasma density increases beyond a critical value.

Numerical results obtained using a 2D full-wave code reproducing the experimental measurements (Figure 5.3) demonstrate the capability of the reflectometer to measure the velocity shear layer with a spatial resolution better than twice the probing wave-lengths in vacuum.

5.3 EDGE PLASMA PHYSICS[3]

5.3.1 Introduction

This research line included in 2004 studies on:

- Energy transfer between parallel flows and turbulence;
- Dynamical relation between parallel flows and instabilities;
- Transport and fluctuations during electrode biasing experiments,

5.3.2. Energy transfer between parallel flows and turbulence

Experiments in the TJ-II have shown radial variations in the cross correlation between parallel and radial velocity fluctuations (comparable to JET) near the LCFS. These gradients are due to the radial variations in the level of poloidal electric field fluctuations and in the cross-phase coherence.

The radial structure of $d < \tilde{v}_r \tilde{M}_{\parallel} > / dr$ changes with the increase of the plasma density; in particular, strong gradients in $d < \tilde{v}_r \tilde{M}_{\parallel} > / dr$ are developed at the radial location where perpendicular sheared flows and double gradient in the Mach number are developed above a critical density.

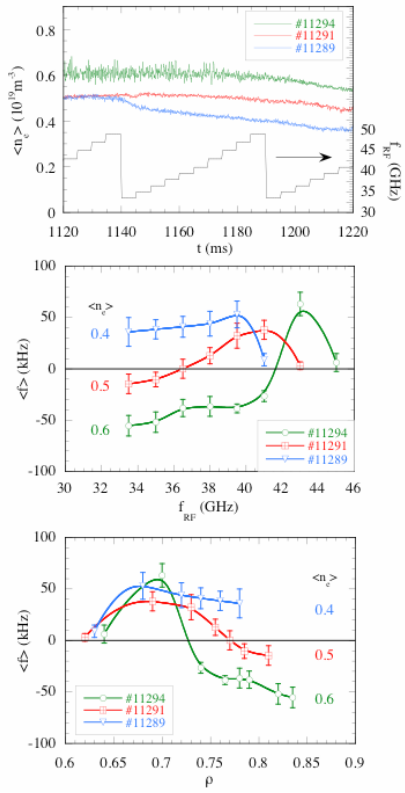

Figure 5.3 - (a) Time evolution of the line-averaged density for three discharges with densities below (open triangles), close (crossed squares) and above (open circles) the critical value ($<n_e> \approx 0.5\ 10^{19} m^{-3}$). The staircase variation of the reflectometer probing frequency is also shown. (b) Mean frequency of the complex amplitude spectra for the different probing frequencies in these three discharges and in a fourth discharge with higher line density ($<n_e> \approx 0.9\ 10^{19} m^{-3}$: full circles) and (c) the same data as a function of the cut-off radius.

From the gradient of the radial profile of the mean parallel flow and the radial-parallel component of Reynolds stress, the turbulence production (P) is given by:

$$P = \left\langle \tilde{v}_r \tilde{M}_{//} \right\rangle \partial M_{//} / \partial r \qquad (5.1)$$

This term combines the velocities cross-correlations $< \tilde{v}_r \tilde{M}_{||} >$ (momentum flux) with the mean velocity gradient ($\partial M_{||} / \partial r$) and gives a measure of the amount of energy per unit mass and unit time that is transferred between mean flow and fluctuations. As can be shown in Figure 5.4 two different signs are found in P, thus implying that the turbulence can act as an energy sink for the mean flow (viscosity) or energy source (pumping) near the shear layer. Figure 5.4 shows that the production term can be of the order of 500 s^{-1} in forward toroidal field. Experiments in TJ-II show production terms with the same order of magnitude as JET for high density plasmas. In low density plasmas the production term is reduced or inexistent.

[3] Work carried out in collaboration with the TJ-II Team. Contact Person: C. Hidalgo

The power per unit of mass necessary to pump the flow up to the velocity value experimentally measured in a turbulence characteristic time (τ_c) is given by: $W = E/\tau_c = M_{//}^2/2\tau_c$. Assuming τ_c in the range of a few turbulence correlation times it follows that W is of the order of 10^3 s^{-1}, which turns out to be comparable to the production term in this region (Figure 5.4). This result suggests that the mean flow generated by turbulent mechanisms is relevant.

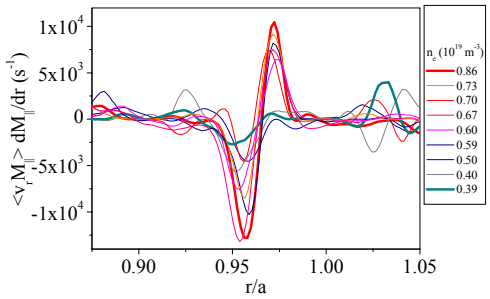

Figure 5.4 - Radial profile of production term in TJ-II

5.3.3. Dynamical relation between parallel flows and instabilities

Following studies previously performed taking advantage of the flexibility of the TJ-II configuration, the time evolution of parallel flows and edge instabilities (indicated by the H_α temporal variation) for configurations with reduced well in the edge have been studied (Figure 5.5). With the appearance of edge instabilities parallel flows are significantly modified, showing a coupling between edge transport and parallel flows. This result is consistent with recent experiments carried in the plasma boundary of JET tokamak.

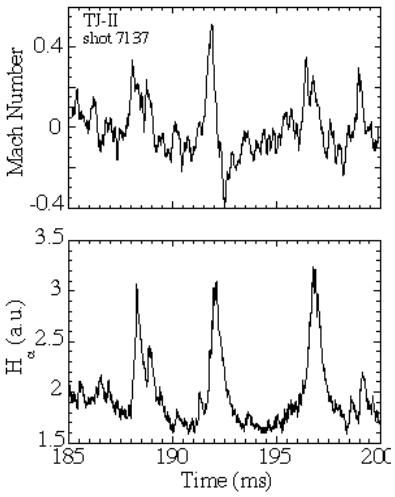

Figure 5.5 - Time evolution of parallel flows and edge instabilities in TJ-II

5.3.4. Transport and fluctuations during electrode biasing

A graphite electrode has been developed for biasing experiments on TJ-II and the first results have been obtained.

As biasing is applied, the biasing current amplitude increases rapidly for both polarities and the floating potential at the plasma edge is also modified in a rather short time scale (<50 μs) leading to a strong modification in the edge radial electric field in the region just inside the limiter. The plasma response is different at densities below and above the threshold value to trigger the spontaneous development of ExB sheared flows. At low densities, the edge plasma potential is fully controlled by external biasing. In this case, strong increase in plasma density and reduction in edge fluctuation level and H_α signals are observed during biasing (Figure 5.6). At higher densities edge plasma potential profiles are determined not only by external biasing but also by the electric fields spontaneous developed. Although an improvement in particle confinement is observed for both polarities, a larger increase is observed for negative electrode biasing.

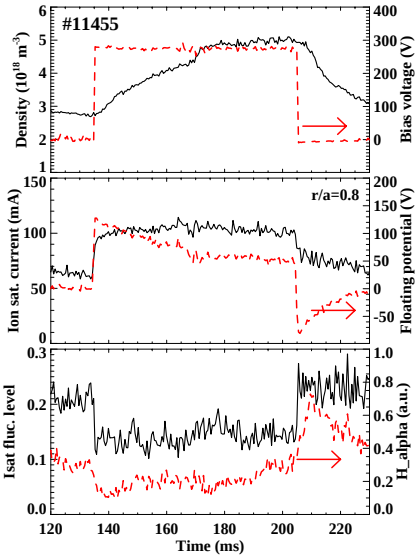

Figure 5.6 - Time evolution of the plasma density, biasing voltage, edge potential, ion saturation current, Isat level of fluctuations and H-alpha signal for a discharge with positive electrode bias.

5.4. HEAVY ION BEAM DIAGNOSTIC[4]

The work in this research line has been mainly focused on the improvement of the dedicated data acquisition system.

Calls for tenders for a new VME computer and a new trigger module have been made. The operating system has been converted from OS-9 to LINUX. The new VME computer has been tested. The operating software has been implemented and the VME drives have been compiled. Thirty-six transimpedance amplifiers have been commissioned and tested.

[4] Work carried out in collaboration with TJ-II and IPP-Kharkov Teams. Contact Person: C. Hidalgo

6. PARTICIPATION IN THE MAST PROGRAMME[1]

M.E. Manso (Head), L. Guimarãis, L. Meneses, A. Silva, F. Silva, P. Varela.

6.1. INTRODUCTION

The main objective of this project is the development and scientific exploitation of a microwave reflectometer for MAST[2], operating in O-mode FM-CW in three frequency bands (K, Ka and U), from 18 to 60 GHz.

During 2004, the VCO oscillator (Ka-band) has been replaced, resulting on a significant reduction of higher order harmonic levels. New static and dynamic calibration curves have been extracted and included in the data processing. The video amplifiers have been replaced improving the signal to noise level. The tuning circuit has been upgrade to fulfil the requirements of full band operation. The dedicated fast data acquisition system based on a VME board developed by CFN with capability to pre-program the samples has been brought to full operation. Several software tools for data analysis have been adapted. The scientific exploitation of the diagnostic has started.

6.2. EXPERIMENTAL RESULTS

6.2.1. Tests

The ASDEX-Upgrade ray-tracing code has been adapted to assess the power losses of the signals received by the MAST microwave antennas. Results (Figure 6.1) show that the diagnostic can accommodate a misalignment smaller than half the dimensions of the antenna mouth.

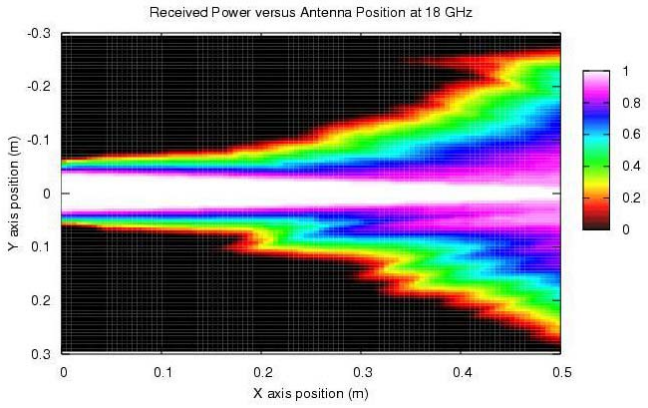

Figure 6.1 – Power received in the antenna (launching frequency 18 GHz) versus the position of the antenna mouth centre. Plasma edge is at 55cm.

6.2.2. Density profiles

Figure 6.2 displays a plasma density profile obtained with the Thomson scattering diagnostic in the plasma core (green) and with the reflectometry diagnostic at the plasma edge (red).

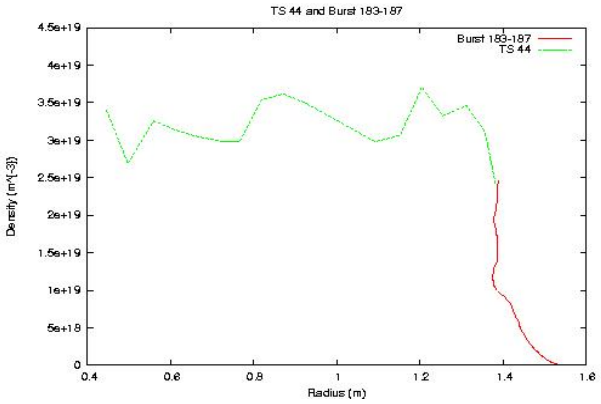

Figure 6.2 – Plasma density profile obtained from Thomson Scattering (green) plus Reflectometry (red).

The MAST reflectometry diagnostic can resolve fast plasma events such as ELMs. Figure 6.3 shows the abrupt outward movements of the probed layer coinciding with the spikes of the D_α signal (in green) at the ELM occurrence, indicating a sudden flattening of the edge density profile.

Additional information is obtained from the time evolution of the spectra of the signal reflected from a probed layer with $n_e = 0.6\times10^{19}$ m^{-3} (Figure 6.4). At each ELM, a broadening of the spectra is observed due to the increase of plasma turbulence at the plasma edge. In the second ELM, the group delay of the probing microwaves (indicating the distance from the antenna to the reflecting layer) increases shortly after the onset of the ELM and the decrease (from 0.224 to 0.2248 s) indicating a recovery phase in agreement with the decrease of the D_α signal.

[1] Work carried out in collaboration with the Association EURATOM/UKAEA. Contact Person: Geoffrey Cunningham.

[2] MAST is a tokamak of the Association EURATOM/UKAEA.

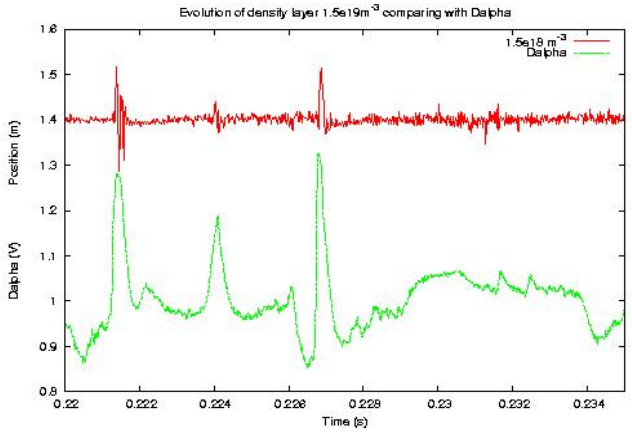

Figure 6.3 - Temporal evolution of a density layer of $1.5x10^{19}$ m^{-3} (in red) compared to the Dalpha signal of the plasma (in green).

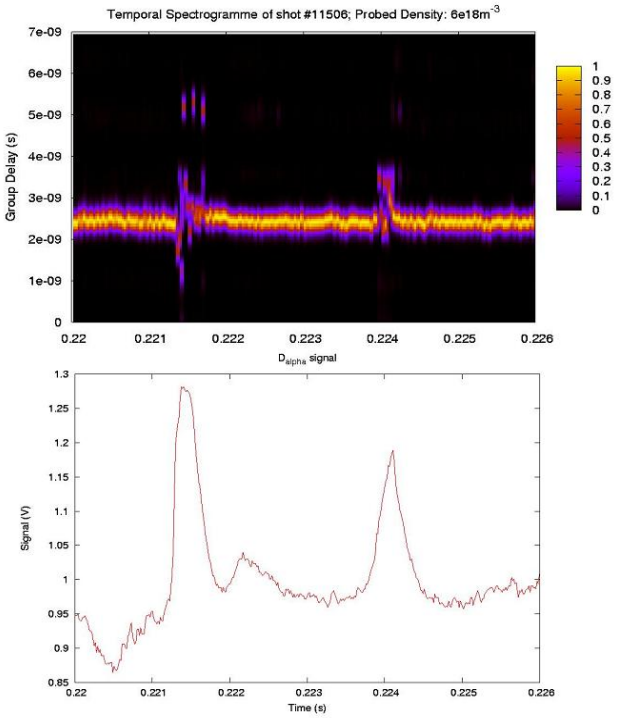

Figure 6.4 – Time evolution of spectra of the signal reflected from density layer $n_e = 0.6e^{19}m^{-3}$.

7. PARTICIPATION IN THE TCV PROGRAMME[1]

C. Varandas (Head), P. Amorim, T.I. Madeira, L.A. Pereira, A.P. Rodrigues.

7.1. INTRODUCTION

The Portuguese participation in the TCV[2] programme has included the development, operation and scientific exploitation of:

- Three X-ray diagnostics: two pulse height analysis (PHA) diagnostics for implementation on an horizontal and a vertical TCV port and a rotating crystal spectrometer;
- An advanced plasma control system (APCS).

7.2. X-RAY DIAGNOSTICS

7.2.1. Horizontal PHA diagnostic

The routine operation of this diagnostic (Figure 7.1), based on a Germanium detector and on a CFN interface amplifier timing generator, has been assured by Portuguese staff.

Software tools for data analysis have been improved, mainly related with the calculation and interpretation of spectra with permanent non-Maxwellian behaviour. Two modified Maxwellian distribution functions were independently tested, accounting for respectively magnetic trapping and anisotropy. The results permit to conclude that, for most of the analysed spectra, only the anisotropy function accounts the observed effects.

Plasma physics studies related with the influence of auxiliary heating on the plasma electron distribution function have been carried out. Results obtained with a bi-Maxwellian function (Figure 7.2) have started to be compared with those provided by other diagnostics.

7.2.2. Vertical PHA diagnostic

7.2.2.1. Introduction

This diagnostic was conceived aiming at providing very high throughput by using a new type of detector and real-time electron temperature and impurity content measurements that might be also used for feedback control by using a CFN multi-DSP-based VME module.

The compact design of the diagnostic has allowed its implementation along a vertical line of sight, in a narrow space between port 14b and a TCV coil. This diagnostic is equipped with a set of DuraBe windows and a variable aperture (Figure 7.3), each one arranged on separate disks actuated by two independent step motors, which are presently remotely controlled by a CRPP master/slave unit.

In 2004, the diagnostic was dismounted from TCV for inspection and repair of some malfunctions, alignment of the detector, replacement of viton rings, calibration of the filters and aperture positions and repair of one motor.

Figure 7.1 – View of the horizontal PHA diagnostic on TCV

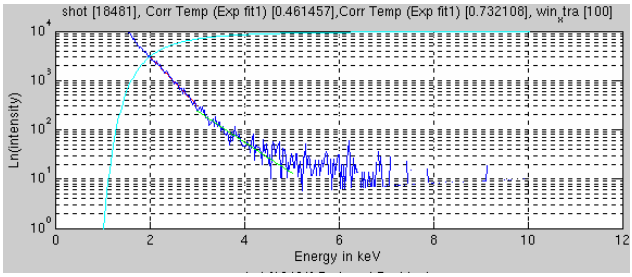

Figure 7.2 - Bi-Maxwellian fit to a spectrum exhibiting a tail

The variable aperture has been redesigned in order to have the correct curvature and gradient. The interface master/slave that actuates the motors has been redesigned aiming at avoiding saturation. A commercial CAMAC data acquisition board (XIA) has been tested, proving not to be stable for X-ray sources of variable flux. A commercial multi-channel analyser board (MCA3-FastComTec) has been installed. Two input channels of this module have been activated to survey the signal coming from the detector pre-amplifier and detection and suppression of the noise sources. The diagnostic has been re-implemented on TCV. The hardware and software for

[1] Work carried out in collaboration with the TCV Team. Contact Person: Basil Duval.

[2] TCV is a tokamak of the Association EURATOM/Suisse Confederation

the calculation of the electron temperature using the CFN real-time multi-DSP-based VME module have been developed, tested and improved.

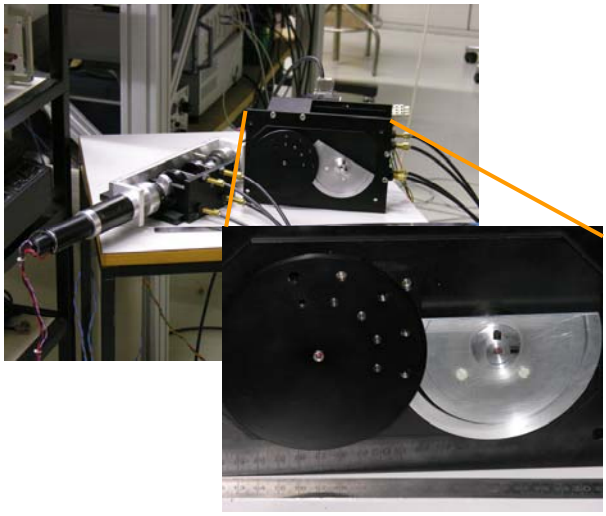

Figure 7.3 - Detail of the filters and aperture holders of the vertical PHA

7.2.2.2. Real-time diagnostic

The real-time diagnostic is being implemented through parallel processing of the acquired data by several digital signal processing algorithms, distributed by the DSPs of the above mentioned CFN module, which construct a sequence of histograms corresponding to the X-ray spectra during a TCV discharge. Each histogram is obtained using the following algorithms: moving average, triangular or trapezoidal filter and custom algorithms that detect the amplitude of the signals and eliminate those that correspond to pile-up. Adequate processing of these histograms, using a custom algorithm to find the linear zone of the histogram data and a linear regression fitting algorithm, allows not only to compute the temperature of the plasma electrons during the discharge, but also to detect and identify the impurities in the central plasma region. An appropriate real-time feedback control algorithm permits to actuate on the gyrotrons of the electron cyclotron heating system in order to avoid disruptions in the plasma due to either excess or missing of the injected power.

7.2.3. Rotating crystal spectrometer

This diagnostic, based on a twenty years old apparatus loaned by the Plasma Physics Princeton Laboratory, has been envisaged to record the soft-X-ray line radiation from highly charged ions of low to medium Z elements from the hot core of the TCV plasma, along a horizontal line of observation.

During the last trimester of 2004, the calls for tenders for the micro-channel plates and crystals have been made. The electronic devices of the diagnostic have been tested. The programmes for the step motor have been revised and improved. The signals that will be provided by TCV system to the diagnostic and from the diagnostic to the TCV data acquisition system have been identified and characterized.

7.3. ADVANCED PLASMA CONTROL SYSTEM

This new digital system for the control of the TCV plasma (Figure 7.4) is based on the CFN real-time multi-DSP-based VME (RTPROV) module.

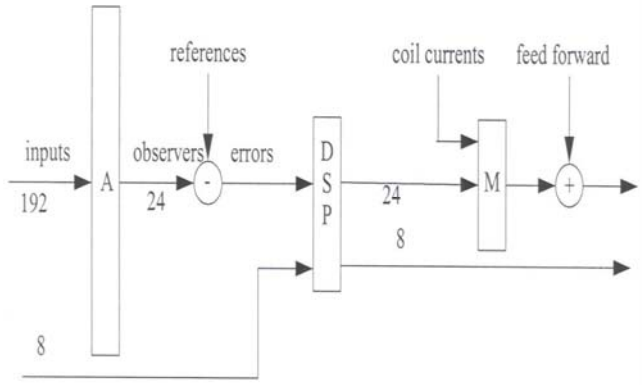

Figure 7.4 – APCS functional diagram

In 2004, the commissioning and testing of twelve RTPROV modules were finalized. The tests of the simultaneous operation of these modules in a VME crate (Figure 7.5) have been initiated. The development and testing of t he data mover bus (DMBUS) have been finalized. The DMBUS and XIO VME modules have been commissioned ad tested. Software for MACH programming and DMBUS management has been developed and tested. The APCS operation system has been developed and tested. Software for the APCS integration in the TCV control and data acquisition system is under development.

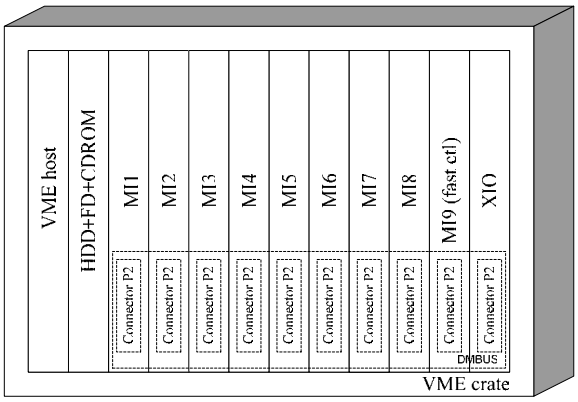

Figure 7.5 – Overview of the APCS hardware

8. PARTICIPATION IN THE ITER PROJECT

M.Manso (Head), L. Cupido, L. Meneses, J. Santos, A. Silva, P. Varela.

8.1. INTRODUCTION

The Portuguese participation in the ITER project included in 2004 activities on microwave diagnostics related with the design analysis of the position reflectometer, development of an advanced FM-CW coherent reflectometer and demonstration experimental studies on ASDEX-Upgrade of plasma position/shape measurements in ITER relevant scenarios.

Concerning the *design analysis of the position reflectometer*, the Association EURATOM/IST has led a Physics Integration Task of the Fusion Technology Programme (TW3-TPDSUP). CATIA models have been developed for the draft design of the waveguide routing of gaps 3, 4 and 5 (Figure 8.1). First simulation studies of the performance of the waveguide routing using HFSS have been performed. The assessment of the possibility to locate the electronics in the port cells has been initiated.

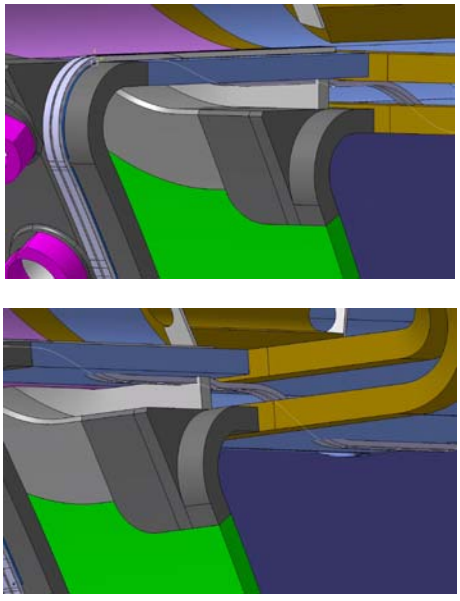

Figure 8.1 –3D Catia models of waveguide routing (gap 4) for the ITER position reflectometer

Regarding the *development of a prototype of a coherent reflectometer*, the basic concept has been developed. The design of the sources and subsequent determination of the operation frequency bands have been finalized. The design of the sweep and digital control has been initiated as well as the study of an integrated FPGA based approach for linear control and frequency synthesis.

Concerning *plasma position/shape measurements*, automatic density have been obtained in ASDEX Upgrade in ITER relevant scenarios, namely in ELMy H modes, demonstrating clearly the possibility to use reflectometry for plasma position/shape measurements in ITER.

8.2. COHERENT REFLECTOMETER

This diagnostic (Figure 8.2.) will be capable of performing both profile and turbulence measurements at very high plasma densities. The use of synthesized sources along with frequency conversions leading to a full coherent system allows both fast sweeps and fixed frequency operation with low phase noise signals. The system is capable of withstanding the long distances from diagnostics to the vessel while using a locally generated reference.

8.3 PLASMA POSITION/SHAPE MEASUREMENTS IN ITER RELEVANT SCENARIOS

ASDEX Upgrade standard ELMy H-mode scenario provides an abundant source of repetitive type I ELMy discharges on which position measurements can be performed. Figure 8.3 shows the positions of densities corresponding to several possible n_{sep}/n_{e_med} ratios after removal of measurements obtained during ELM onset and MHD phases where microwave signals are scattered and cannot be used for data analysis.

The proximity of time traces of position of different tracked layers indicates the location of the ETB (in the steep region of the profile, different density layers are very close in radial distance). Consistently, in both HFS and LFS, after the L-H transition ($t \approx 1.85$ s) and during the initial density ramp up, curves corresponding to a ratio n_{sep}/n_{e_med} of 30% and 40% are closer. Afterwards, the density drops with the increase of ELM frequency but the ratios of curves at the steep region rise to 40-50%. The injection of more 2 MW of neutral heating and a strong fueling gas puff leads to a higher density steady state phase, with higher frequency higher density ELMs (f_{ELM}>200 Hz after t≈5 s). Again, the proximity of the curves suggests a rise of densities at the ETB, corresponding to 50-60% n_{sep}/n_{e_med} values. During this phase, rapid ELM recovery results in oscillations of the positions in the steep gradient region of less than 0.5 cm when compared to the magnetic separatrix changes (black curve).

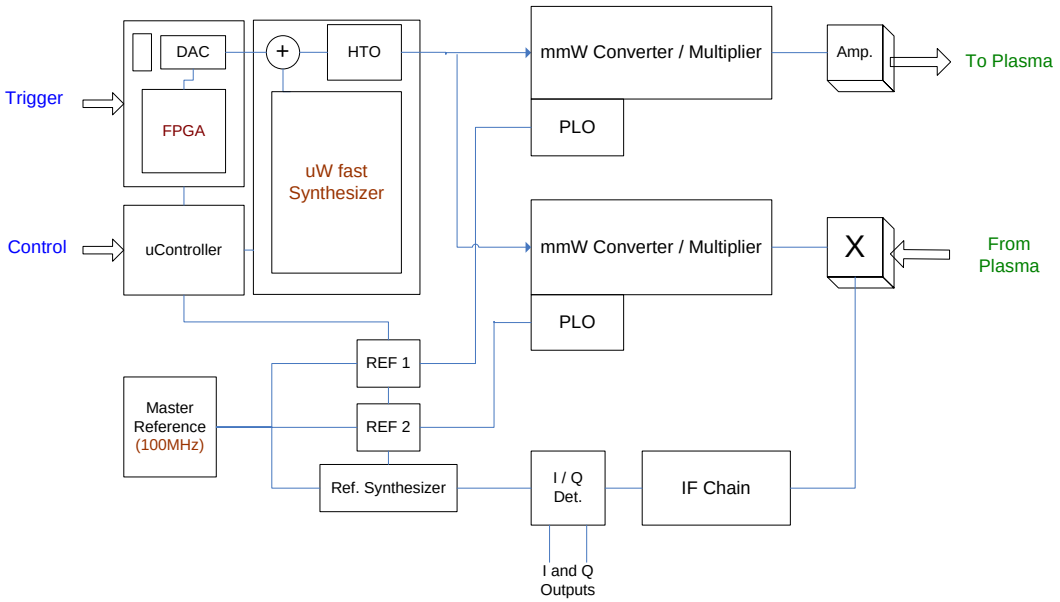

Figure 8.2 – Reflectometer using coherent signal generation and IQ detection

For the profiles that correspond to t=2.66 and 3.76 s, the pedestal is still within the measuring range. For t=6.02 s the edge profile changes considerably, exhibiting higher densities up to the density barrier foot, typical of a gas puffed, non-detached H-mode plasma. In this phase, similar to the foreseen ITER higher density regimes, the pedestal is no longer within the measuring range of the reflectometer. The increase of the density at the barrier foot is consistent with the observed increase of the ratio values of the closest curves. In these circumstances, an alternative n_{sep}/n_c scaling (where n_c is the pedestal density) cannot be used to estimate the density at the separatrix without the upgrading of the ASDEX Upgrade reflectometer to probe higher densities.

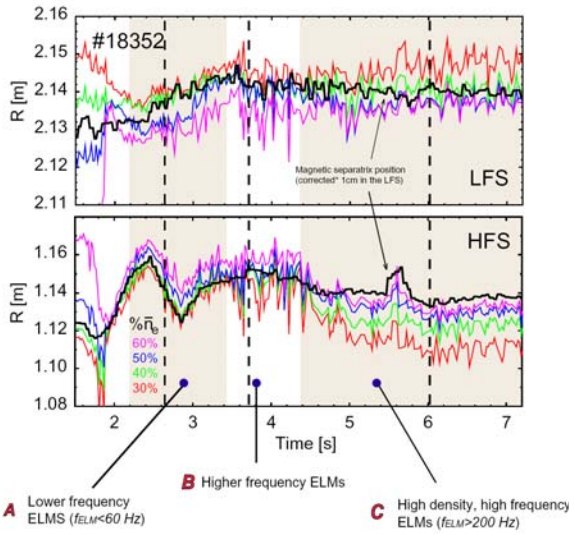

Figure 8.3 - Temporal evolution of edge plasma layers with plasma densities according to the time trace of the magnetic separatrix position.

9. OTHER THEORY AND MODELLING STUDIES

F. Serra and J.P. Bizarro (Heads), J. Belo, D. Borba, R.Coelho J. Ferreira, F. Nave, P. Rodrigues.

9.1. INTRODUCTION

This project included in 2004 three research lines:

- Study of the role of magnetic reconnection processes in the dynamics and confinement of thermonuclear plasmas;
- Studies on lower-hybrid current drive;
- Modelling of Grad-Shafranov equilibrium in tokamak plasmas.

Concerning *the role of magnetic reconnection (ideal and resistive) processes in the dynamics and confinement of thermonuclear plasmas*[1], studies of the poloidal $\vec{E}\times\vec{B}$ velocity, mode coupling effects on plasma braking and NTM triggering and parity and topology of tearing mode perturbations have been carried out.

Regarding the *studies on non-inductive current drive*, a method to measure the scattering matrices of lower-hybrid multi-junctions has been developed. Progress has been made on the study of the spectral-gap problem for lower-hybrid current drive. IST/CFN staff has participated in the design of the ITER-like PAM launcher for lower hybrid current drive[2].

Concerning the *modeling of the Grad-Shafranov equilibrium in tokamak plasmas*, a perturbative GS equilibrium solver, able to deal with realistic pressure and current-density profiles, was adapted to handle the existence of a poloidal-field reversal layer, for which the tangential magnetic field and the enclosed toroidal current do vanish.

9.2. ROLE OF MAGNETIC RECONNECTION PROCESSES IN THE DYNAMICS AND CONFINEMENT OF THERMONUCLEAR PLASMAS

9.2.1. Introduction

The following main studies were performed in 2004:

- Poloidal $\vec{E}\times\vec{B}$ velocity (V_θ^{ExB}) studies;
- Mode coupling effects on plasma braking and NTM triggering;
- Parity and topology of tearing mode perturbations.

9.2.2. Poloidal $\vec{E}\times\vec{B}$ velocity (V_θ^{ExB}) studies

A further investigation on the effect of forced magnetic field line reconnection on plasma poloidal $\vec{E}\times\vec{B}$ velocity (V_{ExB}^{θ}) was conducted. The localised toroidal braking torque, driven by static external magnetic fields, that develops at the resonant q-surface inside the plasma for both the viscous-resistive and ideal-viscous regimes, is shown to be given by the generic form

$$T_\phi \propto \frac{(\delta\Omega\tau_{rec})^{\lambda}}{\beta^2+(\delta\Omega\tau_{rec})^{\nu}} \qquad (9.1)$$

where the constant $\beta>1$, the parameters $\lambda=(1,1/4)$ and $\nu=(2,0)$, $\delta\Omega$ is the local plasma toroidal angular rotation variation and τ_{rec} is the characteristic reconnection time inside the viscous-resistive layer. It is shown that over the viscous time scale, although the localised torque spreads over a similar region both in the viscous-resistive and ideal-viscous regimes, the induced velocity gradient around the resonant surface (favourable to ITB onset) are smeared out. Thus, while differential rotation (shielding the external fields) is the most relevant mechanism preventing ITB formation in the viscous-resistive regime, plasma viscosity limits the maximum obtainable velocity shear in the ideal-viscous regime. It appears less likely that ITB onset in the vicinity of rational q=m/n surfaces may be connected to forced reconnection at such surfaces.

9.2.3. Mode coupling effects on plasma braking and NTM triggering

Magnetic field line reconnection events are potentially hazardous since they may deteriorate the plasma energy confinement and performance. In particular, the onset and growth of neoclassical tearing modes (NTMs), a resistive instability driven by the loss of the bootstrap current fraction within the island chain associated to this instability, is known to limit the maximum achievable plasma beta and prevent safe access to relevant advanced regimes of tokamak operation. Another event that strongly affects confinement, potentially leading to plasma disruptions, is the penetration and amplification of locked modes induced by the intrinsic "error-field" of the machine. Both types of magnetic perturbations are a major concern for a reliable operation of next stage tokamaks such as ITER and for future tokamak fusion reactors.

Mode coupling, through driven reconnection, can drive the NTM island width up to the bifurcation threshold even when there is differential rotation. In such a scenario, the mode frequency evolution is complex and as soon as the island width overcomes the bifurcation threshold, the mode decouples from the coupling drive and acquires its natural rotation frequency (Figure 9.1). Focusing on the role played by mode coupling on the global, self-similar, plasma rotation braking that favours the amplification of locked modes induced by the intrinsic tokamak error-field, it was enlightened that, although toroidal and non-linear mode coupling contribute to a non

[1] Work carried out in collaboration of CNR-Milano, of the Association EURATOM/ENEA. Contact Person: E. Lazzaro.
[2] Work performed in collaboration with the Association EURATOM/CEA.

localised braking of the toroidal rotation around the resonant surfaces inside the plasma (Figure 9.2), coupling to plasma elongation appears to be essential to explain the experimental observations.

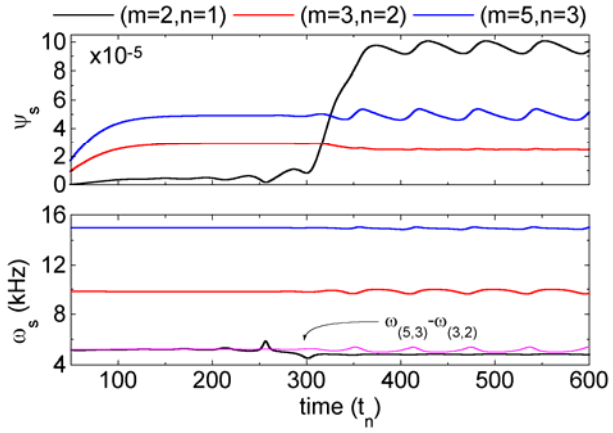

Figure 9.1 - Metastable m=2,n=1 mode triggering and destabilization by nonlinear three wave resonance mode coupling to (3,2) and (5,3) modes.

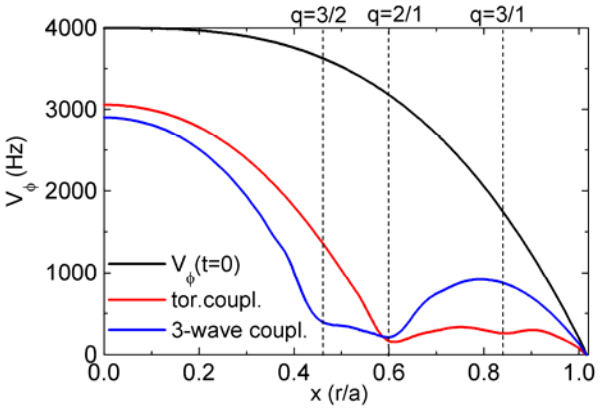

Figure 9.2 - Reduced MHD numerical calculations evidencing the additional plasma braking due to three wave (with driving (2,1) and (3,2) modes) and toroidal coupling (with the (3,1) mode) with a dominant m=2,n=1 error field driving component.

9.2.4. Parity and topology of tearing mode perturbations

The dominantly sheared toroidal plasma rotation (affecting the $\vec{E}\times\vec{B}$ velocity) that is imparted by neutral beam injection can benefit plasma confinement, reducing the scale length of turbulence, shielding plasma reconnection driven by the error-field and stabilising resistive wall modes. Resistive modes, such as the tearing mode, may nonetheless be unstable, deteriorate plasma confinement and eventually lead to disruptions. The effect of toroidal rotation on the reconnection rates and tearing eigenfunctions, as well as on the topology of the rotation and flux contours associated to tearing modes, in a small/medium aspect ratio low-β cylindrical tokamak was addressed.

A single helicity symmetric cylindrical model, valid for all aspect ratios but with imposed incompressible plasma motion was adopted and the reconnection rate dependence on the aspect ratio and on the sheared toroidal rotation was firstly investigated. The magnetic and velocity perturbations parallel to the helical versor at small aspect ratio, are shown to destabilise ideal modes, rendering the growth rate of the fastest m=1,2 growing modes independent of the Reynolds numbers (Figure 9.3).

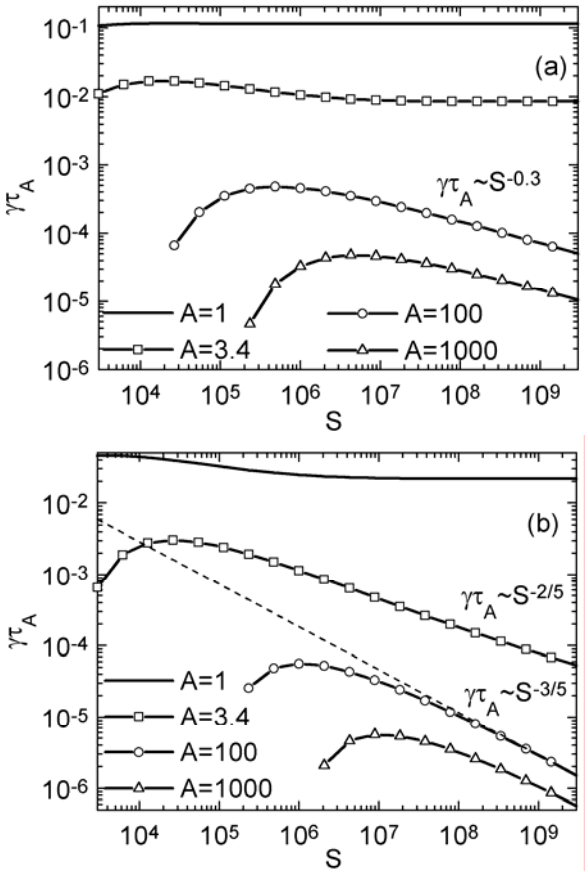

Figure 9.3 - Growth rate scaling of m=1 (a) and m=2 (b) tearing instabilities with the magnetic Reynolds number for several values of the aspect ratio A.

Plasma angular rotation is also shown to have a strong influence on the stability of tearing modes, dependent on the Prandtl number (ratio of the resistive to viscous diffusion times). For low viscosity scenarios (Prandtl <<1), toroidal rotation profiles with decreasing velocity with plasma radius are found to destabilise the mode, doubling the growth rate when rotation is of the order of 20kHz at the magnetic axis. On the other hand, for Prandtl>>1 (typically of the order 10), plasma rotate with the same type of radial profile but with 13 kHz at the magnetic axis is sufficient to stabilise the mode. Sheared plasma rotation and viscosity were also found to have a profound effect on the topology of the ohmic unstable

magnetic island. In fact, for high Prandtl numbers, the island appears deformed as soon as it forms, becoming symmetric only when reaching a steady state. For low viscous plasma the deformation is much smaller.

9.3. STUDIES ON LOWER-HYBRID CURRENT DRIVE

9.3.1. A method to measure the scattering matrices of lower-hybrid multijunctions

Aiming at routinely and reliably testing the S-matrices of the multijunctions that build up lower-hybrid (LH) antennas, a general method for measuring the S-matrices of microwave (mW) devices with any number of ports has been developed using basic network analysis. The broader approach used in this work may prove eventually useful to anyone interested in measuring S-matrices of arbitrary mW components. In fact, such method has been proposed, and is going to be adopted, to test the multijunctions that will build up the ITER-like PAM launcher to be eventually installed on JET.

9.3.2. Progress on the spectral-gap problem for lower-hybrid current drive

One of the possible solutions for the so called spectral-gap problem on the LH current drive could be the effects of the magnetic ripple on the LH wave propagation in plasmas. To correctly assess the extent of these effects in real tokamaks, a fully consistent 3D toroidal equilibrium with magnetic ripple has to be assessed, which can only be done via a numerical solution. A parallel 3D equilibrium code has been developed using a new approach based on a generalized non-conservative variational principle, assuming nested flux surfaces and compatible with fixed or constrained almost-free plasma boundary.

9.3.3. Design of an ITER-like PAM launcher for lower-hybrid current drive

Two main actions were carried out in the framework of the collaboration with CEA-Cadarache on heating and current drive: the studies of a PAM (Passive Active Multijunction) ITER-like LHCD launcher for Tore Supra and the initial studies of a similar launcher for JET.

On the subject of the launcher for Tore Supra the following work was carried out: study of the impact that a vacuum gap inserted between the antenna mouth and the plasma has on the directivity and the coupling properties of the PAM as a function of both the vacuum gap width and the plasma density (above the plasma cut-off density); determination of the effect that the use of passive waveguides with depths different from the original design ($\lambda/4$) have on the directivity and coupling properties of the PAM and, in particular, when combinations of passive guides with distinct depths is used; the phase shifters were appropriately compensated for to take into account the toroidal as well as poloidal shape of the mouth, the RF properties of the first TE_{10}-TE_{30} mode converter prototype were experimentally determined by a team at CEA-Cadarache and the mode converter (as well as the structure used in the corresponding experimental set-up) was then modelled in order to compute the theoretical RF properties and compare them to the measurements; further developments and improvements were introduced to the three new codes (started during the previous year) that are meant to study the stability of the system made up of the PAM + mode-converter.

The preliminary studies of a PAM-type antenna for JET were also started in response to a call from the EFDA Associate Leader for JET relating to the upgrade activities of its LHCD system (a project for which CEA-Cadarache contributes as the Leader Association). This work focused primarily on the coupling and directivity properties of two launcher designsand a variety of studies were carried out. As a conclusion of this work the bijunction was proposed for the design of the PAM type antenna.

9.4. MODELLING OF THE GRAD-SHAFRANOV EQUILIBRIA WITH NEGATIVE CORE TOROIDAL CURRENT IN TOKAMAK PLAMAS

The possibility of reversed Grad-Shafranov (GS) equilibria, with negative toroidal current density flowing in the core and overall positive plasma current, attracted considerable discussion in the fusion community, mainly in connection with improved confinement regimes displaying strongly reversed magnetic shear. Although some of their properties have already been established for a few particular choices of pressure and current-density profiles, a suitable framework was lacking which could provide physical insight into the problem, as well as numerical solutions for more general input profiles. To this end, a perturbative GS equilibrium solver, able to deal with realistic pressure and current-density profiles, was adapted to handle the existence of a poloidal-field reversal (PFR) layer, for which the tangential magnetic field and the enclosed toroidal current do vanish.

It has been explained why reversed equilibria with nested topology are isolated and hardly realizable, as opposed to more structurally stable non-nested solutions (Figure 9.4).

In addition, the island system that unfolds, with its separatrix, in these reversed equilibria is suitably shaped by tailoring the pressure and poloidal-field input profiles (Figure 9.5), a task which is greatly simplified by the ability of the adapted GS solver to handle general input profiles.

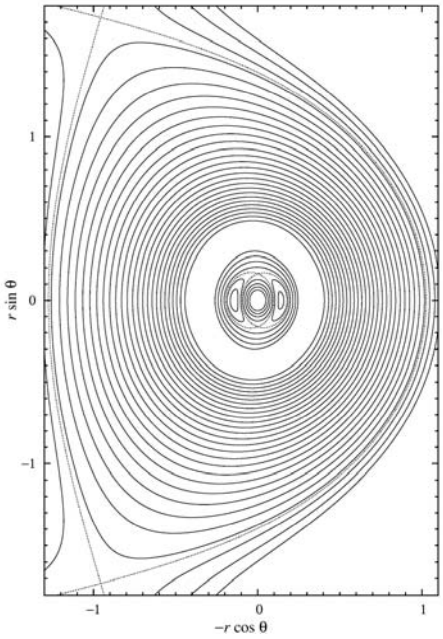

Figure 9.4 - Flux surfaces for typical JET parameters and pressure profile $p(r)=p_0(1-\alpha r)\exp(-\gamma r)$ with $\alpha=9.5$ and $\gamma=10$.

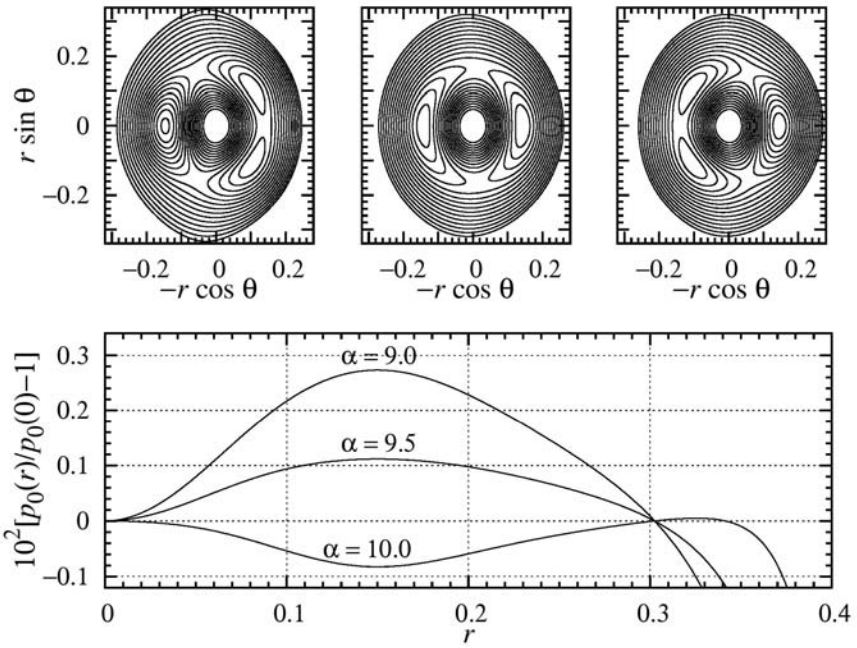

Figure 9.5 - Flux surfaces at the core zone for three different pressure profiles with $\alpha=9.0$, 9

10. OTHER ACTIVITIES ON CONTROL DATA ACQUISITION AND SIGNAL PROCESSING

J. Sousa and C. Varandas (Heads), A. Batista, A. Combo, C. Correia, M. Correia, N. Cruz, R. Pereira, P. Ricardo.

10.1. INTRODUCTION

This project included in 2004 two main research lines:

- Development of a low-cost, fully integrated, event-driven real-time control and data acquisition system for fusion experiments;
- Development of clusters of computers.
  This year adequate embedded development tools for the PowerPC processor have been assessed. A preliminary hardware control core of the system, implemented as a System on Chip (SoC), has been designed. Adequate software tools for programming a reconfigurable real-time processing system have been assessed and tested. A reconfigurable hardware PCI module has been developed. A water-cooled 16 computer cluster has been developed, tested and used for heavy parallel calculus.

10.2. Embedded development tools for Power PC

The performance and cost of the following embedded real-time operating system for PowerPC and cross-compiling tools have been evaluated: WindRiver VxWorks, MontaVista LinuxPPC and LinuxPPC with RTAI extensions. Results allow to conclude that the LinuxPPC with RTAI is the best choice since it has adequate real-time capabilities at a much lower cost. The Xilinx Platform Studio cross-compiling tools are appropriate due to the use of programmable logic devices from this manufacturer for SoC implementation. These tools have been tested to readily compile a version of the Linux kernel that has been specially developed for the target hardware platform.

10.3. Hardware control core of SoC

A basic hardware control core of the system on chip (SoC) has been designed, using the Xilinx Platform Studio (Figure 10.1). A version with only one processor has been successfully tested and implemented on a ML310 board which includes a Xilinx Virtex-II Pro FPGA.

10.4. Software tools for programming a reconfigurable real-time processing system

The reconfiguration of a SoC-based control and data acquisition system can be made at two levels: the processor and the programmable logic. While the former is readily programmable using a computer language compiler, the latter until now was lacking high level programming tools. Nevertheless there are at least two suitable tools for this task: the Mathworks Matlab (with the Xilinx System Generator or AccelChip) and the Mentor Graphics Catapult C Synthesis. This group of tools covers three different, complementary approaches for reconfiguring the programmable logic: integer and floating-point programming in Matlab and high-level language (C) programming.

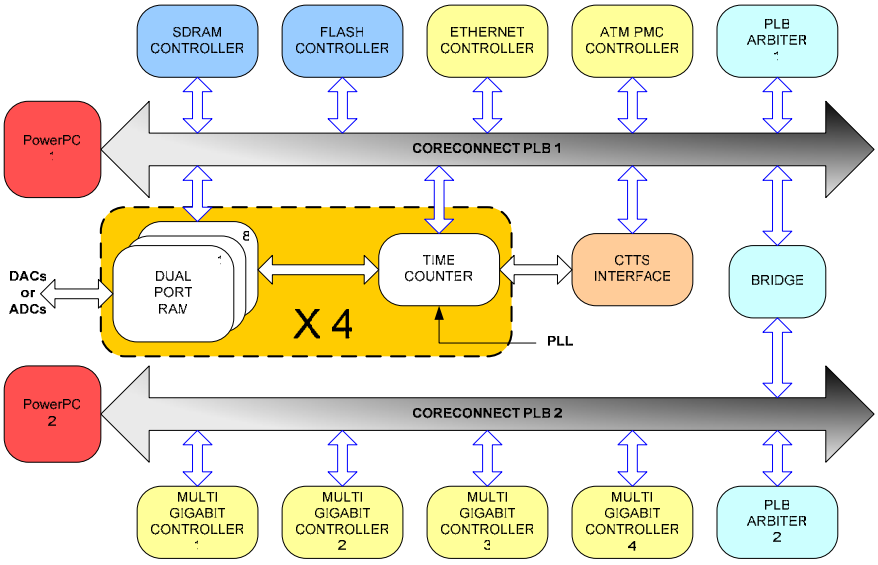

Figure 10.1 - Hardware control core of the SoC system

10.5. Reconfigurable hardware PCI module

A general-purpose multi-channel PCI module for applications on control and data acquisition has been developed. This module includes a reconfigurable DSP/FPGA combination providing up to 8000 MIPS DSP and 3 Million logic gates and can be coupled through a standard connector to new expansion boards.

For new projects the designer will target the application, by designing a specific expansion board and reconfiguring the FPGA equations and/or the DSP code.

The first application was an expansion board (Figure 10.2) with 8 channels, 2 MSPS, 16-bit waveform generator for use on the test-bench platform for the real-time project of JET. A control board with 12 ADC channels with 12-bit@50 MHz and 2 DAC channels as well as a timing generator and event router module is being developed.Generic DSP control software including a library of basic functions and a library of FPGA equations has been developed to facilitate the design of codes for the specific operation of new expansion modules and applied on the development of the waveform generator module.

10.6. Development of clusters of computers

CFN is developing clusters of standard computers (Orionte) (Figure 10.3), with the following main design requirements: (i) reduced cost; (ii) reduced space; (iii) reduced noise; (iv) high ratio between performance and cost; and (v) adequate parallel programming skills for plasma physics.

Orionte has been implemented in two editions with 8 and 16 processors, using exclusively commodity hardware (Table 10.1). In order to get the minimum cost and space, Orionte is made by modules of eight nodes. Each node is put together with one set of components except the switch, which serves up to three modules (Figure 10.4).

Employing water cooling copper blocks, manufactured at IST, it was possible to put eight nodes is one 6U rack. T 1GBit/s ethernet was chosen in order to satisfy network demanding parallel programs. Each module (8 boards) is equipped with one harddrive (120 Gb for Orionte 16), for 7 nodes boot remotely with DHCP and TFTP and mount the master's harddrive through NFS.

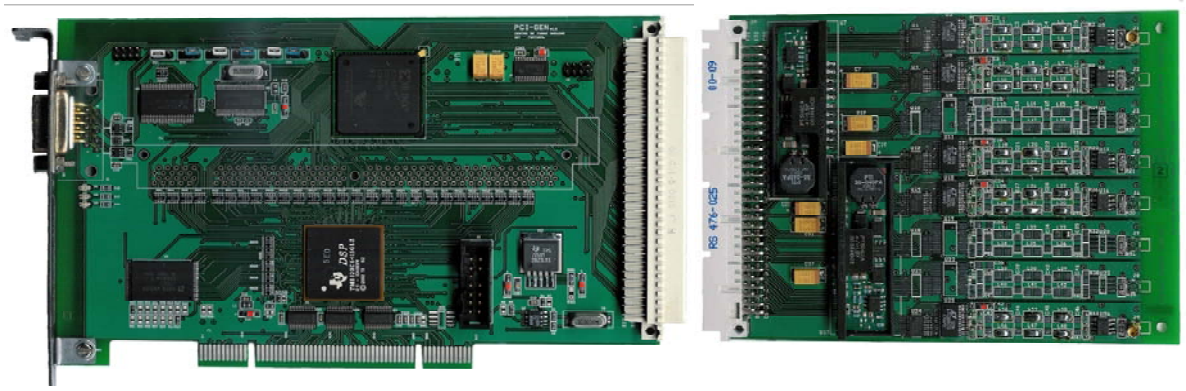

Figure 10.2 - Configurable hardware PCI module with a waveform generator expansion module.

	Orionte 8	Orionte 16
Processor	P4 2,4GHz FSB 533MHz	P4 3 GHz FSB 800MHz
Memory	1GByte (2 x 512Mb)	1GByte (2 x 512Mb)
Network interface	1Gb (onboard)	1Gb (onboard)
Motherboard	Intel D845GERG2	Intel D865GLC
Hard drive	80Gb	2 x 120 Gb
Switch	Ovislink 1Git 8 ports	USRobotics 1Gbit 24 ports

Table 10.1 – Components of Orionte 8 and 16

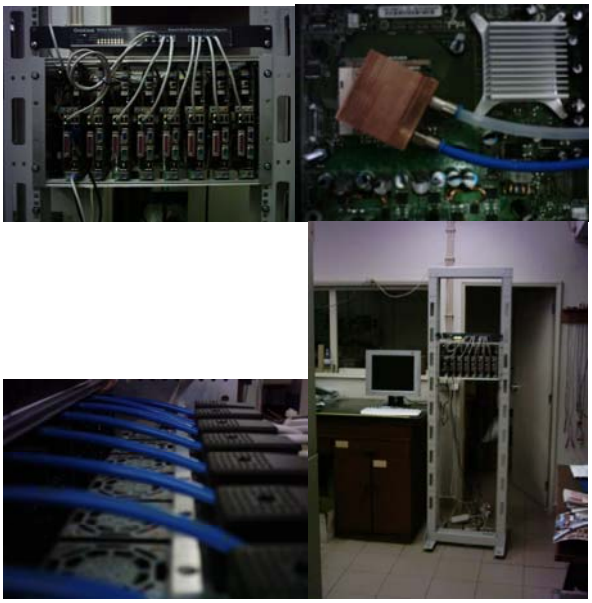

Figure 10.3 - Photographs of the Orionte cluster

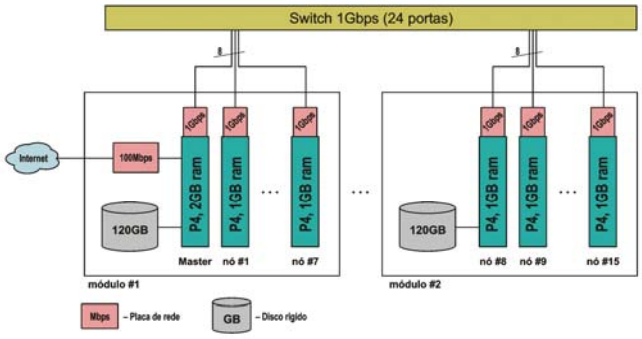

Figure 10.4 – Orionte eight board module diagram

Orionte is a"Beowulf" 2nd generation cluster, running linux Gentoo, with 2.4.28 kernel. Linux offers all the necessary tools for remote booting and simple cluster administration: DHCPD, TFTPD, SSHD, etc. The kernel is patched with OpenMosix, providing single-system-image (automatic migration of processes). An open source batch queue system (Sun Grid Engine) was also installed.

Orionte has many of the most used tools in computational physics (such as state-of-the art compilers for C, C++, Fortran and Java), high performance numeric libraries (like FFTW, Lapack-Atlas), tools and libraries for parallel programming (such as MPICH 1/ 2 or LAM/MPI), visualization tools and libraries (like OpenDX) and high-level technical computing language and interactive development environments (such as Matlab or IDL).

Orionte has been used to develop, test and run parallel applications in C,C++, Fortran and Matab using the MPI paradigm, as well as to run intensive traditional (many-runs) serial codes, graphical applications for physical visualization, computational signal processing and remote data processing and visualization. Several parallel codes have been developed and/or used by CFN Researchers, such as: AXISYMME (for magnetic-equilibria reconstruction in axisymmetric, large-aspect-ratio toroidal plasmas, taking as input the plasma-pressure and the reduced poloidal-magnetic-field profiles), CHOI (for parallel calculation and ready visualization of the Choi–Williams distribution for non-stationary fusion plasma signals processing), CRUNCH (a simplified filament current fitting code to evaluate current profile in ISTTOK tokamak from Mirnov probes), ESBEAM (based on a multidimensional paraxial Wentzel-Kramers-Brillouin approach to yield the distribution of wave potential for electrostatic lower-hybrid wave propagation in tokamak plasmas under current-drive conditions), GEM3 (a three-dimensional electromagnetic gyrofluid code to study turbulence in the boundary region of tokamak plasmas). RAYON (a parallel ray-tracing code for lower-hybrid wave propagation) and REFMUL (a 2D Finite-Difference Time-Domain electromagnetic code used in reflectometry modelling of fusion plasmas).

11. GROUP OF LASERS AND PLASMAS

J.T. Mendonça (Head), R. Azambuja, L. Cardoso, M. Cataluna, H. Crespo, J. Davies, J.M. Dias, J. Encarnação, M. Fajardo, G. Figueira, A. Guerreiro, N. Lopes, A.M. Martins, S. Mota, D. Resendes, J.A. Rodrigues, L.O. Silva, G. Sorasio.

11.1. INTRODUCTION

This project included in 2004 activities mainly related with the following research lines:

- Ultra high power, ultra-short lasers[1];
- Theory and simulation on extreme plasma physics[1];
- Studies on complex and space plasmas.

11.2. ULTRA HIGH POWER, ULTRA-SHORT LASERS

11.2.1. Hardware improvements in laser system and target area of the laboratory for intense lasers

11.2.1.1. Diagnostics

A homebuilt SPIDER (spectral phase interferometer for direct electric-field reconstruction) diagnostic (Figure 11.1) was implemented and used to optimize the compressed pulse duration and pulse shape. A thorough study has been undertaken for this purpose, which allowed a better understanding of the role of the several parameters distorting the pulse shape, and how to compensate for them. In what concerns the SPIDER device, an extension of its working parameters into the highly chirped pulse regime was studied.

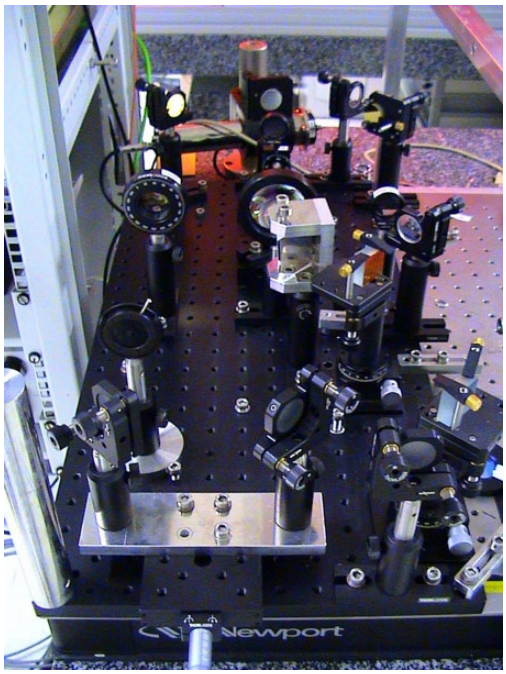

Figure 11.1 – View of SPIDER diagnostic

11.2.1.2. Vacuum pulse compressor

A specially-built vacuum chamber was installed for housing the current grating compressor, compatible with pulse amplification to the 10 Joule level and subsequent compression to the hundreds of fs level, without air-induced pulse distortion. This equipment is composed of a stainless steel vacuum chamber, a mechanically independent internal and external frame where the optical components are attached, a turbomolecular pump and a dry rough vacuum pump (Figure 11.2).

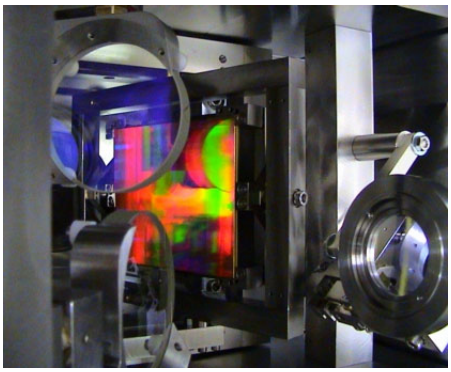

Figure 11.2 – Inside the compressor vacuum chamber, second grating.

11.2.1.3. In-vacuum beam delivery

The new pulse compressor includes a new vacuum beam delivery system (Figure 11.3), composed of a thin polymer window for compressor-target chamber vacuum separation, a gate valve with thick glass window (for low power alignments, a fast gate valve for emergency shutdown and a small vacuum chamber for steering the beam to the target chamber. The compressor vacuum system is automatically controlled by a home made microprocessor based controller. This pulse compressor can be upgraded in future to 50 TW (200 fs) by use of dielectric diffraction gratings.

11.2.1.4. Laser characterization

Following this modification, the laser system was fully characterized (Figure 11.4); in particular given the vertical configuration of the compressor, a new type of tilted pulse front autocorrelator has been successfully tested. A parametrical optimization of the spectral evolution along the laser chain was also performed, in order to minimize the final pulse duration.

[1]In the frame of the project "Keep-in-Touch Activities on Inertial Fusion Energy" of the Contract of Association EURATOM/IST.

Figure 11.3 – View of new in-vacuum beam delivery system

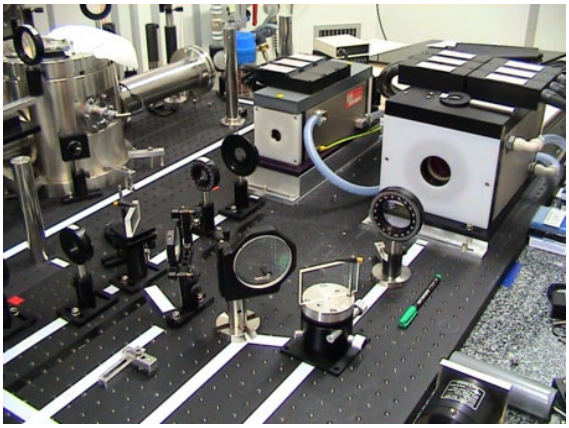

Figure 11.5 – 16 and 45 mm Nd:glass amplifiers

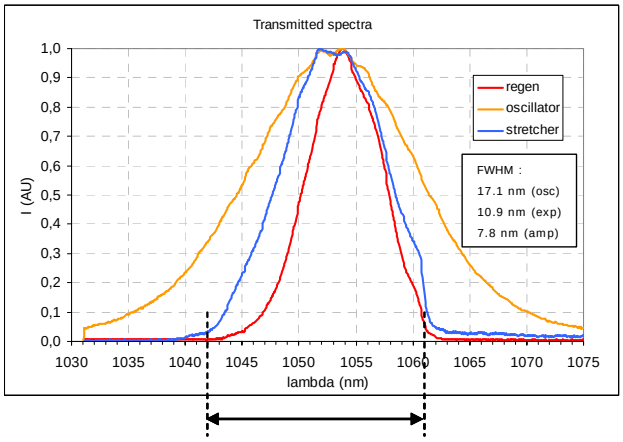

Figure 11.4 – Laser characterization: transmitted spectra at several critical elements in the amplification chain, showing gain-induced spectral narrowing.

11.2.1.5. Nd:glass 45 mm amplifier

This new amplifier was added in April 2004 to the final laser chain, which will allow the envisaged amplification above 10 J (Figure 11.5). Problems in coordinating its triggering sequence with that of the existing Nd:glass amplifier, and a lengthy flashlamp and rod replacement for the latter prevented us from testing both of them together until early 2005, when both situations have been finally solved.

11.2.1.6. Optical parametric chirped pulse amplification (OPCPA)

This work followed its course, and the first experiments are now taking place. A considerable theoretical work was done at this level, concerning the evaluation of ultra broad band optical parametric amplification by using dispersed signal beams. This scheme allows high fidelity amplification of pulses with bandwidths in excess of hundreds of nanometers to the multi-Joule level.

11.2.1.7. Laser modelling

The Miro software package was used for modelling L2I's laser chain; in particular, a thorough study of the best parameters for operating the 16 and 45 mm Nd:glass amplifiers together was undertaken, in terms of pump energy, pulse duration, pulse spectrum and B-integral.

11.2.2. Experiments

11.2.2.1. Electron acceleration

A new experiment on production of plasma channels for electron accelerators has been started. The objective of this experiment was to test the laser triggered-free-plasma-discharge in a differentially pumped gas cell. This is a fundamental step to use this technique in guiding laser pulses at high intensity since it allows reducing ionization-induced refraction of the laser beam at capillary entrance. These first experiments produced no conclusive results on laser guiding due to the difficulty of controlling the pre-pulses with the present laser setup. However, the plasmas lines produced in the gas cell show the same characteristics as those of previous experiments in a filled chamber. The laser system up-grade for 2005 with a new OPCPA arm and better contrast will allow solving the problems found in this experiment.

11.2.2.2. Collaboration with UCLA laser plasma group

A collaboration with the Laser Plasma Group of the University of California – Los Angeles aiming the development of plasma sources for laser plasma interaction was started in 2004. Under this collaboration Portuguese staff has participated in an experiment to test a UCLA-developed plasma source and we started the development of a new generation of plasma sources aiming the production of energetic electron beams by laser-plasma interaction.

11.2.2.3. X-ray lasers and XUV diagnostics

In inertial confinement fusion, high-density plasmas are produced. Optical probes have been widely used to understand laser-produced plasmas, but they have limitations in the study of higher densities such as compressed capsules or high power laser-solid interaction.

These difficulties include high absorption of optical light, strong refraction, and most of all the impossibility of probing beyond the critical density.

X-ray lasers are an ideal tool for studying these types of plasmas, because they can probe higher density regions with novel tools such as XUV interferometer or holography. Highly emitting sources are necessary, however, because one has to overcome the self-emission from the hot dense plasmas. In that context, we have worked in three major fields: improving the emissivity of the XUV source using High Harmonic seeding, designing new XUV diagnostics for plasmas and studying relativistic plasma effects on the propagation of X-ray lasers.

11.3. THEORY AND SIMULATIONS

11.3.1. Theoretical studies of fast ignition inertial confinement fusion

Preliminary theoretical studies of fast ignition using laser generated electron beams were carried out in 2004, leading to the successful submission of a grant proposal on this topic. This project should start in the first half of 2005.

The studies aimed at identifying key physics issues related to the process of fast ignition that need to be understood in order for the scheme to be implemented. Issues that have been considered include energy deposition by a beam with a broad energy spectrum and current limitation by the self-generated magnetic field of the beam.

The original calculations of the electron energy required for the electrons to stop in the core considered a mono-energetic beam, but laser generated electron beams have broad energy spectra. A simple analytical model has been used to estimate the ideal mean energy and the fraction of the beam energy that provides useful heating from the required stopping distance and electron energy distribution.

The minimum current required for fast ignition greatly exceeds the Alfvén limit, so can only propagate while the plasma provides an almost coincident return current. The return current is formed with a separation from the beam current of the order of the collisionless skin depth and the separation then increases as a result of the mutual repulsion of the currents and the decay of the return current due to collisions. The initial current neutralization that can be provided even in the core is insufficient to allow the beam to propagate and the decay time of the return current due to collisions is lower than the pulse duration. Possible solutions to this problem have been considered, and two practical solutions have been identified. A higher mean energy could overcome the problem since this lowers the current and raises the Alfvén limit, which compensates for the expected loss in efficiency. Schemes that could allow an increase in the mean energy without a loss in efficiency are being studied. Multiple beams could overcome the problem since each beam carries a fraction of the total current.

The obvious choice in this case is to use spherical illumination, which theoretically eliminates the problem altogether.

11.3.2. Plasma simulation

The main research theme is high energy density science, or extreme plasma physics. This rapidly emerging field encompasses a wide range of scenarios whose unifying aspects of are established by the methodology followed to tackle the different problems, with a combination of relativistic kinetic theory, plasma physics, accelerator physics, theoretical astrophysics with state-of-the art massively parallel numerical simulations using particle-in-cell codes or hybrid/reduced codes.

The team on extreme plasma physics has developed a strong expertise in plasma simulation codes, theoretical plasma physics, plasma-based accelerators, and advanced simulation techniques. We are now becoming recognized as the leading plasma simulation group in Europe, and achieving worldwide recognition. Collaboration with the leading research programs in the US, and in France in our fields of research is tight and strong, guaranteeing us access to state-of-the-art computing facilities such as the newly commissioned Dawson cluster at UCLA or the IBM SP3 at NERSC, Oakland, California, and the most up to date experimental results.

Our work deals with different aspects of laser-plasma interactions at extreme radiation intensities, ranging from laser-solid interactions to large-scale length plasma accelerators, from fast ignition of fusion targets to shocks in Coulomb explosions of cluster, from theory of stimulated scattering instabilities to sources of energetic protons for cancer therapy.

As a spin-off of the work on inertial fusion energy related problems, we have also extended some of our work to astrophysical problems, namely the nonlinear evolution of magnetic fields generated from collisionless instabilities[2].

The need for a hierarchy of simulation codes capable of covering a wide range of time and length scales has motivated our further development of the hybrid code dhybrid[3].

The CFP cluster has been upgraded to an extra 40 CPU PowerPC G5 over Gigabit Ethernet, for an aggregate cluster size of 80 CPUs, 65 GB RAM (Figure 11.6).

Next sections described the main results obtained in ten research topics.

11.3.2.2. Beam-plasma instability

In fast ignition, huge currents, in excess of hundreds of MA, need to be transported across background plasma whose density varies within more than 4 orders of magnitude. Depending on the properties of the beam, such high fluxes of free energy can drive plasma instabilities. These instabilities can be deleterious if occurring near the coronal region of the plasma, or they can be beneficial if occurring near the core of the compressed fusion pellet.

[2] This work is performed in collaboration with the University of Kansas

[3] This code is being developed in collaboration with the Rutherford Appleton Laboratory.

A systematic analysis of the filamentation instability has been performed by GoLP, using relativistic kinetic theory, exploring the scenarios where this instability can be of relevance. Some of these results have also been applied to the study of equivalent scenarios in astrophysical scenarios, namely gamma ray bursters, with a detailed emphasis on magnetic field generation and nonlinear evolution from collisionless plasma processes.

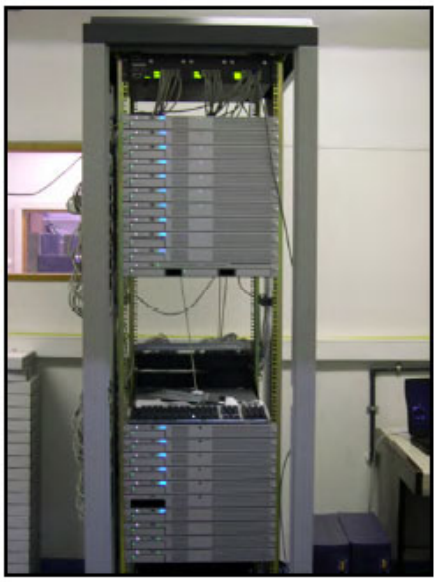

Figure 11.6 – The expp cluster at GoLP.

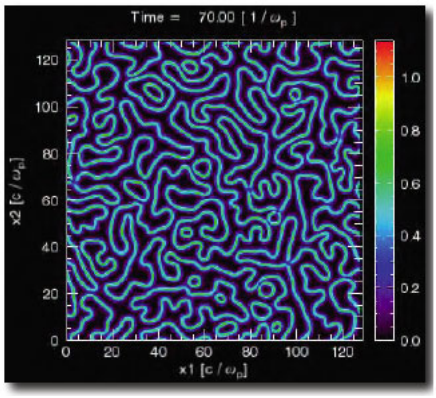

Figure 11.7 – Two-dimensional filamentation instability.

11.3.2.3. Fast electron transport in realistic ICF targets

In 2004, fast electron transport in realistic geometries have been addressed for the first time,. This is a critical issue for fat ignition since all previous simulations have been performed in scenarios not realistic and, thus leading to unphysical results solely associated with boundary conditions. In particular, demonstration that for fast ignition conditions a well-defined electron beam is not formed was made. Furthermore, the role of cone-shaped targets for coupling of the laser radiation to the electrons has been explored.

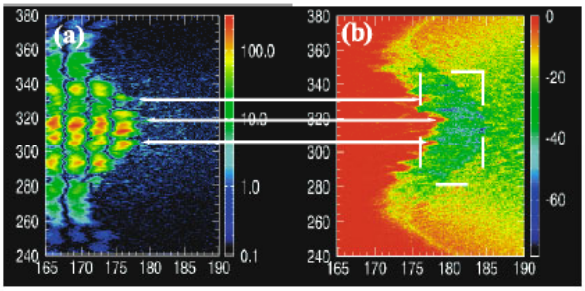

Figure 11.8 – Laser filamention in the interaction region. (a) laser field, and (b) electron density

11.3.2.4. Photon accelerator

In the same way as relativistic plasma waves can accelerate electrons with GeV/cm gradients, they can also upshift photons riding the waves. Such phenomena can be used as a novel way to tune radiation over a wide range of frequencies but also as a diagnostic tool for relativistic structures.

A numerical exploration of the photon accelerator either in a pre-formed plasma or including ionization effects on the short laser pulse driving the wake was performed. As a novel diagnostic the Wigner transform concept was employed, which allows for a clear identification of the relevant physics.

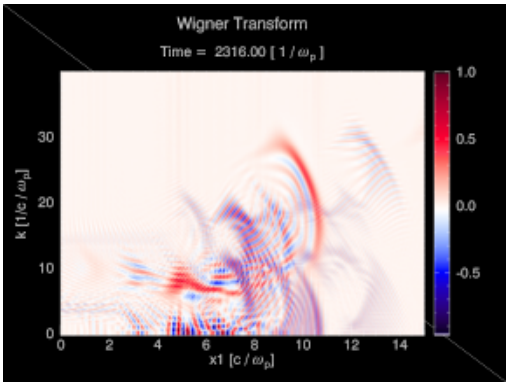

Figure 11.9 – Wigner transform of ultra short laser pulse riding a laser wakefield

11.3.2.5. Osiris 2.0 development

In 2004, IST released osiris 2.0, the novel version of the massively parallel fully relativistic particle-in-cell code osiris, which has been developed within the Osiris consortium. Among the new features, osiris 2.0 includes several ionization models (impact, tunnel, and barrier suppression), binary collisions, and novel laser initialization configurations (Bessel beams, tilted wavefronts). This release of osiris 2.0 has been accompanied by the implementation of a software development infrastructure, based on subversion, for collaborative development, management, and version tracking of the project. In order to achieve performance gains, tight integration between osiris 2.0 and the clusters where this code runs has also been pursued. The

availability of significantly more computational power has also pushed for the development of further features in idl.zamb, the visualization infrastructure for large data sets.

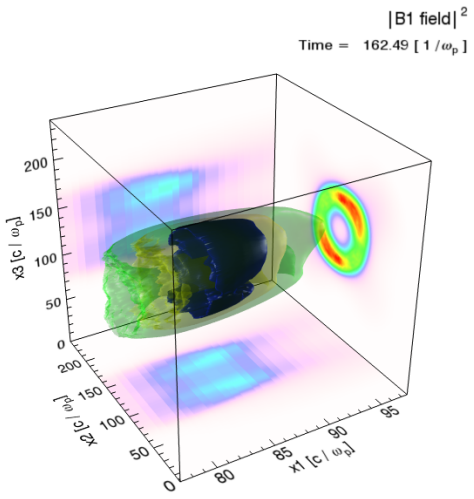

Figure 11.10 – Longitudinal B-field driven by a Bessel beam

11.3.2.6. dHybrid

The first version of dhybrid has now been completed, with major improvements in the hybrid algorithm, and expanded capabilities. The range of scenarios that dhybrid can now deal with has significantly increased from the initial version of dcomet. In this code, the ions are treated as kinetic particles, and the electrons as a massless fluid. The length scale and the time scale is then determined by the ion dynamics thus allowing the simulation of larger/longer scenarios. This code has been employed to study artificial magnetospheres and artificial comets. The current version of dhybrid is now prepared for the next step, which will lead to the parallelization of this code, which will then be the state-of-the-art hybrid code.

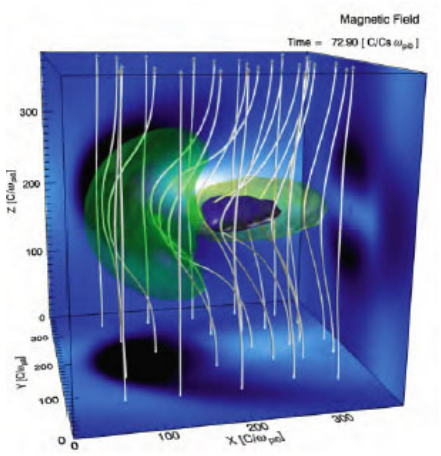

Figure 11.11 – Simulation with dhybrid of an artificial magnetosphere

11.3.2.7. Collisionless shocks for fast ignition and proton acceleration

Demonstration that ultra intense lasers can drive electrostatic shocks that can be very effective in accelerating particles was made. This scenario has been further explored, in order to optimize the proton acceleration mechanisms, and to analyze the possible consequences of these shocks for fast ignition. Significant effort is also been put into the theoretical description of such nonlinear structures, in particular, relativistic collisionless shocks, with shocks velocities comparable to the speed of light.

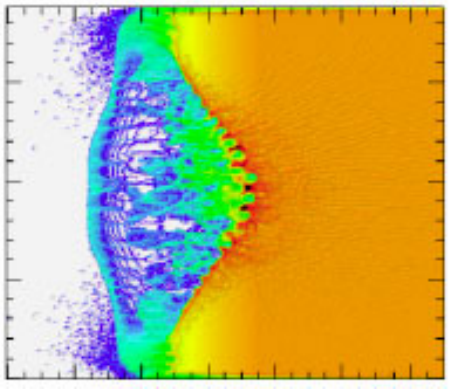

Figure 11.12 – Electron density of collisionless shock from hole boring driven by ultra intense laser in the front surface of solid target (laser is moving from left to right)

11.3.2.8. Explosion of clusters and neutron yield increase from controlled shock shells

A novel technique to control the explosion of nano to sub-micron deuterium clusters was proposed. The possibility to control such explosions opens the way to the increase of the neutron yield due to intra-cluster reactions. This scenario has been explored, optimizing the double pulse technique, generalizing the concept to heteronuclear clusters. The possibility to extend these ideas to other intense radiation sources in the VUV and soft x-ray domains was proposed. Preliminary work on this topic has been pursued.

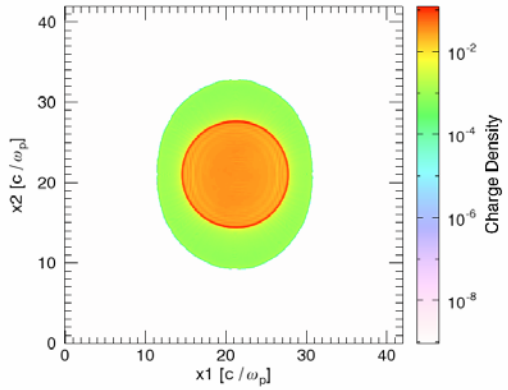

Figure 11.13 – Formation of shock shells: the inner ions overtake the outer ions

11.3.2.9. Blow out, wave breaking and self-injection

The possibility for electron acceleration up to 1 GeV in the laser wakefield configuration in a 1 cm long plasma channel has been identified. The physics that allows for such extreme energies is highly nonlinear and includes the blow-out of the electrons and the formation of an ion channel behind the short laser pulse driving the wake, the wave breaking on the nonlinear plasma wave formed in the trail of the laser pulse, and the self-injection of the electrons into the accelerating bucket.

A detailed theoretical study of these coupled nonlinear phenomena as well as a large number of simulations to test the theoretical model and to interpret the results of experiments under way all over the World have been carried out.

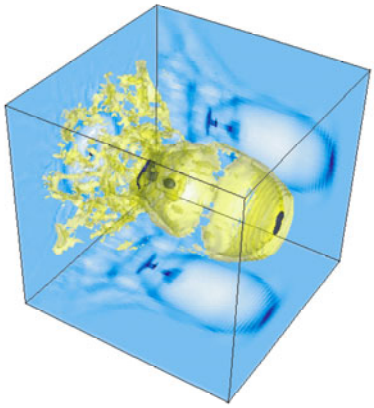

Figure 11.14– Electron density from ultra intense laser blow-out in a preformed plasma

11.3.2.10. B-field generation and the inverse Faraday effect

One of the most interesting phenomena in laser-plasma interactions is the generation of magnetic fields up to the MG level. Different mechanisms can lead to B-field generation in plasmas, but one mechanism is still eluding experimentalists and theorists: the inverse Faraday effect. Detailed numerical simulations of the inverse Faraday effect have been performed, while a new theoretical model including the role of ionization has been studied. Our findings indicate the presence of the inverse Faraday effect, and show that ionization can increase the B-field level.

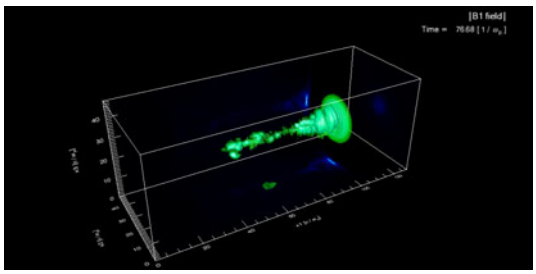

Figure 11.15 – B-field generated by circularly polarized laser in underdense plasma

11.3.2.11. Stimulated scattering instabilities driven by broadband radiation sources

Ultra intense lasers have a large bandwidth either because these pulses are short in duration or due to their interaction with the background media. Furthermore, spectrally broadened long laser pulses (e.g. using random phase plates) are commonly used in ICF since the growth rate for stimulated scattering instabilities is strongly decreased for such laser light conditions. No self-consistent theory exists for stimulated scattering instabilities that accounts for the bandwidth of the radiation source.

A novel theory has been developed by Golp for stimulated scattering instabilities with broadband radiation sources by generalizing the Wigner-Moyal formalism to variable mass Klein-Gordon like systems. In the limit of zero bandwidth (monochromatic pump) the standard results for stimulated Raman scattering for all intensities and all angles have been recovered. The generalized dispersion relation has been derived and explored as a function of the bandwidth of the pump radiation.

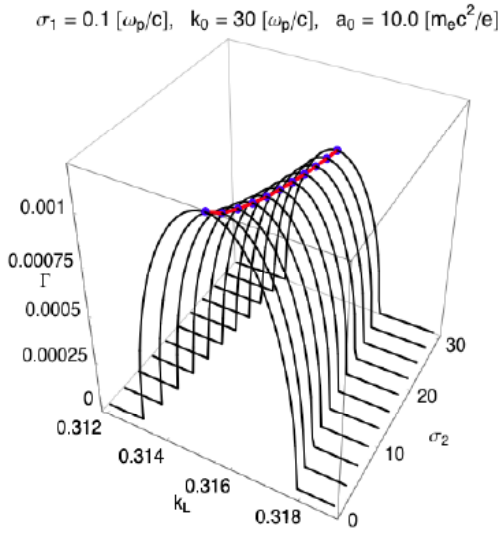

Figure 11.16 – Growth rate for Raman forward scattering including bandwidth effects

11.3.3. Quantum information theory

Together with some work on the foundations of Quantum Mechanics, the research on quantum information theory has been twofold: on multiparticle quantum walks and their algorithmic applications, as well as on how to use electron scattering to entangle magnetic impurities in a solid.

Quantum walks are the quantum version of the random walks. Classically, random walks with *K* particles are equivalent to *K* independent single-particle random walks. In the quantum case though, a walk with *K* particles may contain entanglement, thus offering a resource unavailable in the classical scenario and which can present interesting advantages. Moreover, in the case of identical particles the effects of quantum statistics have to be taken into account,

giving an additional feature to quantum walks that can also be exploited. In this work[4], we show how the entanglement and the relative phase between the states describing the *coin degree of freedom* of each particle will influence the evolution of the quantum walk. In particular, the probability to find at least one particle in a certain position after *N* steps of the walk, as well as the average distance between the two particles, can be larger or smaller than the case of two unentangled particles, depending on the initial conditions we choose. This resource can then be tuned according to our needs, in particular to enhance a given application (algorithmic or other) based on a quantum walk. Experimental implementations were also discussed.

Motivated by the importance of entanglement in quantum computation and in some difficulties to generate it in solid state systems, a scheme to entangle two magnetic impurities (stationary spins 1⁄2) embedded in a solid state system have been proposed[5]. The main idea is to use a ballistic electron as an agent which scatters one the two impurities in succession and entangles them. Being a scattering based scheme, it requires no control over the ability to switch interactions on and off between entities in a solid, as is required by many existing entangling proposals. Moreover, even in comparison to other reduced control proposals, such as those based on scattering or two particle interference, our current scheme has the simplicity that it involves only one mobile entity, namely the ballistic electron, and does away with the difficulty of having to make two electrons coincide at the same place at the same time. This already is focused on how two magnetic impurities embedded in a solid can be entangled by an injected electron scattering between them and by subsequent measurement of the electron's state. The first step was the investigation of an ideal case where only the electronic spin interacts successively through the same unitary operation with the spins of the two impurities. In this case, high (but not maximal) entanglement can be generated with a significant success probability. Afterwards a more realistic description which includes both the forward and back scattering amplitudes was considered. In this scenario, the entanglement between the impurities as a function of the interaction strength of the electron-impurity coupling was obtained. The results led to conclude that our scheme allows us to entangle the impurities maximally with a significant probability (Figure 11.17).

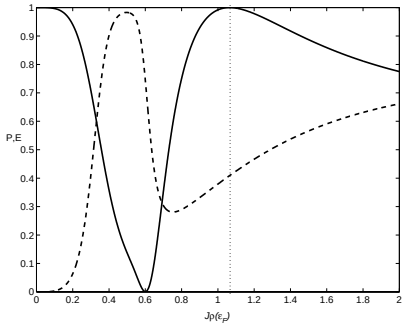

Figure 11.17 – Plots of the probability P (dashed line) of detecting the transmitted electron in the spin down state, and the amount of entanglement E (solid line) obtained between the impurity spins in that case, as a function of the interaction strength $J\rho$ (ε_F), for the realistic scenario of the electron successively scattering of the two impurities.

11.4. STUDIES ON COMPLEX AND SPACE PLASMAS

11.4.1. The science of laboratory colloidal plasmas and mesospheric charged aerosols"[6]

11.4.1.1. Interaction forces and dust dynamics in strongly coupled systems

A large number of laboratory observations reveal the formation of ordered linear chains and sheets composed of charged dust grains levitated in the sheath region of radio-frequency (rf) or dc plasma discharges at very low pressures. At higher pressures, three-dimensional structures are typically formed. Recently, a number of low gas pressure experiments have explored the generation of large amplitude vertical oscillations by lowering either the background pressure or the plasma number density, or by imposing an external force that arises from a low-frequency sinusoidal voltage in the sheath region. A theoretical model has been developed that successfully describes the phenomenology in existing experiments, including the observed self excited oscillations, nonlinear resonance and parametric oscillations. This work was further extended to a self-consistent theory for melting dynamics as well as particle temperature of charged dust grains in plasma sheaths.

11.4.1.2. Waves and instabilities in dusty plasmas

Linear as well as nonlinear mechanisms for the generation of electrostatic and electromagnetic waves in fully and partially ionized dusty plasmas with and without the external magnetic field have been considered. A unified theory describing the effects of charge fluctuations on low frequency phenomena has been developed. The results of this investigation are being applied to the Earth's mesosphere where both negative and positive dust layers are observed. In particular the origin of ELF/ULF waves triggered by positive cloud to ground lightning above mesoscale convective systems has been investigated.

11.4.2. Laser propulsion: ground to orbit launch

The work programme for 2004 involved a review of the state-of-the-art in Laser Propulsion as well as modelling laser thruster flows.

11.4.2.1. State-of-the-art thrusters

The American Lightcraft, the German Bell Thruster, the Japanese Laser driven In-Tube Accelerator (LITA), the Russian Aerospace Laser Propulsion Engine (ASLPE), the

[4] Done in collaboration with S. Bose from UCL and N. Paunkovic and L. Sheridan from the University of Oxford.
[5] Work performed in the frame of the S. Bose from UCL, A. Costa from Universidade Federal de Lavras
[6] In the frame of the European Research Network on Complex Plasmas

Brazilian Laser Supported Directed Energy Air Spike (DEAS), and the American Heat Exchanger Thruster (HX), were reviewed. Of these, only the Lightcraft is a "complete" vehicle. The remaining thruster configurations allow experimental and theoretical study of relevant physical and fluid dynamic issues but are further removed from a thruster application. The Heat Exchanger is technologically close to chemical propulsion and does not take advantage of the high specific impulse which laser propulsion can provide.

11.4.2.2. Laser technology

Full advantage of the promise of laser propulsion for Low Earth Orbit (LEO) requires a high power pulsed laser and consequent efficient propellant absorption, energy confinement, and gas expansion. The real problem is a nonlinear optimization problem involving the propellant, the laser wavelength, the pulse duration, the pulse repetition frequency and the laser power (energy). The selection of the laser wavelength is a critical issue for laser propulsion. Most work to date has concentrated on the 10.6 μm wavelength because of the availability of high power CO_2 lasers. The optimal wavelength will depend on tradeoffs between a variety of parameters, including transmission, absorption, laser efficiency, and the specific mission. Absorption favours longer wavelengths, whereas transmission through the atmosphere and optics favours shorter wavelengths. State-of-the-Art CO2 lasers typically reach 100 kW average power on the order of a few minutes of operation. Closed cycle designs exist which would allow for continous operation.

11.4.2.3. Laser heated flow modelling

Steady laser heated LSD wave flows using LiH as propellant have been modelled. Both an equilibrium and a two-temperature kinetic model were investigated. The resulting structure of the LSD waves have been derived. For completeness, an LSC steady model with H as propellant was also investigated. Thruster performance calculations for the equilibrium LiH model have been obtained. It is seen that the calculated performance is comparable, within factors of 2-3, to the Lightcraft vehicle performance which uses air as propellant. Figures 11.18 and 11.19 present results from the kinetic flow modelling.

11.4.2.4. Trajectory modelling

Numerical simulations were performed to gain insight into the mechanics of laser propulsion ascent trajectories and how these are influenced by the most relevant mission parameters. The simulations were performed using Colvet. This is a WindowsTM application coded in Fortran 95. The vehicle is approximated by a point-mass. There are no moments and the only forces acting on the vehicle are gravity, aerodynamic drag and propulsive thrust. Several interesting results were found in the simulations performed. A simple steering program made of steps and slopes performs close to that of optimized pitch programs. This allows for a small number of parameters to completely define a steering program, greatly decreasing the complexity of analyzing laser propulsion. The general trend of 1kg of payload for every mega-Watt of laser power was confirmed. There is an optimum laser power for a given launch mass, within a given mission. Drag losses strongly influence low mass vehicles. Aerodynamic design should be a major design driver. It is beneficial to use as high specific impulse as possible, as long as it allows enough thrust for a given power setting to lift the vehicle fully loaded. Comparison with flight results shows very good agreement.

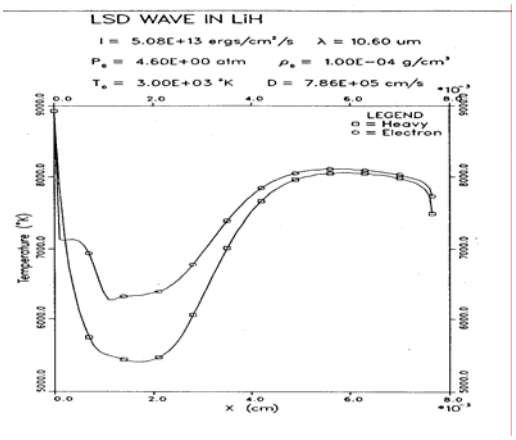

Figure 11.18 - Finite kinetic 2-T temperature profile.

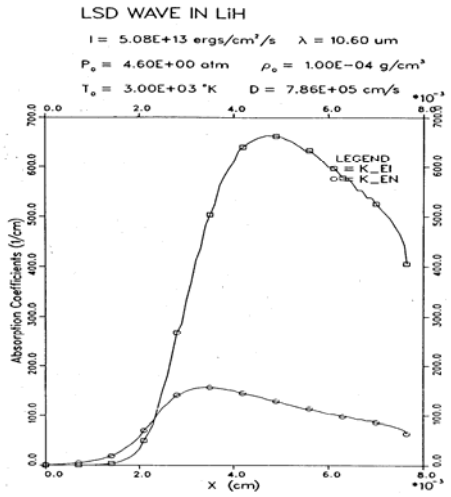

Figure 11.19 - Laser Supported Detonation (LSD) wave absorption coefficients.

11.4.3 Lidar guidance navigation and control (GNC)

The activity involved applied research into the applicability of single photon counting Lidar as an altimeter for both landing and rendezvous missions of a space vehicle. Functional Lidar requirements were determined from mission requirements. Simulation of a complete laser altimeter system was performed including the appropriate transmitter and detector array receiver. The basic equations were applied to this novel altimeter and appropriate design parameters were derived. The figures below (11.20 to 11.22) present typical results, showing the variation of the average laser power and receiver aperture

as a function of laser PRF between 1-30 000 Hz. An array detector with 64 elements is simulated. The range is fixed at 5000 m for a scan angle of 20º. The power decreases monotonically but eventually saturates. At a PRF of 30000 Hz, the transmitter power is 1 Watt, a very acceptable value. The radius increases monotonically but eventually begins to saturate. Even at 30 000 Hz, the upper PRF frequency for single pulse TOF, the detector radius is 3 cm. Current available commercial technology which could implement the design was indicated.

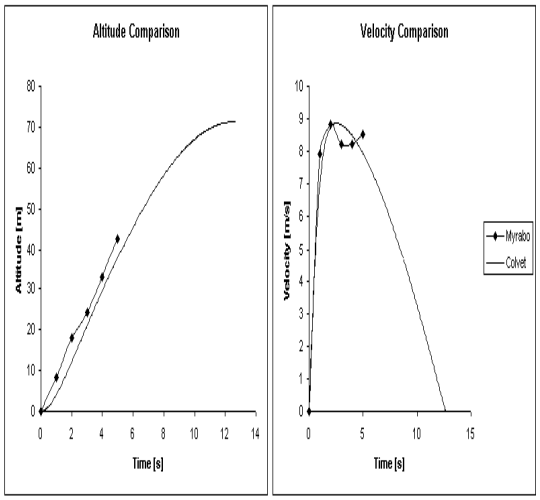

Figure 11.20 - Altitude and Velocity Profile Comparison with Myrabo Flight Results

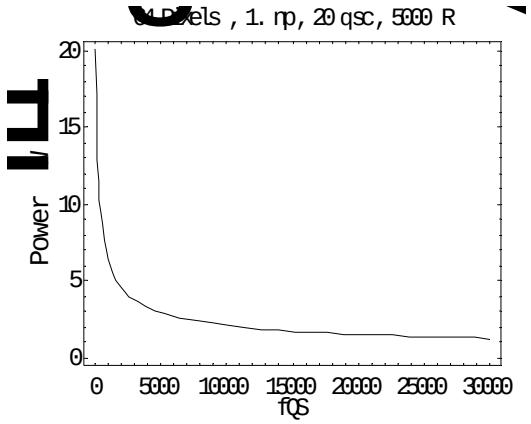

Figure 11.21 - Average Laser Power vs Laser PRF (64 Element Detector) Landing.

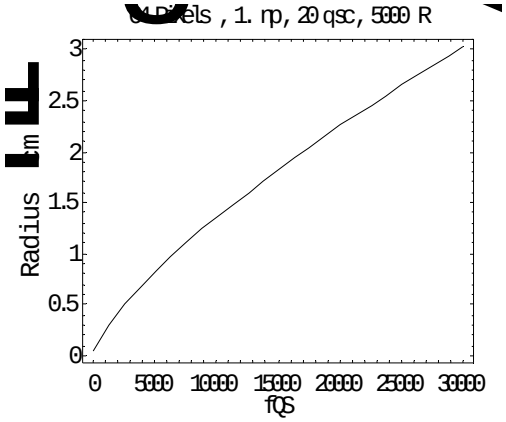

Figure 11.22 - Receiver Aperture vs Laser PRF (64 Element Detector) Landing.

12. GROUP OF SPACE PLASMA

A. L. Brinca (Head), M. H. Marçal and F. J. Romeiras.

12.1. INTRODUCTION

The research work carried out by the Space Plasma Group in 2004 follows naturally from the previously reported activity. During this period, three main areas were under investigation:

- Interpretation of Totem Pole emissions;
- Effects of large-amplitude waves on linear instabilities;
- Assessment on the feasibility of the *magnetic bubble* as a means of space propulsion.

12.2. TOTEM POLE EMISSIONS[1]

12.2.1. Introduction

Totem Pole emissions were first observed near the dayside magnetopause by the Geotail spacecraft in 1997[2]. They are electrostatic electron Bernstein waves whose characteristics are not fully explained by the standard model invoked for the generation of this type of wave activity. In particular, the occurrence of harmonic branches above the upper hybrid frequency and the fine spectral structure of the lower frequency emissions could not be interpreted in the context of the model adopted to study Bernstein waves in the magnetosphere.

12.2.2 . Approach and results

The classical paradigm associated with electron Bernstein emissions uses an admixture of cold and hot electron populations neutralized by a background of immobile ions, with the perpendicular velocity distribution of the hot species providing the free energy, and the emphasis placed on modes propagating slightly away from the perpendicular (with respect to the background magnetic field).

In a previous work[3], we adopted an alternative source of free energy to stimulate electron Bernstein waves: the almost monoenergetic ion (AMI) beams recently observed by the Interball 1 spacecraft. The success of this model led to its utilization in the context of the Totem Pole emissions, where it was demonstrated that AMI beams could generate electron Bernstein emissions both below and above the upper hybrid frequency (as observed by the Geotail spacecraft) and provided a simple means of accounting for the fine spectral structure found in the lower harmonic bands.

12.3. LARGE AMPLITUDE WAVES AND INSTABILITIES[4]

12.3.1. Introduction

The richness and variety of free energy sources in space plasma environments warrants the study of the influence of large amplitude waves (stimulated by a given free energy source) on the characteristics of instabilities (eventually fed by another
free energy source).

12.3.2. Previous and present work

The study of the effect of large-amplitude circularly polarized waves on linear beam-plasma electromagnetic instabilities was followed by the investigation of electrostatic instabilities induced by large-amplitude left-hand polarized waves and the triggering of ion acoustic instabilities in the solar wind by finite amplitude waves.

12.4. MAGNETIC BUBBLE AND SPACE PROPULSION[5]

12.4.1. Introduction

In the year 2000, Winglee and collaborators proposed a new means of spacecraft propulsion[6]: tapping the energy of the solar wind with an (artificially created) 'magnetic bubble'.The basic objective of the so called Mini-Magnetospheric Plasma Propulsion system is to deflect the solar wind particles by a large magnetic bubble whose field lines are attached to the spacecraft; as the charged particles of the solar wind are reflected by the magnetic field, the force that they exert is transmitted along the field lines to the spacecraft to produce its acceleration.

---

[1] This research line has been carried out in collaboration with Prof. Luis Gomberoff, Physics Department, University of Chile at Santiago and partially funded by FONDECYT (Chilean Institute).

[2] Matsumoto, H. and H.Usui, Intense bursts of electron cyclotron harmonic waves near the dayside magnetopause observed by Geotail, *Geophys. Res. Lett.*, *24*, 49, 1997.

[3] Brinca, A.L., F.J. Romeiras and L. Gomberoff, Stimulation of electron Bernstein modes by perpendicular ion beams, *Geophys. Res. Lett.*, *30*, 2175, doi: 10.1029/2003GL017501, 2003.

[4] This research line has been carried out in collaboration with the Physics Department of the University of Chile at Santiago and partially funded by FONDECYT (Chilean Institute).

[5] This research line was carried out by all the groups in the Centro de Física de Plasmas and was partially funded by ESA.

[6] Winglee, R.M., J. Slough, T. Ziemba and A. Goodson, Mini-magnetospheric plasma propulsion: Tapping the energy of the solar wind for spacecraft propulsion, *J. Geophys. Res.*, *105*, 21067, 2000.

The spacecraft to be propelled carries a current loop to generate a dipolar magnetic field and a plasma source. The success of the propulsion mechanism hinges on the magnitude of the force that, via the interaction of the solar wind with the created magnetic bubble, acts upon the spacecraft. Many complex phenomena influence the outcome of the interaction (for example, the characteristics of the plasma created by the spacecraft source); the investigation made a preliminary assessment of several of them.

13. GROUP OF GAS DISCHARGES AND GASEOUS ELECTRONICS

C. M. Ferreira (Head), L. Alves, F.M. Dias, V. Guerra, J. Henriques, S. Letout, J. Loureiro, L. Marques, L. Novo, M. Pinheiro, E. Tatarova.

13.1. INTRODUCTION

This Group carried out activities in 2004 mainly related with two research areas:

- Environment plasma engineering;
- Modelling of plasma reactors.

13.2. ENVIRONMENT PLASMA ENGINEERING LABORATORY

13.2.1. Introduction

Having in view environmental issues, the main activity of the "Gaseous Electronics" research group during 2004 was focused on detailed experimental and theoretical investigations of large-scale microwave molecular plasmas. Plasma sources operating in N_2, O_2, H_2 and their mixtures are presently the subject of many investigations due to their importance in plasma-based technologies and in atmospheric physics. For example, gas discharges operating in nitrogen-oxygen mixtures are used for cold sterilization of medical devices, removal of nitrogen oxides (NO_x) from flue and exhaust gases. Nitrogen-hydrogen mixtures are important as sources of ground state atoms. Large-scale plasma sources based on microwave propagation are of interest for new-generation technologies because of the high number densities of active species they yield. The effect of the plasma in the treatment process is strongly correlated with the spatial distribution of the species and the plasma parameters, as is well known.

13.2.2. Experiment

13.2.2.1. Experimental system development

An improvement in the operation of the large-scale plasma source has been done during 2004. A schematic diagram of the plasma source is shown in Figure 13.1. The discharge chamber is a stainless steel tube (d = 30 cm) headed by a water-cooled aluminium block and closed at the top by a 10 mm-thick quartz window. A 2.45 GHz microwave power supply is coupled to the plasma using a pair of slot antennas formed on a waveguide base plane. The generator is isolated from the discharge chamber by a high power circulator with high power matched load used for matching the impedance of the discharge chamber to the waveguide.

The plasma is created by the energy carried by surface waves propagating radially (r) and azimuthally (φ) along the interface between the plasma and a quartz dielectric plate located at the top wall. In the discharge, two different zones are formed due to the exponential decrease of the electric field. The first one is the active discharge zone close to the interface, where the surface waves propagate and sustain the discharge, and the second one is the remote, "electric field-free" plasma zone (Figure 13.1).

In order to get spatial resolution of the emission spectroscopy measurements, an "optical periscope" system has been designed and constructed. The "optical periscope" is placed inside the plasma (Figure 13. 2).

Figure 13.1 – Large-scale source: experimental set-up.

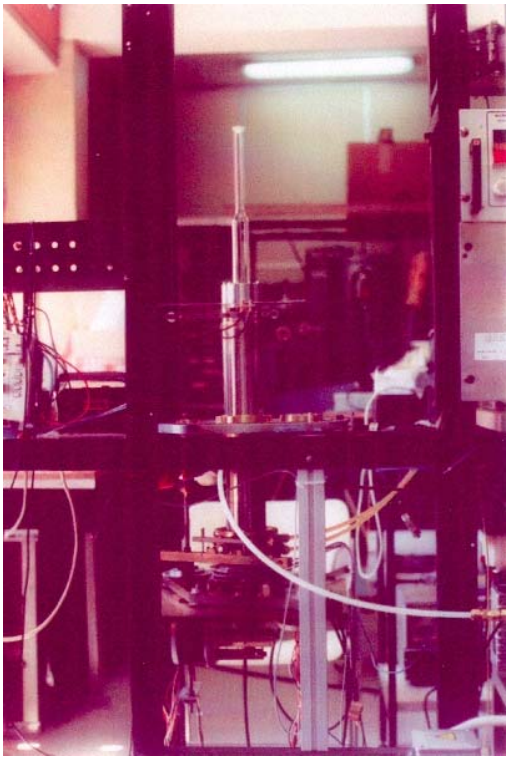

Figure 13.2 - "Optical periscope"

It consists of a hollow stainless steel piston with an optical fibre located inside. The piston is terminated at the top by an optical quality window and a right-angle prism. The "periscope" can be moved in the axial and azimuthal directions. The plasma radiation impinging radially on the prism is deflected towards the axis, collimated by a lens and then collected by the optical fibre, which guides it into the input slit of a spectrometer. The volume of plasma under investigation is determined by the apparatus function. Photons emitted by the plasma are transferred by the optical system into the entrance slit of a SPEX 1250M spectrometer (2400 g/mm grating) with a Hamamatsu R928 photomultiplier. The current generated by the photomultiplier is sent to data acquisition electronics DataScan2, and processed by Spectramax software.

13.2.2.2. Surface mode identification

An electrodynamical analysis of the plasma source has been performed. The waves form a resonant eigenmode satisfying the pertinent boundary conditions and the plasma takes discrete density values, which ensure that the resonant eigenmodes exactly appear at the excitation frequency (2.45 GHz). Selective excitation of a proper mode is necessary for stable operation of the system. For this reason, spatially resolved 3D measurements of the electric field components are performed and compared with the theoretical results to identify the mode sustaining the discharge. Electric field measurements have been performed by using a 0.5 mm tungsten wire probe (of length l = 5 mm), which is movable in the azimuthal (φ), radial (r), and axial (z) directions.

The 2D (azimuthal and radial) total electric field intensity pattern at a constant axial distance z=0.3 cm is depicted in Figure 13.3. The experimentally obtained azimuthal distribution of the radial electric field component, measured at fixed axial z and radial r positions, is shown in Figure 13.4. As seen, the measured distributions of the field components clearly correspond to the transverse magnetic TM_{330} mode, as considered theoretically.

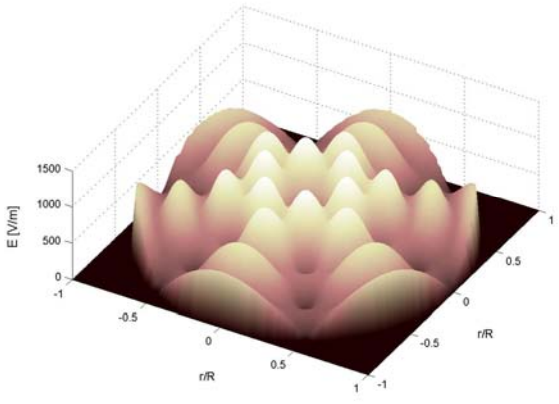

Figure 13.3 - 2D (r-φ) distribution of the total electric field.

13.2.2.3. Emission spectroscopy measurements

13.2.2.3.1. Emission from radiative states

Emission spectroscopy was used to measure the $N_2(C^3\Pi_u)$, $N_2^+(B^2\Sigma_u)$ and NO(γ) band intensities and the emission of excited hydrogen atoms [H_δ, H_γ], as a function of the spatial position in N_2–xO_2 and N_2–xH_2 , He–xH_2 mixtures[1].

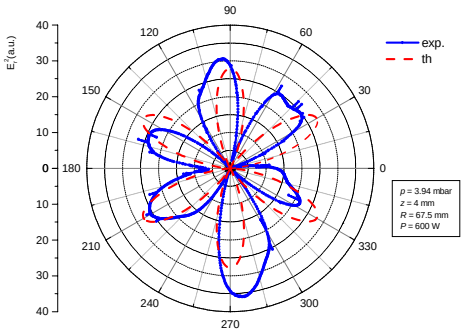

Figure 13.4 - Azimuthal variation of the square of the measured radial component of the electric field (z = 4 mm, r = 67.5 mm, p = 3 Torr).

The experimental data are discussed in the framework of kinetic considerations. The investigated intensity of the emission lines of the 2nd positive and 1st negative systems of N_2, and of NO(γ) and hydrogen atoms in the discharge zone of a large-scale N_2-O_2 and N_2-H_2 plasma source follows the spatial variation of the local electric field peculiar for the TM_{140} surface mode, as the obtained results demonstrate. On the contrary, the population in vibrational and rotational levels of the $N_2(C^3\Pi_u, v)$ state is spatially homogeneous. The vibrational spectrum of the NO(γ) band [$NO(A^2\Sigma^+, v' \rightarrow X^2\Pi, v'')$] has been detected in the UV range, between 230 and 290 nm. As seen from Figure 13.5 the azimuthal variations of the band head intensities of the lines corresponding to different vibrational transitions follow the variations in electric field intensity (TM_{140} mode) in the discharge zone.

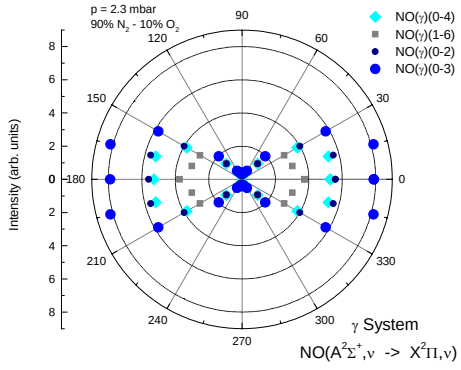

Figure 13.5 - Azimuthal variations of the band head intensities corresponding to different vibrational transitions of the NO(γ) system (Δz = 1 cm).

[1] Work carried out in collaboration with CPAT-URS (France), and the Lebedev Physical Institute of the Russian Academy of Sciences (Rússia).

13.2.2.3.2. Gas heating

The rotational distribution of the intensity of the R-branch in the $N_2(C^3\Pi_u, v'=0 \rightarrow B^3\Pi_g, v''=2)$ band of N_2 was used for temperature determination taking into account the Hönl-London factors. Because the measured distributions nearly follow Boltzmann´s law, the rotational temperature for the state can be introduced. The azimuthal distribution of T_r in the active plasma zone, i.e. close to the interface for two different N_2-O_2 mixture compositions is shown in Figure 6. As seen, the measured values are around 1000 K, independently of the azimuthal position. Thus, significant homogeneity of the rotational excitation of N_2 molecules is observed. Due to fast rotational–translational energy exchanges, these temperatures are also indicative of the gas temperature and of the spatial distribution of gas heating.

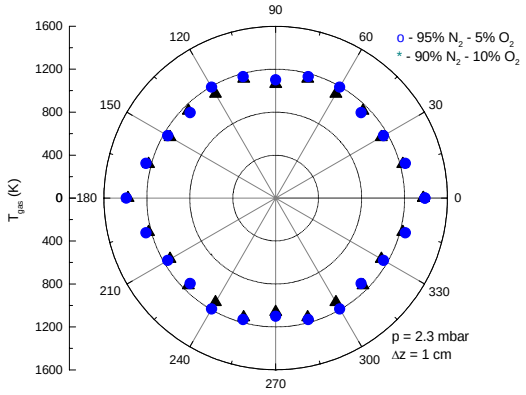

Figure 13.6 - Azimuthal distribution of T_r in a N_2-O_2 discharge.

13.2.2.3.3. Doppler broadening technique

The Doppler broadening technique has been applied to investigate a new effect associated with excessive broadening (and excess of energy generated) of the H_α atomic line in hydrogen containing mixtures, like Ar-H_2 and He-H_2. Recent spectroscopic diagnostics of He-xH_2 and H_2 plasmas generated by a slot antenna excited microwave plasma source, operating at $\omega/2\pi$=2.45 GHz, reveal that the emission profile of the Balmer-α line shows larger broadening than the Balmer-β and the helium line at 5875.7A [transition $3^3D \rightarrow 2^3P$] (Figure 13.7). The temperatures corresponding to the H_α and H_β lines profiles are 0.28 eV and 0.17 eV, respectively, much higher than the wall temperature and the rotational temperatures calculated from the Q-branch of the Fulcher-α band [$d^3\Pi_u$ (v=0) → $a^3\Sigma_g^+$ (v=0)] under the same conditions. The measured full width at half maximum (FWHM) of the H_α and H_β lines is nearly constant in the axial direction, i.e., does not change along the transition between the discharge and the remote plasma in He-H_2, (Figure 13.8).

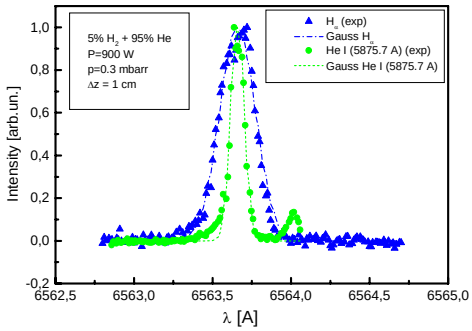

Figure 13.7 - Typical H_α, and helium 5875.7 A line profiles recorded in the discharge zone of a He-H_2 plasma.

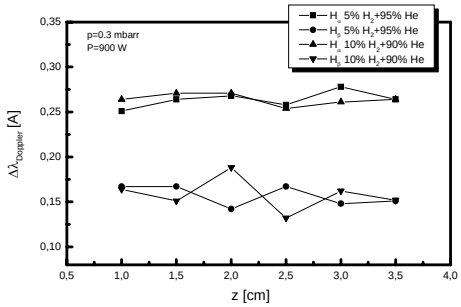

Figure 13.8 - Axial variation of FWHM of H_α and H_β lines in He-H_2 plasma.

13.2.3. Theoretical analysis

13.2.3.1. Large scale plasma source

A self-consistent numerical model for a large-scale Ar plasma source excited by a pure TM_{330} surface mode was developed and used to investigate the 3D spatial structure of the discharge during 2004[2]. The model is based on the solution of a coupled system of equations including the electron Boltzmann equation, the particle balance equations for all the relevant charged and neutral species, the gas thermal balance, and the equations describing the TM_{330} surface mode electrodynamics. Probe diagnostic techniques and radiophysics methods have been applied to validate the model predictions. The density distributions of plasma electrons, positive ions and electronically excited states of Ar atoms were shown to be strongly correlated with the electric field intensity distribution in the discharge zone, close to the plasma-dielectric interface (Figure 13.8). In fact, the spatial 3D distributions of these species in the discharge clearly follow the electric field pattern, demonstrating that electron collision processes play a dominant role in the active part of the plasma source. As observed, close to the interface the density distribution follows the field distribution; the maxima of the electron density coincide with those of the field. Azimuthal homogeneity at z = 25 mm, i.e. at the end of the discharge zone, is nearly achieved (Figure 13.9). It should be stressed that the experimental results confirm the main trends predicted by the model (Figure 13.10). To our knowledge these are the first experimental and theoretical results with 3D resolution concerning these plasma sources.

[2] Work carried out in collaboration with the Department of Electrical Engineering, Nagoya University (Japan).

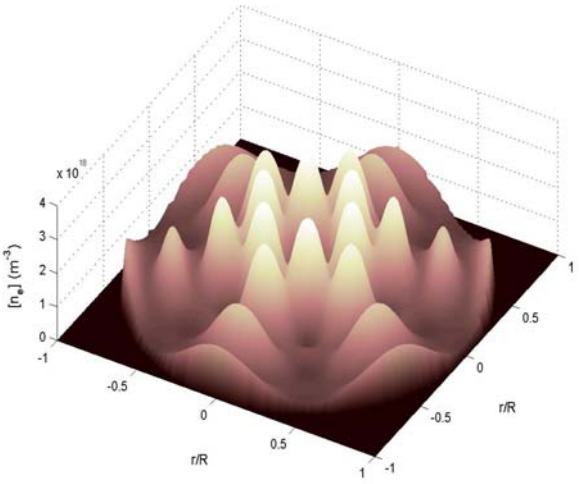

(z = 3 mm)

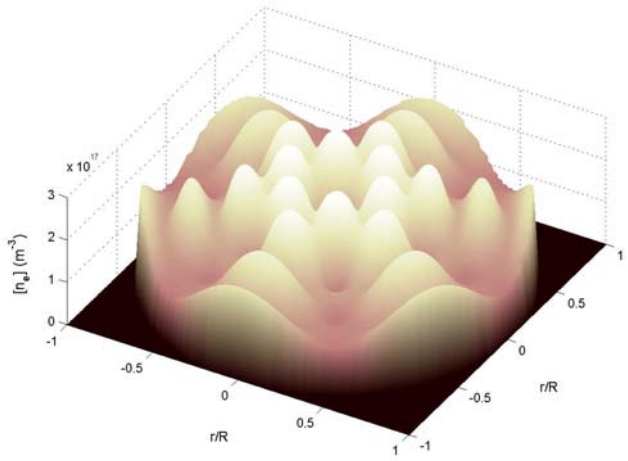

(z = 14 mm)

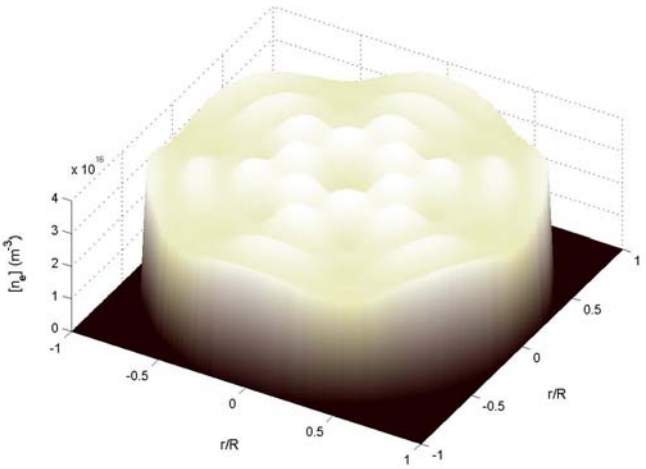

(z = 25 mm)

Figure 13.9 - 2D (r-φ) distribution of the electron density (a) z = 3 mm; (b) z = 14 mm; (c) z = 25 mm (p = 3 Torr, P = 600 W).

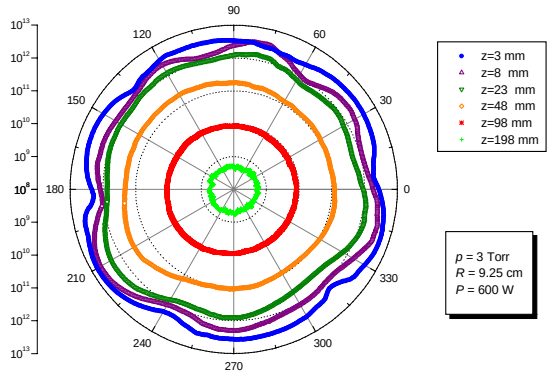

Figure 13.10 - Experimental axial dependence of the electron density azimuthal profile.

13.2.3.2. Afterglow studies

In recent years, there has been growing interest in the study of sterilization by afterglow plasmas due to the possibility of achieving such a process at relatively low temperatures. Plasma sterilization is an alternative to conventional sterilization systems in hospitals. Afterglows of flowing microwave discharges in N_2–O_2 to inactivate *Bacillus subtilis* spores have been the subject of preliminary studies by other groups[3]. It seems the spores are ultimately inactivated by UV photons, through destruction of their DNA strands. Simultaneously, the increased erosion of O_2 on the spores as time elapses reduces the number of photons required to reach the lethal dose. The action of O_2 probably results from the impinging of $O(^3P)$ atoms, while the action of UV radiation, as suggested by spectroscopic measurements, is due to the relatively strong intensity of the NOβ system bands (250–320 nm) emitted in the afterglow by NO(B) molecules. The major role attributed to UV photons in the sterilization process has also been confirmed.

In order to get physical insight into the processes occurring in these afterglow plasmas, we have developed detailed theoretical models first for pure nitrogen, which are currently being extended to N_2-O_2 . The kinetic model for the discharge starts with the determination of the electron energy distribution function (EEDF), the vibrational distribution functions (VDFs) of $N_2(X,v)$ and $O_2(X,v)$ molecules, the concentrations of N_2 and O_2 electronic states, N and O atoms, NO, NO_2 and O_3 species, and of the various positive and negative ions formed in the discharge. For atomic nitrogen, we consider both ground and excited states $N(^4S, ^2D, ^2P)$, whereas for oxygen we take into account atomic oxygen in the ground-state $O(^3P)$ only. Nitric oxides are also included with both ground and excited states, $NO(X, A, B)$ and $NO_2(X, A)$.

Figure 13.11 shows the calculated and measured concentrations of the first electronically excited metastable state $N_2(A)$ of nitrogen in the afterglow of a pure nitrogen microwave discharge operating at $(\omega/2\pi)$=433 MHz, in a Pyrex tube with inner radius R=1.9 cm, at a pressure p=440 Pa and flow rate Q=1.5 slpm. The data points were obtained by a French laboratory in Grenoble. This

[3] Work carried out in collaboration with the University of Montreal (Canada).

metastable state is an important energy carrier in the afterglow, and plays a crucial role in the post-discharge. It is very striking that an increase is observed in the population of $N_2(A)$ metastables in the field-free post-discharge. There must exist a local production of $N_2(A)$ molecules, which has been shown to be due to near resonant vibration-vibration (V-V) energy exchanges, followed by electronic-vibration (V-E) exchanges. The latter can be induced by collisions of highly vibrationally excited $N_2(X,v)$ molecules with both N atoms and electrons.

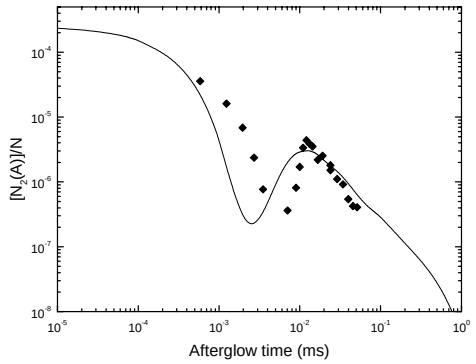

Figure 13.11 – Calculated and measured temporal evolution of the fractional concentration of $N_2(A)$ metastables in the afterglow of a microwave nitrogen discharge.

Once $N_2(A)$ states are created, they transfer energy to other states and to ionization. Therefore, many other excited states, as well as electrons and positive ions, have a similar profile during the afterglow. Figures 13.12 and 13.13 exhibit a comparison of calculations and measurements[4] for metastable $N(^2P)$ atoms and the radiative $N_2(B)$ state, respectively.

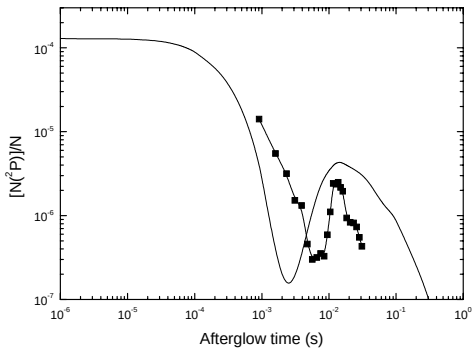

Figure 13.12 – Calculated and measured temporal evolution of the fractional concentration of $N(^2P)$ metastable in the afterglow of a microwave nitrogen discharge.

The detailed explanation of the energy transfers that take place in a nitrogen afterglow was a major achievement of our group. The knowledge obtained in the investigation of pure nitrogen plasmas is now being transferred to the more complicated case of a mixture N_2-O_2. The final goal is to understand the behaviour of such plasmas and to obtain the conditions that optimize the plasma sterilization process.

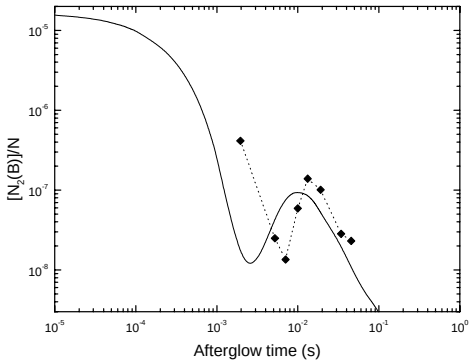

Figure 13.13 – Calculated and measured temporal evolution of the fractional concentration of the $N_2(B)$ radiative state in the afterglow of a microwave nitrogen discharge.

13.3. MODELLING OF PLASMA REACTORS

13.3.1. Introduction

Plasma Reactors (PR) are nowadays an essential tool used in different types of industrial chains with electronics, photovoltaic, optics, food industry, or surface modification. In recent years, new reactor configurations have been proposed in order to give adequate effective answers, according to the objectives of each application.

The main objective with this research line is the development of simulation tools to optimize, in an effective realistic way, the operation conditions of different PR's. The validation of such tools requires a strong interaction between modeling and experiment, without which it will not be possible to improve the understanding of the main mechanisms controlling discharge operation. Such interaction is ensured here through different collaborations with foreign research teams.

13.3.2. Modelling of a capacitively-coupled radio-frequency reactor[5]

Modeling of a capacitively-coupled radio-frequency (ccrf) reactor (Figure 13.14), based on low-pressure (p<1 Torr) pure hydrogen discharges, operating at frequencies up to 80 MHz, has been pursuit.

The systematic characterization of ccrf hydrogen discharges has been achieved, by comparing model results to experimental measurements for various electrical parameters (the self-bias voltage, the plasma potential and impedance, and the power coupled to the plasma), obtained at different rf applied voltages, frequencies and pressures (Figures 13.15 and 13.16). It was possible to simulate and control the development of Double Ionization Structures with hydrogen radio-frequency discharges, by inducing its occurrence in a modified hydrogen-like gas (Figure 13.17).

[4] Also performed in Grenoble, France.

[5] This research was carried out in collaboration with *the Laboratoire de Physique et Technologie des Plasmas*, (LPTP, Palaiseau, France) and the *Laboratoire de Physique des Gaz et des Plasmas* (LPGP, Orsay, France).

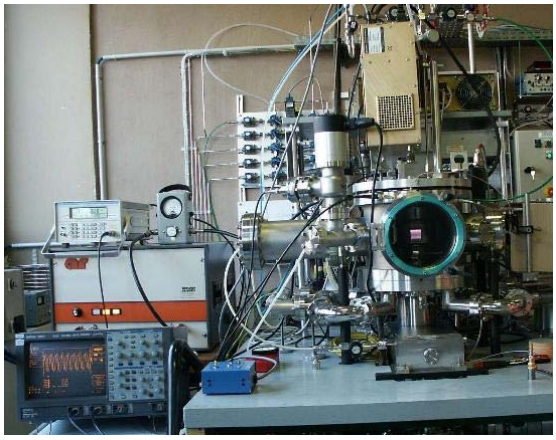

Figure 13.14 – Capacitively coupled radio-frequency reactor, (LPTP, Ecole Polytechnique, Palaiseau, France).

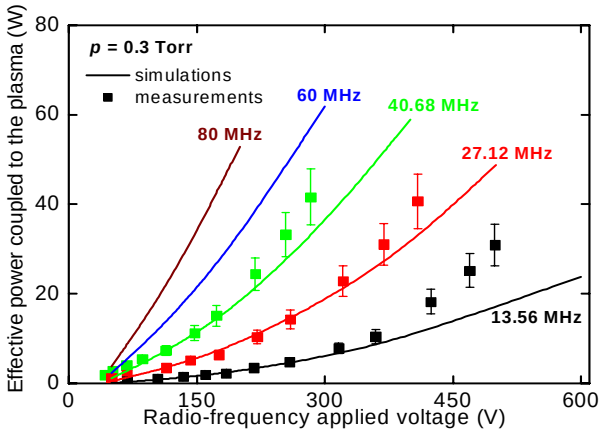

Figure 13.15 – Effective power coupled to the hydrogen plasma.

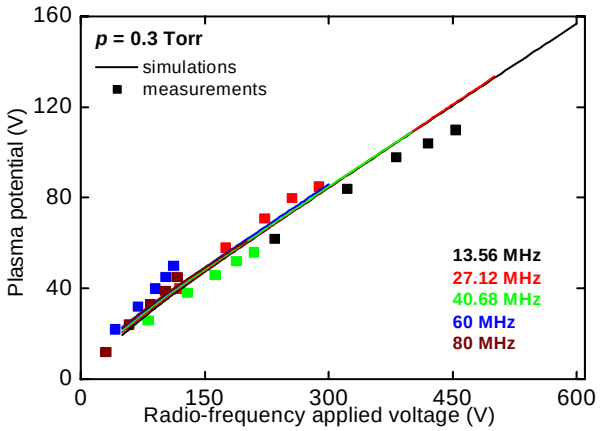

Figure 13.16 – Plasma potential at discharge axis.

The improvement of the comparison between measurements (obtained by probe measurements and LIF) and simulations for the densities of electrons and H-atoms, at different discharge operating conditions has been initiated (Figures 13.18 and 13.19). This goal requires the coupling between (i) a two-dimensional, time-dependent, collisional-radiative model (based on a solution to the Navier-Stokes / Saint-Venant equations), including the reactive multi-component diffusion transport of H(n=1-5) electronically excited atoms and $H_2(X^1\Sigma_g^+,v=0..14)$ vibrationally excited ground state molecules; and (ii) a two-dimensional, time-dependent, fluid code for the transport of charged particles (electrons and H^+, H_2^+, H_3^+ and H ions).

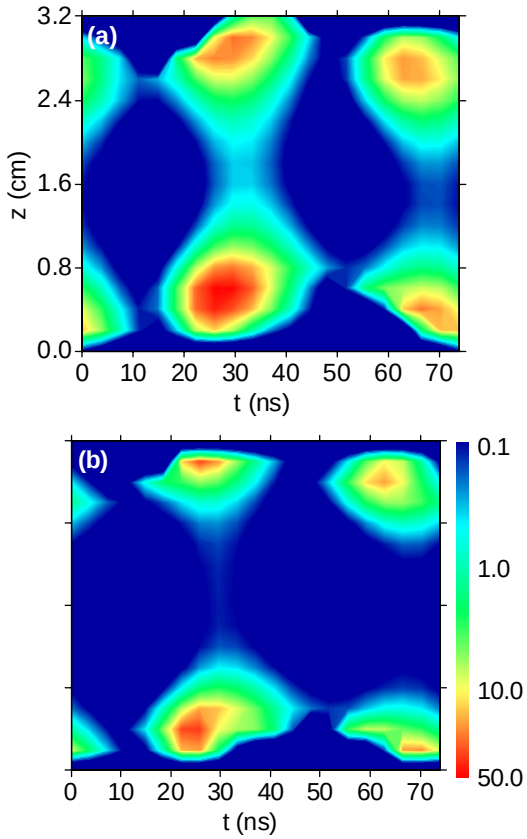

Figure 13.17 – Space-time variation (at discharge axis and during one rf cycle) with the ionization rate (in 10^{14} cm^{-3} s^{-1}), for a ccrf discharge operating at 13.56 MHz frequency, 217 V applied voltage and 1 torr pressure, in (a) standard hydrogen; (b) modified hydrogen adopting $\mu(H_3^+)/10$.

13.3.3. Theoretical and experimental studies of microwave excitation structures

The interplay between modeling and experiment in the characterization of microwave excitation structures, currently used in plasma reactors for thin films deposition, has been intensified. The following activities have been carried out: (i) probe measurements in order to determine, as a function of radial and axial positions, the electron energy distribution function, the electron density and the electron temperature; and (ii) spectroscopy measurements aiming at determining the relative populations of some excited states with the background gas.

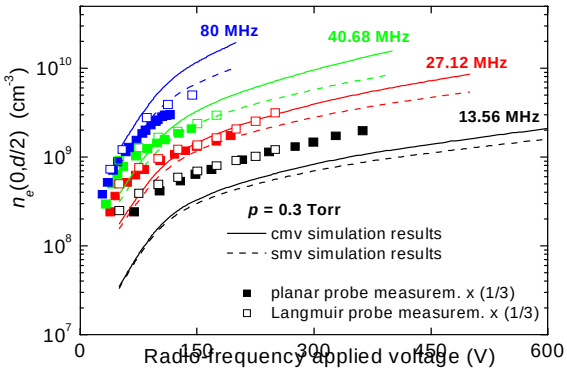

Figure 13.18 – Electron density at discharge axis, obtained with various model versions (cmv and svm).

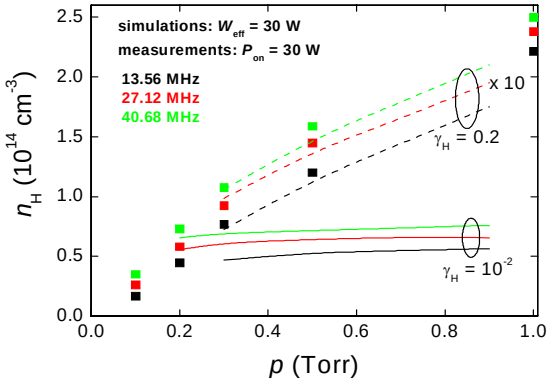

Figure 13.19 – H-atoms density, as a function of pressure, obtained at various wall-recombination coefficients (γ_H).

This task concerned the study of two excitation structures.

(i) A cylindrical excitation structure (corresponding to the sequence plasma-dielectric-air-metal of propagation media, within a 1cm tube radius), operating at 2.45 GHz frequency in argon, for intermediate pressures (~1Torr) and average electron densities around 10^{12} cm^{-3} [6].

(ii) A coaxial excitation structure (corresponding to the sequence metal-air-dielectric-plasma-metal of Torr) and average electron densities bellow 10^{12} cm^{-3} [7].

A collisional-radiative model (CRM) at 30 levels for the argon gas has been developed, proposing a new set of electron collision cross-sections and/or rate coefficients, for the direct and stepwise excitation/de-excitation of argon levels. The CRM results yield a general good agreement with spectroscopic measurements of different line intensity ratios with the 4p and 5p systems (Figure 13.22).

Figure 13.20 – Microwave reactor (cylindrical configuration), (ICMS, Sevilla, Spain).

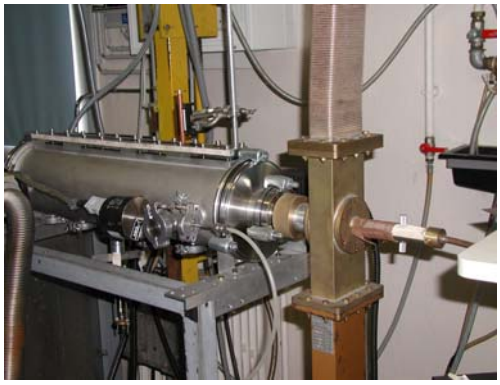

Figure 13.21 – Surface-wave discharge (coaxial configuration), (LPGP, Orsay, France).

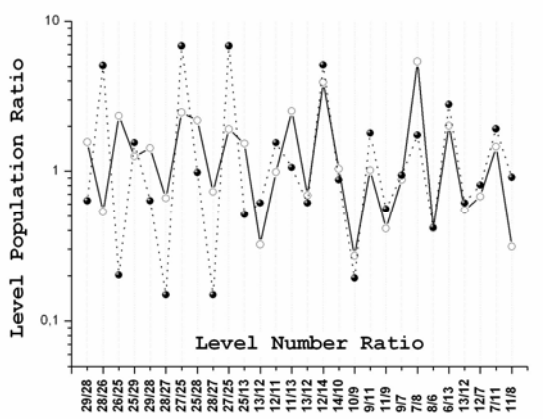

Figure 13.22 – Measured (solid line) and calculated (dashed) line intensity ratios, at 60 mTorr pressure and 400 W power.

[6]This research work was carried out in collaboration with the *Instituto de Ciencias de Materiales de Sevilla* (ICMS, Sevilla, Spain) and the *Facultad de Física* of the *Universidad de Sevilla*, under the framework of the *Acções Integradas Luso-Espanholas* (2003-2004 CRUP – CSIC's agreement, project E-51/02).

[7]This research work was developed in the framework of the *Acções Integradas de Cooperação Científica e Técnica Luso-Francesas* (2004 GRICES – EGIDE's agreement), with the *Laboratoire de Physique des Gaz et des Plasmas* (LPGP, Orsay, France).

Simulation of the electron density and temperature radial distributions within the microwave discharge has been achieved, by using a one-dimensional fluid code for the transport of charged particles. Model results were compared with probe measurements of these quantities (Figures 13.23 and 13.24)

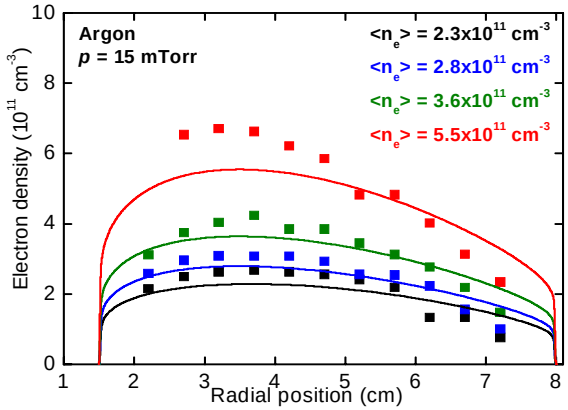

Figure 13.23 – Electron density radial profiles

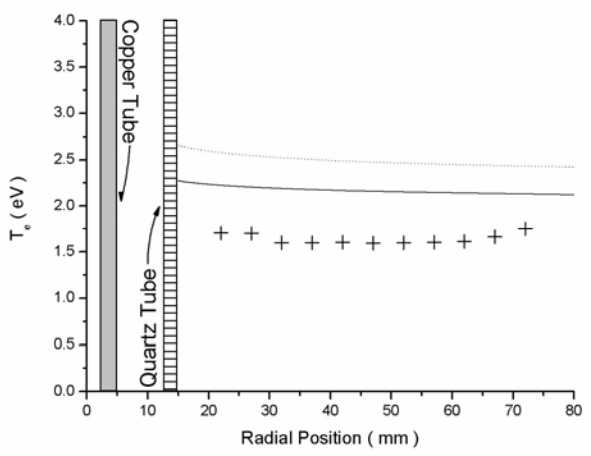

Figure 13.24 – Electron temperature radial profiles, at 30 mTorr pressure and 700 W power. Calculations were obtained with CRM (solid line), and without CRM (dotted).

First experimental evidence has been found, in support of model predictions, of the presence of supra-thermal electrons, issuing from a plasma-resonance region within the space-charge region, near the wall (Figures 13.25 and 13.26).

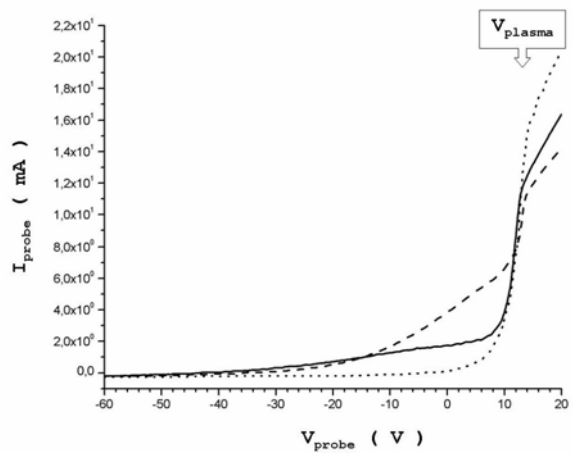

Figure 13.25 – Planar probe characteristics at a constant radial position of 2 mm, for 30 mTorr gas pressure and 200 W power, and for different probe orientations: solid line (radial), dashed (axial) and dotted (azimuthal).

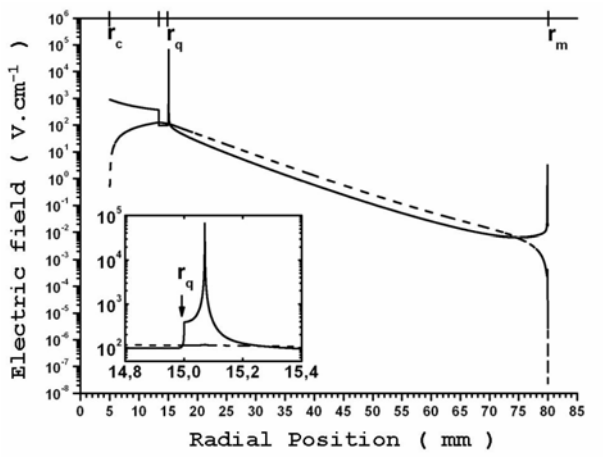

Figure 13.26 – Calculated radial distribution of the wave electric field components (Er, solid line; Ez, dashed), at 30 mTorr pressure and ~ 500 W power. The lower left graph is a blow-up of the inner resonance region.

14. OTHER ACTIVITIES

14.1. CENTRO DE FUSÃO NUCLEAR

14.1.1. Collaboration with Brazil

IST/CFN has proceeded with the collaboration on nuclear fusion with two Brazilian Institutions:

- Laboratório de Plasmas (LP), do Instituto de Física, da Universidade de São Paulo;
- Laboratório Associado de Plasmas (LAP), do Instituto Nacional de Pesquisas Espaciais, de São José dos Campos.

In 2004, a working programme for the collaboration between IST and IFUSP in nuclear fusion was elaborated, with activities on tokamak operation, control and data acquisition, diagnostics and MHD. The design of a microwave reflectometer for TCA/Br has been jointly performed. A joint project on "identification of local Alfvén wave resonances with reflectometry" to be submitted to the EFDA JET Close Support Unit and to the ASDEX-Upgrade Programme Committee has been elaborated. New software for the CFN VME transient recorder modules in operation on TAC/Br was made. Collaboration with LAP in the development of a multi-point Thomson scattering diagnostic for ETE has proceeded.

14.1.2. Organization of scientific meetings and exhibitions

- CFN has collaborated with IAEA on the organization of the "20th Fusion Energy Conference" (FEC-2004), held in Vilamoura, Portugal, in November 2004, with 604 participants from 32 countries.
- CFN organized an axhibition of the "EXPO Fusion", in Vilamoura, from 1 to 6 November 2004. The exhibition has been visited by about 500 students of secondary schools of the south of Portugal.
- Dr. Duarte Borba was member of the Programme Committee of FEC-2004.
- Dr. Carlos Silva was member of the Programme Committee of the "Workshop on the Role of Electric Field in Plasma Confinement and Exhaust".

14.1.3. Participation in the management of Fusion Programmes

- Some members of the IST/CFN staff are delegates to Committees of the European Fusion Programme and of the European Fusion Development Agreement (Table 14.1).
- Prof. Carlos Varandas is/was:
  - Chairman of the EFDA Steering Committee;
  - Vice-Chairman of the "CCE-FU[1] Special Working Group on Possible Joint Implementation of ITER";
  - Member of the Steering Committees of the Bilateral Agreements of EURATOM with Russia, Japan and the US Department of Energy;
  - Member of the European Union Delegation to the ITER negotiations.
- Prof. Horácio Fernandes and Dr. Paulo Varela were members of the JET Remote Participation Users Group.
- Dr. Duarte Borba was Deputy Leader of the JET Task Force M and Leader of the ASDEX-Upgrade Task Force on MHD.
- Prof. Fernando Serra is/was a member of:
  - Ad-Hoc Group for the Monitoring of 2003 and Overview of 2003 EFDA Technology Activities: Diagnostic;
  - Ad-Hoc Group from STAC for the "Monitoring of W7-X project";
  - Member of the ITPA (International Tokamak Physics Activity) Topical Group on Diagnostics.
- Prof. Maria Emília Manso was:
  - Member of the Programme Committee of the ASDEX-Upgrade project;
  - Chairperson of the International Advisory Board on Reflectometry.

14.2. CENTRO DE FÍSICA DOS PLASMAS

14.2.1. Organization of scientific meetings and exhibitions

- Prof. Matos Ferreira was:
  - Chairman of an exhibition called "À luz de Einstein 1905-2005", organized in the frame of the "2005 World Year of Physics", in collaboration with Fundação Calouste Gulbenkian.;
  - Member of the International Advisory Board of International Summer School on Vacuum, Electron and Ion Technology organized by Bulgarian Academy of Sciencies and Institute of Ion Beam Physics and Materials Research, Rossendorf Centre (Germany);
  - Member of the International Scientific Committee of International Workshop: Microwave Discharges, Fundamentals and Applications;
- Profs. Luís Silva, João Mendanha Dias and Ricardo Fonseca and Dr. Gonçalo Figueira are also members of the Organizing team of the exhibition "À luz de Einstein 1905-2005".
- Prof. V. Guerra was member of the International Scientific Committee European Conference on Atomic and Molecular Physics of Ionized Gases (ESCAMPIG).

[1] CCE-FU means "Consultative Committee for the EURATOM Specific Research and Training Programme in the Field of Nuclear Energy Fusion

- Prof. Tito Mendonça was co-chairman of the Workshop on Theoretical Plasma Physics, Abdus Salam ICTP Trieste
- Prof. Luís Silva:
  - Was appointed member of the Programme Committee of the 47th Annual Meeting of the Division of Plasma Physics of the American Physical Society
  - Is member of the Scientific Committee of the Workshop on Laser and Plasma Accelerators, and member of the Scientific Committee of the International Workshop on Fast Ignition and High-Field Physics.

14.2.2. Participation in the management of International Programmes

- Prof. Tito Mendonça is member of the Inertial Fusion Energy Coordinating Committee (Table 14.1).
- Prof. Matos Ferreira is member of:
  - COST Technical Committee on Physics;
  - Academia Europeia of the European Physical Society.

14.2.3. Prizes and Awards

- Prof Luis Silva was the recipient of the 2003 IBM Scientific Prize.
- Mr Nuno Brites was the recipient of the Prémio António da Silveira 2004.
- Prof. Tito Mendonça and Prof. Luis Silva are Fellows of the Centre for Fundamental Physics, Rutherford Appleton Laboratory.

Name	Member of
Carlos Varandas	CCE-FU
	EFDA Steering Committee
	FTC[2]
	CFI[3]
	STC[4]
	EFDA Technology Sub-Committee
Maria Emília Manso	CCE-FU
	EFDA Steering Committee
	EFDA Public Information Sub-Committee
Fernando Serra	STAC[5]
	EFDA/PIG[6]
J.P. Bizarro	STAC
P. Silva	STC
	EFDA Technology Sub-Committee
Carlos Silva	AFAC[7]
J.T. Mendonça	IFEC[8]

Table 14.1 – Participation of members of the Association EURATOM/IST on the management of the European Fusion Programme and of the European Fusion Development Agreement

[2] FTC means "Fusion Technology Committee"
[3] CFI means "Committee Fusion Industry"
[4] STC means "Scientific and Technical Committee"
[5] STAC means "Scientific and Technical Advisory Committee"
[6] PIG means "Public Information Group"
[7] AFAC means "Administrative and Financial Advisory Committee"
[8] IFEC means "Inertial Fusion Energy Committee"

15. PUBLICATIONS

15.1. CENTRO DE FUSÃO NUCLEAR

15.1.1. Ph.D thesis

- *"Edge density studies of ELMy H-modes in ASDEX Upgrade using reflectometry"*
  Isabel Nunes, June 2004
  Universidade Técnica de Lisboa

15.1.2. Master thesis

- *"Operação e controlo remoto do sistema de reflectometria do tokamak ASDEX Upgrade"*
  Sílvia Graça, November 2004
  Universidade Técnica de Lisboa

15.1.3. Articles in scientific journals

- *"Real-time motional Stark effect in JET"*
  Alves, D., A. Stephen, N. Hawkes, S. Dalley, A. Goodyear, R. Felton, E. Joffrin, H. Fernandes, EFDA-JET contributers
  Fusion Engineering and Design, 71**,** 175, 2004

- *"Li ceramic pebbles chemical compatibility with Eurofer samples in fusion relevant conditions"*
  Alves, L.C., E. Alves, M.R. da Silva, A. Paúl, A. La Barbera
  Journal of Nuclear Materials B 329-33, 1295-1299, 2004.

- *"JET divertor geometry and plasma shape effects on the L-H transition threshold"*
  Andrew, Y., N.C. Hawkes, M.G.O'Mullane, R. Sartori, M. de Baar, I Coffey, K. Guenther, I Jenkins, A. Korotkov, P. Lomas, G.F. Matthews, A. Matilal, R. Prentice, M. Stamp, J. Strachan, P. de Vries and JET-EFDA Contributors
  Plasma Physics and Controlled Fusion, 46**,** (5), A87, 2004

- *"Edge ion parameters at the L-H transition on JET"*
  Andrew, Y., N.C. Hawkes, M.G.O' Mullane, R. Sartori, M.N.A. Beurskens, I. Coffey, E. Joffrin, A. Loarte, D.C. McDonald, R. Prentice, G. Saibene, W. Suttrop, K-D Zastrow and JET EFDA Contributers.
  Plasma Physics and Controlled Fusion, 46**,** (2), 337, 2004

- *"Density response to central electron heating: theoretical investigations and experimental observations in ASDEX Upgrade"*
  Angioni, C., A.G. Peeters, X. Garbet, A. Manini, F. Ryter and ASDEX Upgrade Team.
  Nuclear Fusion, 44**,** (8), 827, 2004

- *"Scintillator probe for lost alpha measurements in JET"*
  Baeumel, S., A. Werner, R. Semler, S. Mukherjee, D.S. Darrow, R. Ellis, F.E. Cecil, L. Pedrick, H. Altmann, V. Kiptily, J. Gafert, and JET-EFDA Contributors.
  Review of Scientific Instruments, 75, (10)**,** 3563, 2004

- *"On the link between the q-profile and internal transport barriers"*
  Baranov, Yu F., X. Garbet, N.C. Hawkes, B. Alper, R. Barnsley, C.D. Challis, C. Giroud, E. Joffrin, M. Mantsinen, F. Orsitto, V. Parail, S.E. Sharapov and the JET-EFDA contributers
  Plasma Physics and Controlled Fusion, 46**,** (8), 1181, 2004

- *"Design study for International Thermonuclear Experimental Reactor high resolution x-ray spectroscopy array"*
  Barnsley, R., M. O'Mullane, L.C. Ingesson, A. Malaquias.
  Review of Scientific Instruments, 75, (10)**,** 3743, 2004

- *"A test-bench for the real-time project phase 2 of JET"*
  Batista, A.J.N., H. Fernandes, J. Sousa, C.A.F. Varandas, E. Joffrin, R. Felton, J. Farthing
  Fusion Engineering and Design, 71**,** 83, 2004

- *"Impurity penetration through the edge transport barrier"*
  Belo, P., V. Parail, G. Corrigan, D. Heading, W. Houlberg, P. Monier-Garbet, J. Ongena and the JET-EFDA contributers
  Plasma Physics and Controlled Fusion, 46**,** (8), 1299, 2004

- *"Multipoint Thomson scattering diagnostic for the ETE tokamak"*
  Berni, L.A., M.P. Alonso, R.M. Oliveira.
  Review of Scientific Instruments, 75, (10)**,** 3884, 2004

- *"Improvement of the T_e profile on Joint European Torus measured by electron cyclotron emission"*
  Blanchard, P., Elena de la Luna, C. Gowers, and JET-EFDA Contributors.
  Review of Scientific Instruments, 75, (10)**,** 3828, 2004

- *"Two-dimensional full-wave code for reflectometry simulations in TJ-II"*
  Blanco, E., S. Heuraux, T. Estrada, J. Sánchez, L. Cupido.
  Review of Scientific Instruments, 75, (10)**,** 3822, 2004

- *"High frequency MHD activity related to type I ELMs in ASDEX Upgrade"*
  Bolzonella, T., H. Zohm, M. Maraschek, E. Martines, S. Saarelma, S. Günter and ASDEX Upgrade Team
  Plasma Physics and Controlled Fusion, 46**,** (5), A143, 2004

- *"First MeV ion loss measurements using activation technique in reversed B experiments at JET"*
  Bonheure, G., S. Popovichev, L. Bertalot, A. Murari, S. Conroy, and JET-EFDA Contributors.
  Review of Scientific Instruments, 75, (10)**,** 3540, 2004

- *"Destabilization of TAE modes using ICRH in ASDEX Upgrade"*
  Borba, D., G.D. Conway, S. Günter, G.T.A. Huysmans, S. Klose, M. Maraschek, A. Mück, I. Nunes, S.D. Pinches, F. Serra and the ASDEX Upgrade Team
  Plasma Physics and Controlled Fusion, 46**,** (5), 809, 2004

- *"Recent H-mode density limit studies at JET"*
  Borras, K., A. Loarte, C.F. Maggi, V. Mertens, P. Monier,

R. Monk, J. Ongena, J. Rapp, G. Saibene, R. Sartori, J. Schweinzer, J. Stober, W. Suttrop and EFDA-JET Workprogramme contributers
Nuclear Fusion, 44**,** (7), 752, 2004

- *"On the interpretation of fluctuation and ExB turbulent transport measured by Langmuir probes in fusion plasmas"*
  Calderón, E., C. Hidalgo, M.A. Pedrosa and C. Silva.
  Review of Scientific Instruments, 75, (10)**,** 4293, 2004

- *"A high performance reconfigurable hardware platform for digital pulse processing"*
  Cardoso, J.M., J.B. Simoes, C.M.B.A. Correia, A. Combo, R. Pereira, J. Sousa, N. Cruz, P. Carvalho, C.A.F. Varandas,
  IEEE Transactions on Nuclear Science, Vol. 51, issue 3, June 2004

- *"Real-time DSP-based shape determination and plasma position control in the ISTTOK tokamak"*
  Carvalho, B., H. Fernandes, C. Silva, D. Borba, C.A.F. Varandas
  Fusion Engineering and Design, 71, 77, 2004

- *"Real-time digital signal processor-based system for MHD mode identification in ISTTOK"*
  Carvalho, B.B., H. Fernandes, J. Sousa and C.A.F. Varandas.
  Review of Scientific Instruments, 75, (10)**,** 4265, 2004

- *"Design of the new magnetic sensors for Joint European Torus"*
  Coccorese, V., R. Albanese, H. Altmann, S. Cramp, T. Edlington, K. Fullard, S. Gerasimov, S. Huntley, N. Lam, A. Loving, V. Riccardo, F. Sartori, C. Marren, E. McCarron, C. Sowden, J. Tidmarsh, F. Basso, A. Cenedese, G. Chitarin, F. DegliAgostini, L. Grando, D. Marcuzzi, S. Peruzzo, N. Pomaro, E.R. Solano and JET-EFDA Contributors.
  Review of Scientific Instruments, 75, (10)**,** 4311, 2004

- *"Bifurcation of generic metastable tearing modes interacting with resonant magnetic fields"*
  Coelho, R. and E. Lazzaro
  Physics of Plasmas 11, 1440, 2004

- *"First tritium operation of ITER-prototype VUV spectroscopy on JET"*
  Coffey, I.H., R. Barnsley and JET EFDA Contributors.
  Review of Scientific Instruments, 75, (10)**,** 3737, 2004

- *"A PCI transient recorder module for the JET magnetic proton recoil neutron spectrometer"*
  Combo, A., R. Pereira, J. Sousa, N. Cruz, P. Carvalho, C.A.F. Varandas, S. Conroy, J. Källne, M. Weiszflog
  Fusion Engineering and Design, 71**,** 151, 2004

- *"Plasma rotation profile measurements using Doppler reflectometry"*
  Conway, G.D., J. Schirmer, S. Klenge, W. Sutrop, E. Holzhauer and the ASDEX Upgrade Team
  Plasma Physics and Controlled Fusion, 46**,** (6), 951, 2004

- *"A low-cost galvanic isolated fast PCI transient recorder with signal processing capabilities"*
  Correia, M., A.J.N. Batista, A. Combo, N. Cruz, P. Carvalho, C. Correia, J. Sousa, C.A.F. Varandas
  Fusion Engineering and Design, 71**,** 159, 2004

- *"Calibration of the charge exchange recombination spectroscopy diagnostic for core poloidal rotation velocity measurements on JET"*
  Crombé, K., Y. Andrew, C. Giroud, N.C. Hawkes, A. Murari, M. Valisa, G. Van Oost, K.-D. Zastrow and JET-EFDA Contributors.
  Review of Scientific Instruments, 75, (10)**,** 3452, 2004

- *"A large memory VME data acquisition system for the jet heterodyne radiometer upgrade"*
  Cruz, N., J. Sousa, R. Pereira, A. Combo, C.A.F. Varandas, M. Beldishevski, S. Dorling, B. Alper, contributers of the EFDA-JET work programme
  Fusion Engineering and Design, 71**,** 167, 2004

- *"Frequency hopping millimeter wave reflectometer"*
  Cupido, L., J. Sánchez and T. Estrada.
  Review of Scientific Instruments, 75, (10)**,** 3865, 2004

- *"Methods for the mitigation of the chemical reactivity of beryllium in steam"*
  Druyts F, Alves EC, Wu CH
  Journal of Nucleal Materials B 329-33, 1353-1356, 2004.

- *"Impurity transport in internal transport barrier discharges on JET"*
  Dux, R., C. Giroud, K.-D. Zastrow and the JET-EFDA contributers
  Nuclear Fusion, 44**,** (2), 260, 2004

- *"Spurious oscillations affecting FIR polarimetry measurements"*
  Elbèze, D., C. Gil, R. Giannella, L. De Pasqual and JET-EFDA Contributors
  Review of Scientific Instruments, 75, (10)**,** 3405, 2004

- *"Neutron measurements on Joint European Torus using an NE213 scintillator with digital pulse shape discrimination"*
  Esposito, B., L. Bertalot, D. Marocco, M. Riva, Y. Kaschuck, S. Skopintsev, A. Zimbal, M. Reginatto, H. Schuhmacher, J.M. Adams, A. Murari, and JET-EFDA Contributors.
  Review of Scientific Instruments, 75, (10)**,** 3550, 2004

- *"Time-frequency analysis of non-stationary signals in fusion plasmas using the Choi-Williams distribution"*
  Figueiredo, A.C.A., M.F.F. Nave and EFDA-JET Contributers
  Nuclear Fusion, 44, (10), L17, 2004

- *"Time-frequency analysis of nonstationary fusion plasma signals: A comparison between the Choi-Williams distribution and wavelets"*
  Figueiredo, A.C.A, M.F.F. Nave and EFDA-JET Contributors.
  Review of Scientific Instruments, 75, (10)**,** 4268, 2004

- *"Electron emissive electrode for the plasma biasing experiment on tokamak ISTTOK"*
  Figueiredo, H., I.S. Nedzelskiy, C. Silva, C.A.F. Varandas, J.A.C. Cabral and R.M.O. Galvão.
  Review of Scientific Instruments, 75, (10)**,** 4240, 2004

- *"Boundary plasma energy transport in JET ELMy H-modes"*
  Fundamenski, W., S. Sipilä and the JET-EFDA contributers
  Nuclear Fusion, 44**,** (1), 20, 2004

- *"Physics of transport in tokamaks"*
  Garbet, X., P. Mantica, C. Angioni, E. Asp, Y. Baranov, C. Bourdelle, R. Budny, F. Crisanti, G. Cordey, L. Garzotti, N. Kirneva, D. Hogeweij, T. Hoang, F. Imbeaux, E. Joffrin, X. Litaudon, A. Manini, D.C. McDonald, H. Nordman, V. Parail, A. Peeters, F. Ryter, C. Sozzi, M. Valovic, T. Tala, A. Thyagaraja, I. Voisekhovitch, J. Weiland, H. Weisen, A. Zabolotsky and the JET EFDA Contributors
  Plasma Physics Controlled Fusion 46, (12B), B557, 2004

- *"Profile stiffness and global confinement"*
  Garbet, X., P. Mantica, F. Ryter, G. Cordey, F. Imbeaux, C. Sozzi, A. Manini, E. Asp, V. Parail, R. Wolf and the JET-EFDA contributers
  Plasma Physics and Controlled Fusion, 46**,** (9), 1351, 2004

- *"Regime identification in ASDEX Upgrade"*
  Giannone, L., A.C.C. Sips, O. Kardaun, F. Spreitler, W. Suttrop and the ASDEX Upgrade Team
  Plasma Physics and Controlled Fusion, 46**,** (5), 835, 2004

- *"Operation of a multiple cell array detector in plasma experiments with a heavy ion beam diagnostic"*
  Gonçalves, B., A. Malaquias, I.S. Nedzelskiy, L. Pereira, C. Silva, C.A.F. Varandas, J.A.C. Cabral, S.M. Khrebtov, N.B. Dreval, L.I. Krupnik, C. Hidalgo and J. Depablos.
  Review of Scientific Instruments, 75, (10)**,** 3511, 2004

- *"Hybrid advanced scenarios: perspectives for ITER and new experiments with dominant RF heating"*
  Gormezano, C., A. Becoulet, P. Buratti, L. Carraro, F. Crisanti, B. Esposito, G. Giruzzi, R. Guirlet, G.T. Hoang, E. Joffrin, X. Litaudon, T. Luce, V. Pericoli-Ridolfini, O. Sauter, A.C.C. Sips, A. Tuccillo and JET EFDA Contributors
  Plasma Physics Controlled Fusion 46, (12B), B435, 2004

- *"Upgrade to the control system of the reflectometry diagnostic of ASDEX Upgrade"*
  Graça, S., J. Santos, M.E. Manso and CFN Reflectometry Team.
  Review of Scientific Instruments, 75, (10)**,** 3852, 2004

- *"Approximate method to extract the pure Faraday and Cotton-Mouton effects from polarimetry measurements in a tokamak"*
  Guenther, K. and JET-EFDA contributers
  Plasma Physics and Controlled Fusion, 46**,** (9), 1423, 2004

- *"The frequency interrupted regime of neoclassical tearing modes (FIR-NTMs): required plasma parameters and possibilities for its active control"*
  Günter, S., M. Maraschek, M. De Baar, D.F. Howell, E. Poli, E. Strumberger, C. Tichmann and the ASDEX Upgrade Team
  Nuclear Fusion, 44**,** (4), 524, 2004

- *"Upgrade of the X-mode reflectometry diagnostic for radial correlation measurements in the Joint European Torus"*
  Hacquin, S., L. Meneses, L. Cupido, N. Cruz, L. Kokonchev, R. Prentice, C. Gowers.
  Review of Scientific Instruments, 75, (10)**,** 3834, 2004

- *"Comparison of m=2,n=1 neo-classical tearing mode limits in JET and DIII-D"*
  Hender, T.C., D.F. Howell, R.J. Buttery, O. Sauter, F. Sartori, R.J. La Haye, A.W. Hyatt, C.C. Petty, JET-EFDA contributers and the DIII-D team
  Nuclear Fusion, 44**,** (7), 788, 2004

- *"Power deposition outside the divertor in ASDEX Upgrade"*
  Herrmann, A., T. Eich, V. Rohde, C.J. Fuchs and J. Neuhauser and the ASDEX Upgrade Team
  Plasma Physics and Controlled Fusion, 46**,** (6), 971, 2004

- *"Improved confinement regimes induced by limiter biasing in the TJ-II stellarator"*
  Hidalgo, C., M.A. Pedrosa, N. Dreval, K.J. McCarthy, L. Eliseev, M.A. Ochando, T. Estrada, I. Pastor, E. Ascasíbar, E. Calderón, A. Cappa, A.A. Chmyga, A. Fernández, B. Gonçalves, J. Herranz, J.A. Jiménez, S.M. Khrebtov, A.D. Komarov, A.S. Kozachok, L. Krupnik, A. López-Fraguas, A. López-Sánchez, A.V. Melnikov, F. Medina, B. van Milligen, C. Silva, F. Tabarés and D. Tafalla
  Plasma Physics and Controlled Fusion, 46**,** (1), 287, 2004.

- *"A high throughput spectrometer system for helium ash detection on JET"*
  Hillis, D.L., D.T. Fehling, R.E. Bell, D.W. Johnson, K.-D. Zastrow, A. Meigs, C. Negus, C. Giroud, M. Stamp, and JET-EFDA Contributors.
  Review of Scientific Instruments, 75, (10)**,** 3449, 2004

- *"ITER-relevant H-mode physics at ASDEX Upgrade"*
  Horton, L.D., G.D. Conway, A.W. Degeling, T. Eich, A. Kallenbach, P.T. Lang, J.B. Lister, A. Loarte, Y.R. Martin, P.J. McCarthy, H. Meister, J. Neuhauser, J. Schirmer, A.C.C. Sips, W. Suttrop and the ASDEX Upgrade Team
  Plasma Physics Controlled Fusion 46, (12B), B511, 2004

- *"Optimization of the lines of sight of the ITER x-ray crystal spectrometer diagnostic"*
  Ingesson, L.C., R. Barnsley, A. Malaquias, M. O'Mullane.
  Review of Scientific Instruments, 75, (10)**,** 3696, 2004

- *"Arrangement of emissive and cold probes for fluctuation and Reynolds stress measurements"*
  Ionita, C., P. Balan, R. Schrittwieser, H.F.C. Figueiredo, C. Silva, C.A.F. Varandas and R.M.O. Galvão.
  Review of Scientific Instruments, 75, (10)**,** 4331, 2004

- *"EDGE2D modeling of edge profiles obtained in JET diagnostic optimized configuration"*
  Kallenbach, A., Y. Andrew, M. Beurskens, G. Corrigan, T.

Eich, S. Jachmich, M. Kempenaars, A. Korotkov, A. Loarte, G. Matthews, P. Monier-Garbet, G. Saibene, J. Spence, W. Suttrop and JET-EFDA Contributers.
Plasma Physics and Controlled Fusion, 46**,** (3), 431, 2004

- *"Comparison of multialkali and GaAs photocathode detectors for Joint European Torus edge light detection and ranging Thomson scattering profiles"*
  Kempenaars, M., P. Nielsen, R. Pasqualotto, C. Gowers, M. Beurskens and JET-EFDA Contributors.
  Review of Scientific Instruments, 75, (10)**,** 3894, 2004

- *"Toroidal interferometer/polarimeter density measurement system on ITER"*
  Kondoh, T., A.E. Costley, T. Sugie, Y. Kawano, A. Malaquias, C.I. Walker.
  Review of Scientific Instruments, 75, (10)**,** 3420, 2004

- *"Frequency control of type-I ELMs by magnetic triggering in ASDEX Upgrade"*
  Lang, P.T., A.W. Degeling, J.B. Lister, Y.R. Martin, P.J. McCarthy, A.C.C. Sips, W. Suttrop, G.D. Conway, L. Fattorini, O. Gruber, L.D. Horton, A. Herrmann, M.E. Manso, M. Maraschek, V. Mertens, A. Mück, W. Schneider, C. Sihler, W. Treutterer, H. Zohm and ASDEX Upgrade Team
  Plasma Physics and Controlled Fusion, 46**,** (11), L31, 2004

- *"ELM pace making and mitigation by pellet injection in ASDEX Upgrade"*
  Lang, P.T., G.D. Conway, T. Eich, L. Fattorini, O. Gruber, S. Günter, L.D. Horton, S. Kalvin, A. Kallenbach, M. Kaufmann, G. Kocsis, A. Lorenz, M.E. Manso, M. Maraschek, V. Mertens, J. Neuhauser, I. Nunes, W. Suttrop, H. Urano and the ASDEX Upgrade Team.
  Nuclear Fusion, 44**,** (5), 665, 2004

- *"Characterization of pedestal parameters and edge localized mode energy losses in the Joint European Torus and predictions for the International Thermonuclear Experimental Reactor "*
  Loarte, A., G. Saibene, R. Sartori, T. Eich, A. Kallenbach, W. Suttrop, M. Kempenaars M. Beurskens, M. de Baar, J. Lönnroth, P.J. Lomas, G. Matthews, W. Fundamenski, V. Parail, M. Becoulet, P. Monier-Garbet, E. de la Luna, B. Gonçalves, C. Silva, Y. Corre and Contributers to the EFDA-JET Workprogramme.
  Physics of Plasmas, 11, Nº 5**,** 2668, 2004

- *"Predictive modeling of ELMy H-modes with a new theory-motivated model for ELMs"*
  Lönnroth, J-S, V. Parail, C. Figarella, X. Garbet, G. Corrigan, D. Heading and JET-EFDA Contributers
  Plasma Physics and Controlled Fusion, 46**,** (5), A249, 2004

- *"Predictive transport modeling and MHD stability analysis of mixed type I-II ELMy H-mode JET plasmas"*
  Lönnroth, J-S, V. Parail, G. Huysmans, G. Saibene, H. Wilson, S. Sharapov, G. Corrigan, D. Heading, R. Sartori, M. Bécoulet and JET-EFDA contributers
  Plasma Physics and Controlled Fusion, 46**,** (5), 767, 2004

- *"Predictive transport modeling of type I ELMy H-mode dynamics using a theory-motivated combined ballooning-peeling model"*
  Lönnroth, J-S, V. Parail, A. Dnestrovskij, C. Figarella, X. Garbet, H. Wilson and the JET-EFDA contributers
  Plasma Physics and Controlled Fusion, 46**,** (8), 1197, 2004

- *"Electron cyclotron emission radiometer upgrade on the Joint European Torus (JET) tokamak"*
  Luna, E. de la, J. Sánchez, V. Tribaldos, G. Conway, W. Suttrop, J. Fessey, R. Prentice, C. Gowers, J.M. Chareau, and JET-EFDA Contributors.
  Review of Scientific Instruments, 75, (10)**,** 3831, 2004

- *"Studies of burning plasma physics in the Joint European Torus"*
  Mayoral, M.L., R. Buttery, T.T.C. Jones, V. Kiptily, S. Sharapov, M.J. Mantsinen, S. Coda, O. Sauter, L.G. Eriksson, F. Nguyen, D.N. Borba, A. Mück, S.D. Pinches, J.M. Noterdaeme and JET-EFDA Contributers
  Physics of Plasmas, 11, Nº 5**,** 2607, 2004

- *"Active beam spectroscopy diagnostics for ITER: Present status"*
  Malaquias, A., M. von Hellermann, S. Tugarinov, P. Lotte, N. Hawkes, M. Kuldkepp, E. Rachlew, A. Gorshkov, C. Walker, A. Costley and G. Vayakis
  Review of Scientific Instruments, 75, (10)**,** 3393, 2004

- *"Experimental study of electron heat transport in ion heated H-modes in ASDEX Upgrade"*
  Manini, A., F. Ryter, C. Angioni, A.G. Peeters, J. Stober, G. Tardini, M. Apostoliceanu, F. Leuterer, C.F. Maggi, D. Nishijima, A. Stäbler, W. Suttrop, D. Wagner and the ASDEX Upgrade Team
  Plasma Physics and Controlled Fusion, 46**,** (11), 1723, 2004

- *"Localized bulk electron heating with ICRF mode conversion in the JET tokamak"*
  Mantsinen, M.J., M.-L Mayoral, D. Van Eester, B. Alper, R. Barnsley, P. Beaumont, J. Bucalossi, I. Coffey, S. Conroy, M. de Baar, P. de Vries, K. Erents, A. Figueiredo, A. Gondhalekar, C. Gowers, T. Hellsten, E. Joffrin, V. Kiptily, P.U. Lamalle, K. Lawson, A. Lyssoivan, A. Lyssoivan, J. Mailloux, P. Mantica, F. Meo, F. Milani, I. Monakhov, A. Murari, F. Nguyen, J.-M. Noterdaeme, J. Ongena, Yu. Petrov, E. Rachlew, V. Riccardo, E. Righi, F. Rimini, M. Stamp, A.A. Tuccillo, K.-D. Zastrow , M. Zerbini and the JET-EFDA contributers
  Nuclear Fusion, 44**,** (1), 33, 2004

- *"The beta scalling of energy confinement in ELMy H-modes in JET"*
  McDonald, D.C., J.G. Corday, C.C. Petty, M. Beurskens, R. Budny, I. Coffey, M. de Baar, C. Giroud, E. Joffrin, P. Lomas, A. Meigs, J. Ongena, G. Saibene, R. Sartori, I Voitsekhovitvh and JET-EFDA contributers
  Plasma Physics and Controlled Fusion, 46**,** (5), A215, 2004

- *"ELMY H-modes in JET helium-4 plasmas"*
  McDonald, D.C., J.G. Cordey, E. Righi, F. Ryter, G. Saibene, R. Sartori, B. Alper, M. Becoulet, J. Brzozowski, I

Coffey, M. de Baar, P. de Vries, K. Erents, W. Fundamenski, C. Giroud, I Jenkins, A. Loarte, P.J. Lomas, G.P. Maddison, J. Mailloux, A. Murari, J. Ongena, J. Rapp, R.A. Pitts, M. Stamp, J. Strachan, W. Suttrop and JET-EFDA Contributers
Plasma Physics and Controlled Fusion, 46**,** (3), 519, 2004

- *"Z_{eff} from spectroscopic bremsstrahlung measurements at ASDEX Upgrade and JET"*
  Meister, H., R. Fischer, L.D. Horton, C.F. Maggi, D. Nishijima and ASDEX Upgrade Team, C. Giroud, K.-D. Zastrow, B. Zaniol and JET-EFDA Contributors.
  Review of Scientific Instruments, 75, (10)**,** 4097, 2004

- *"Plasma potential measurements by the heavy ion beam probe diagnostic in fusion plasmas: biasing experiments in the TJ-II stellarator and T-10 tokamak"*
  Melnikov, A.V., C. Hidalgo, A.A. Chmyga, N.B. Dreval, L.G. Eliseev, S.M. Khrebtov, A.D. Komarov, A.S. Kozachok, L.I. Krupnik, I. Pastor, M.A. Pedrosa, S.V. Perfilov, K. McCarthy, M.A. Ochando, G. Van Oost, C. Silva, B. Gonçalves, Yu. N. Dnestrovskij, S.E. Lysenko, M.V. Ufimtsev, and V.I. Tereshin
  Fusion Science and Technology, 46, Nº 2**,** 299, 2004

- *"On the use of MHD mode analysis as a technique for determination of q-profiles in JET plasmas"*
  Nave, M.F.F., D. Borba, R. Galvão, S. Hacquin, B. Alper, C. Challis, S. Gerasimov, N. Hawkes, J. Mailloux, S. Sharapov, C. Boswell, M. Brix, E. Joffrin, E. de la Luna, P. Smeulders and EFDA-JET Contributors.
  Review of Scientific Instruments, 75, (10)**,** 4274, 2004

- *"Time-of-flight energy analyzer for the plasma potential measurements by a heavy ion beam diagnostic"*
  Nedzelskiy, I.S., A. Malaquias, B. Gonçalves, C. Silva, C.A.F. Varandas, and J.A.C. Cabral.
  Review of Scientific Instruments, 75, (10)**,** 3514, 2004

- *"Characterization of the density profile collapse of type I ELMs in ASDEX Upgrade with high temporal and spatial resolution reflectometry"*
  Nunes, I., G.D. Conway, A. Loarte, M. Manso, F. Serra, W. Suttrop and the CFN and ASDEX Upgrade teams.
  Nuclear Fusion, 44**,** (8), 883, 2004

- *"Towards the realization on JET of an integrated H-mode scenario for ITER"*
  Ongena, J., P. Monier-Garbet, W. Suttrop, Ph. Andrew, M. Bécoulet, R. Budny, Y. Corre, G. Cordey, P. Dumortier, Th. Eich, L. Garzotti, D.L. Hillis, J. Hogan, L.C. Ingesson, S. Jachmich, E. Joffrin, P. Lang, A. Loarte, P. Lomas, G.P. Maddison, D. McDonald, A. Messiaen, M.F.F. Nave, G. Saibene, R. Sartori, O. Sauter, J.D. Strachan, B. Unterberg, M. Valovic, I. Voitsekhovitch, M. von Hellermann, B. Alper, Y. Baranov, M. Beurskens, G. Bonheure, J. Brzozowski, J. Bucalossi, M. Brix, M. Charlet, I. Coffey, M. De Baar, P. De Vries, C. Giroud, C. Gowers, N. Hawkes, G.L. Jackson, C. Jupen, A. Kallenbach, H.R. Koslowski, K.D. Lawson, M. Mantsinen, G. Matthews, F. Milani, M. Murakami, A. Murari, R. Neu, V. Parail, S. Podda, M.E. Puiatti, J. Rapp, E. Righi, F. Sartori, Y. Sarazin, A. Staebler, M. Stamp, G. Telesca, M. Valisa, B. Weyssow, K.D. Zastrow and the JET-EFDA contributers
  Nuclear Fusion, 44**,** (1), 124, 2004

- *"High resolution Thomson scattering for Joint European Torus (JET)"*
  Pasqualotto, R., P. Nielsen, C. Gowers, M. Beurskens, M. Kempenaars, T. Carsltrom, D. Johnson and JET-EFDA Contributors.
  Review of Scientific Instruments, 75, (10)**,** 3891, 2004

- *"Type-I ELM precursor modes in JET"*
  Perez, C.P., H.R. Koslowski, G.T.A Huysmans, T.C. Hender, P. Smeulders, B. Alper, E. de la Luna, R.J. Hastie, L. Meneses, M.F.F. Nave, V. Parail, M. Zerbini and JET-EFDA Contributers
  Nuclear Fusion, 44**,** (5), 609, 2004

- *"Study and optimization of lower hybrid wave coupling in advanced scenario plasmas in JET"*
  Pericoli, V., Ridolfini, A. Ekedahl, S.K. Erents, J. Mailloux, S. Podda, Y. Sarazin, A.A. Tuccillo and the EFDA-JET Workprogramme Contributers.
  Plasma Physics and Controlled Fusion, 46**,** (2), 349, 2004

- *"Spectroscopic determination of the internal amplitude of frequency sweeping TAE"*
  Pinches, S.D., H.L. Berk, M.P. Gryaznevich, S.E. Sharapov and JET-EFDA Contributers
  Plasma Physics and Controlled Fusion, 46**,** (7), S47, 2004

- *"The role of energetic particles in fusion plasmas"*
  Pinches, S.D., H.L. Berk, D.N. Borba, B.N. Breizman, S. Briguglio, A. Fasoli, G. Fogaccia, M.P. Gryaznevich, V. Kiptily, M.J. Mantsinen, S.E. Sharapov, D. Testa, R.G.L. Vann, G. Vlad, F. Zonca and JET-EFDA Contributors
  Plasma Physics Controlled Fusion 46, (12B), B187, 2004

- *"Predicting the behaviour of magnetic reconnection processes in fusion burning plasma experiments"*
  Porcelli, F., S.V. Annibaldi, D. Borgogno, P. Buratti, F. Califano, R. Coelho, E. Giovannozzi, D. Grasso, E. Lazzaro, F. Pegoraro, M. Ottaviani and A.I. Smolyakov
  Nuclear Fusion, 44**,** (2), 362, 2004

- *"Formation criteria and positioning of internal transport barriers in ASDEX Upgrade"*
  Quigley, E.D., A.G. Peeters, P.J. McCarthy, M. Apostoliceanu, J. Hobirk, V. Igochine, H. Meister and the ASDEX Upgrade Team
  Nuclear Fusion, 44, (11), 1189, 2004

- *"Lithium beam charge exchange diagnostic for edge ion temperature measurements at the ASDEX Upgrade tokamak"*
  Reich, M., E. Wolfrum, J. Schweinzer, H. Ehmler, L.D. Horton, J. Neuhauser and ASDEX Upgrade Team
  Plasma Physics and Controlled Fusion, 46**,** (5), 797, 2004

- *"Analysis of JET halo currents"*
  Riccardo, V., T.C. Hender, P.J. Lomas, B. Alper, T. Bolzonella, P. De Vries and G.P. Maddison and JET-EFDA Contributers

Plasma Physics and Controlled Fusion, 46**,** (6), 925, 2004

- *"Asymptotic, closed integral solutions for the reconstruction of Grad-Shafranov equilibria in axisymmetric, large-aspect-ratio toroidal plasmas"*
  Rodrigues, P. and J.P.S. Bizarro
  Physics of Plasmas, 11, 186, 2004.

- *"Dimensionless pedestal identity experiments in JT-60U and JET in ELMy H-mode plasmas"*
  Saibene, G., T. Hatae, D.J. Campbell, J.G. Cordey, E de la Luna, C. Giroud, K. Guenther, Y. Kamada, M.A.H. Kempenaars, A. Loarte, J. Lönnroth, D. Mc Donald, M.F.F. Nave, N. Oyama, V. Parail, R. Sartori, J. Stober, T. Suzuki, M. Takechi, K. Toi and JET-EFDA contributers.
  Plasma Physics and Controlled Fusion, 46**,** (5), A195, 2004

- *"Frequency modulation continuous wave reflectometry measurements of plasma position in ASDEX Upgrade ELMy H-mode regimes"*
  Santos, J., S. Hacquin, M. Manso and ASDEX Upgrade Team.
  Review of Scientific Instruments, 75, (10)**,** 3855, 2004

- *"Study of type III ELMs in JET"*
  Sartori, R., G. Saibene, L.D. Horton, M. Becoulet, R. Budny, D. Borba, A. Chankin, G.D. Conway, G. Cordey, D. McDonald, K. Guenther, M.G. von Hellermann, Yu Igithkanov, A. Loarte, P.J. Lomas, O. Pogutse, J. Rapp and JET-EFDA contributers
  Plasma Physics and Controlled Fusion, 46**,** (5), 723,

- "*Error estimation and parameter dependence of the calculation of the fast ion distribution function, temperature, and density using data from the KF1 high energy neutral particle analyzer on Joint European Torus"*
  Schlatter, C., D. Testa, M. Cecconello, A. Murari, M. Santala, and JET-EFDA Contributors.
  Review of Scientific Instruments, 75, (10)**,** 3547, 2004

- *"Monitoring Alfven cascades with interferometry on the JET tokamak"*
  Sharapov S E, Alper B, Fessey J, Hawkes N C, Young N P, Nazikian R, Kramer G J, Borba D N, Hacquin S, De La Luna E, Pinches S D, Rapp J, Testa D, JET-EFDA contributors
  Physical Review Letters, 93, 16, p.165001-1-4, 2004

- *"Influence of electrode and limiter biasing on the ISTTOK plasma"*
  Silva, C., H. Figueiredo, I. Nedzelsky, B. Gonçalves, J.A.C. Cabral, C.A.F. Varandas and G. Van Oost
  Plasma Physics and Controlled Fusion, 46**,** (1), 163, 2004

- *"Improved confinement events triggered by emissive electrode biasing on the tokamak ISTTOK"*
  Silva, C., I. Nedzelskiy, H. Figueiredo, R.M.O. Galvão, J.A.C. Cabral and C.A.F. Varandas
  Nuclear Fusion, 44**,** (7), 799, 2004

- *"Fluctuation measurements using a five-pin triple probe in the Joint European Torus boundary plasma"*
  Silva, C., B. Gonçalves, C. Hidalgo, M.A. Pedrosa, K. Erents, G. Matthews and R.A. Pitts.
  Review of Scientific Instruments, 75, (10)**,** 4314, 2004

- *"Global full-wave simulation of the Tore-Supra Doppler reflectometer"*
  Silva, F. da, S. Heuraux, N. Lemoine, C. Honoré, P. Hennequin, M. Manso, R. Sabot.
  Review of Scientific Instruments, 75, (10)**,** 3816, 2004

- *"A PCI time digitizer for the new JET time-of-flight neutron spectrometer"*
  Sousa, J., A.J.N. Batista, A. Combo, R. Pereira, N. Cruz, P. Carvalho, C.A.F. Varandas, S. Conroy, G. Ericsson, J. Källne
  Fusion Engineering and Design, 71**,** 101, 2004

- *"PCI data acquisition and signal processing hardware modules for long pulse operation"*
  Sousa, J., A.J.N. Batista, A. Combo, R. Pereira, M. Correia, N. Cruz, P. Carvalho, C. Correia and C.A.F. Varandas.
  Review of Scientific Instruments, 75, (10)**,** 4271, 2004

- *"Numerical investigations of axisymmetric equilibria with current holes"*
  Strumberger, E., S. Günter, J. Hobirk, V. Igochine, D. Merkl, E. Schwarz, C. Tichmann and the ASDEX Upgrade Team
  Nuclear Fusion, 44**,** (3), 464, 2004

- *"Study of quiescent H-mode plasmas in ASDEX Upgrade"*
  Suttrop, W., G.D. Conway, L. Fattorini, L.D. Horton, T. Kurki-Suonio, C.F. Maggi, M. Maraschek, H. Meister, R. Neu, Th Pütterich, M. Reich, A.C.C. Sips, and the ASDEX Upgrade Team
  Plasma Physics and Controlled Fusion, 46**,** (5), A151, 2004

- *"Control and monitoring system for fusion neutron spectroscopy on the Joint European Torus"*
  Tardocchi, M., G. Gorini, D. Palma, C. Sozzi, J. Källne, S. Conroy, G. Ericsson, L. Giacomelli, W. Glasser, H. Henriksson, A. Hjalmarsson, E. Ronchi, H. Sjöstrand, M. Weiszflog, S. Popovichev, and JET-EFDA Contributors.
  Review of Scientific Instruments, 75, (10)**,** 3543, 2004

- *"Materials design data for reduced activation martensitic steel type EUROFER"*
  Tavassoli AAF, Alamo A, Bedel L, et al. ,
  Journal of Nuclear Materials B 329-33, 257-262, 2004

- *"Alfvén mode stability and wave-particle interaction in the JET tokamak: prospects for scenario development and control schemes in burning plasma experiments"*
  Testa, D., A. Fasoli, D. Borba, M. de Baar, M. Bigi, J. Brzozowski, P. de Vries and JET-EFDA Contributers
  Plasma Physics and Controlled Fusion, 46**,** (7), S59, 2004

- *"Fully pellet-controlled ELMs sustaining identical pedestal conditions of natural ELMy H-mode in ASDEX Upgrade"*
  Urano, H., W. Suttrop, P.T. Lang, L.D. Horton, A. Herrmann and ASDEX Upgrade Team
  Plasma Physics and Controlled Fusion, 46**,** (5), A315, 2004

- *"ITER diagnostic: Integration and engineering aspects"*
  Walker, C.I., A.E. Costley, K. Itami, T. Kondoh, T. Sugie, G. Vayakis and A. Malaquias.
  Review of Scientific Instruments, 75, (10)**,** 4243, 2004

- *"Shear and collisionality dependences of particle pinch in JET L-mode plasmas"*
  Weisen, H., A. Zabolotsky, X. Garbet, D. Mazon, L. Zabeo, C. Giroud, H. Leggate, M. Valovic, K-D Zastrow and contributers to the JET-EFDA Workprogramme
  Plasma Physics and Controlled Fusion, 46**,** (5), 751, 2004

- *"Density peaking in low collisionality ELMy H-mode in JET"*
  Valovic, M., R. Budny, L. Garzotti, X. Garbet, A.A. Korotkov, J. Rapp, R. Neu, O. Sauter, P. de Vries, B. Alper, M. Beurskens, J. Brzozowski, D. McDonald, H. Leggate, C. Giroud, V. Parail, I. Voitsekhovitch and JET EFDA Contributors
  Plasma Physics Controlled Fusion 46, (12), 1877, 2004

- *"A model-based strike point sweeping technique applied to JET"*
  Villone, F. and contributers to the EFDA-JET Workprogramme
  Plasma Physics and Controlled Fusion, 46**,** (9), 1375, 2004

- *"Tritium transport experiments on the JET tokamak"*
  Zastrow, K-D, J M Adams, Yu Baranov, P Belo, L Bertalot, J H Brzozowski, C D Challis, S Conroy, M de Baar, P de Vries, P Dumortier, J Ferreira, L Garzotti, T C Hender, E Joffrin, V Kiptily, J Mailloux, D C McDonald, R Neu, M O'Mullane, M F F Nave, J Ongena, S Popovichev, M Stamp, J Stober, D Stork, I Voitsekhovitch, M Valovic, H Weisen, A D Whiteford, A Zabolotsky and JET EFDA Contributors
  Plasma Physics Controlled Fusion 46, (12B), B255, 2004

- *"Compact NE213 neutron spectrometer with high energy resolution for fusion applications"*
  Zimbal, A., M. Reginatto, H. Schuhmacher, L. Bertalot, B. Esposito, F. Poli, J.M. Adams, S. Popovichev, V. Kiptily, A. Murari, and JET-EFDA Contributors.
  Review of Scientific Instruments, 75, (10)**,** 3553, 2004

15.1.4. Papers in international conferences

- **15th Topical Conference on High Temperature Plasma Diagnostics, 19-22 of April, 2004, San Diego, USA**

- *"On the interpretation of fluctuations and ExB turbulent transport measured by Langmuir probes in fusion plasmas"*
  Calderon, E., C. Hidalgo, C. Silva, M.A. Pedrosa

- *"A Real-Time DSP-Based System for MHD Mode Identification in ISTTOK"*
  Carvalho, B., H. Fernandes, J. Sousa and C.A.F. Varandas

- *"Frequency Hopping MMW Reflectometer"*
  Cupido, L., M. E. Manso, L. Meneses, J. Sánchez and F. Serra

- *"A Current Profile Diagnostic Based on a Linux Cluster Running MatLab"*
  Fernandes, H., D. Alves, T. Pereira, J. Ferreira, C. Varandas and B. Carvalho

- *"Time–Frequency Analysis of Nonstationary Fusion Plasma Signals: A Comparison Between the Choi-Williams Distribution and Wavelets"*
  Figueiredo, A.C.A., M.F.F. Nave and the JET-EFDA Contributors

- *"Electron Emissive Electrode for the Plasma Biasing Experiments on Tokamak ISTTOK"*
  Figueiredo, H., C. Silva, I.S. Nedzelskiy, C.A.F. Varandas, J.A.C. Cabral and R.M.O. Galvão

- *"Upgrade to the Control System of the Reflectometry Diagnostics of ASDEX Upgrade"*
  Graça, S., J.Santos and the CFN Reflectometry Team

- *"Possibilities of X-mode Correlation Reflectometry Measurements from the Upgraded KG8b Diagnostic on JET"*
  Hacquin, S., L. Meneses, I. Nunes, N. Cruz, L. Cupido, R. Prentice and the JET-EFDA Contributors

- *"On the use of MHD mode analysis as a technique for determination of q-profiles in JET plasmas"*
  Nave, M.F.F., D. Borba, R. Galvão, S. Hacquin, B. Alper, C. Challis, S. Gerasimov, N. Hawkes, J. Mailloux, S. Sharapov, C. Boswell, M. Brix, E. Joffrin, E. de la Luna, P. Smeulders and EFDA-JET Contributors.

- *"Time-of-Flight Energy Analyzer for the Plasma Potential Measurements by a Heavy Ion Beam Diagnostic*"
  Nedzelskiy, I.S., A. Malaquias, B. Gonçalves, C. Silva, C.A.F. Varandas and J.A.C. Cabral

- *"FM-CW Reflectometry Measurments of Plasma Position in ASDEX Upgrade ELMY-H Mode Regimes"*
  Santos, J., S. Hacquin, M. Manso and the ASDEX Upgrade Team

- *"Fluctuations Measurements Using a 5-pin Triple Probe in the JET Boundary Plasma"*
  Silva, C., C. Hidalgo, B. Gonçalves, K. Erents, G. Matthews, M.A. Pedrosa and R. Pitts

- *"Global Full-Wave Simulation of the Tore Supra Doppler Reflectometer"*
  Silva, F. da, S. Heuraux, N. Lemoine, C. Honoré, P. Hennequin, M. Manso and R. Sabot

- *"PCI Data Acquisition and Signal Processing Hardware Modules for Long Pulse Operation"*
  Sousa, J., A.J.N. Batista, A. Combo, R. Pereira, Miguel Correia, N. Cruz, P. Carvalho, Carlos Correia and C.A.F. Varandas

- **16th International Conference on Plasma Surface Interactions in Controlled Fusion Devices, 24-28 of May, Portland, Maine, USA**

- *"Statistical Description of the Radial Structure of Turbulence in the JET Plasma Boundary Region"*
  Gonçalves, B., C. Hidalgo, C. Silva, M.A. Pedrosa and K. Erents

- *"Edge and Divertor Physics with Reversed Toroidal Field in JET"*
  Pitts, R. A., P. Andrew, X. Bonnin, A. V. Chankin, Y. Corre, G. Corrigan, D. Coster, I. Duran, T. Eich, S. K. Erents, W. Fundamenski, A. Huber, S. Jachmich, G. Kirnev, M. Lehnen, P. J. Lomas, A. Loarte, G. F. Matthews, J. Rapp, C. Silva, M. F. Stamp, J. D. Strachan, E. Tsitrone and contributors to the EFDA-JET workprogramme

- *"On the Energy Transfer Between Flows and Turbulence in the Plasma Boundary of Fusion Devices"*
  Sánchez, E., C. Hidalgo, B. Gonçalves, C. Silva, M.A. Pedrosa, M. Hronc and K. Erents

- *"Determination of the Particle and Energy Fluxes in the JET far SOL during ELMs using the Reciprocating Probe Diagnostic"*
  Silva, C., B. Gonçalves, C. Hidalgo, K. Erents, A. Loarted, G. Matthews and M. Pedrosa

- *"Comparison of Limiter and Emissive Electrode Bias on the Tokomak ISTTOK"*
  Silva, C., I. Nedzelskiy, H. Figueiredo, R.M.O. Galvão, J.A.C. Cabral and C.A.F. Varandas

- **31st EPS on Plasma Physics, 28 June to 1 July, Imperial College, London**

- "*Coupling properties of Tore Supra's ITER-like LH PAM launcher*"
  Belo, J.H., Ph. Bibet

- *"Observation and Implication of MHD Modes for the Hybrid Scenario in JET"*
  Belo, P., P. Buratti, R.J. Buttery,T.C. Hender, D.F. Howell, A. Isayama, E. Joffrin, M.F.F. Nave, G. Sips e os contributos do JET-EFDA

- *"Role of Impurity and Deuterium Fuelling in Evolution of Trace Tritium in JET ELMy H-mode: Transport Analysis and Predictive Modelling"*
  Belo, P., V. Parail, G. Corrigan, D. Heading, L. Garzotti, P. Monier-Garbet, J. Ongena, G. Bonheure, I. Voitsekhovitch e os contributos do JET-EFDA

- *"Supersonic molecular beam fuelling at ASDEX Upgrade"*
  Bucalossi, J., P. T. Lang, G. Martin, V. Mertens, J. Neuhauser, V. Rohde, L. Fattorini and the ASDEX Upgrade Team.

- *"Observation of slow sawtooth reconnection in JET low-shear discharges"*
  Buratti, P., B. Alper, A. Becoulet, P. Belo, C. Gormezano, P. Smeulders

- *"Dual feedback controlled high performance Ar seeded ELMy H-Mode discharges in JET including trace tritium experiments"*
  Dumortier, P., G. Bonheure, R. Felton, J. Harling, E. Joffrin, A. Messiaen, J. Ongena, P. Belo, I. Coffey, Y. Corre, K. Crombe, M. de_Baar, A. Huber, D. Kalupin, A. Kreter, S. Jachmich, G. Maddison, P. Monier-Garbet, M.F.F.Nave, V. Parail, M.E. Puiatti, G. Telesca, M. Tokar', B. Unterberg, M.Valisa, I. Voitsekhovitch, M. von Hellermann and contributors to the EFDA-JET workprogramme

- *"Z-Dependence of Impurity Transport in the Hybrid Scenario at JET"*
  Giroud, C., P. Belo, R. Barnsley, I. Coffey, R. Dux, M. von Hellermann, E. Joffrin, C. Jupen, A. Meigs, M. O'Mullane, V. Pericoli Ridolfini, A.C.C. Sips, A. Whiteford, K-D Zastrow and JET EFDA Contributors

- *"Trace-Tritium Measurement of Magnetic Island Effect on Particle Confinement"*
  Hender, T C, R J Buttery, E de la Luna, J S Ferreira, D F Howell, D C McDonald, M F F Nave, J D Strachan, A D Whiteford, K-D Zastrow e os contributos do JET EFDA

- *"On the Momentum Re-distribution via Fluctuations in Fusion Plasmas"*
  Hidalgo, C., B. Gonçalves, M.A. Pedrosa, C.Silva, O. Orozco, E. Calderón, G. Falchetto, X. Garbet and M. Hron

- *"Small Sawtooth Regimes in JET Plasmas"*
  Nave, M.F.F., S. Coda, R.Galvão, J. Graves, R. Koslowski, M.Mantsinen, F.Nabais, S. Sharapov, P. de Vries, R. Buttery, M. de Baar, C. Challis, J. Ferreira, C. Giroud, M. Mayoral, S. D.Pinches, M.Stamp e os contributos do JET-EFDA

- *"Tritium Fuelling of JET Plasmas with Internal Transport Barriers"*
  Mailloux, J., C.D. Challis, K-D. Zastrow, J.M. Adams, B. Alper, Yu. Baranov, P. Belo, L. Bertalot, P. Beaumont, R. Buttery, S. Conroy , E. De La Luna, P. de Vries, C. Giroud, N.C. Hawkes, E. Joffrin, P.J. Lomas, D.C. McDonald, S.D. Pinches, S. Sharapov, I. Voitsekhovitch, and JET EFDA Contributors

- *"Study of the Density Pedestal Width in ASDEX Upgrade using Reflectometry"*
  Nunes, I., L.D.Horton, A.Loarte, G.D.Conway, F.Serra, M.Manso and the CFN and ASDEX Upgrade Teams

- *"Tokamak turbulence computations on closed and open magnetic field lines"*
  Ribeiro T., B. Scott, D. Coster and F. Serra

- *"Small ELM experiments in H-mode plasmas in JET"*
  Saibene, G, P J Lomas, R Sartori, A Loarte, P R Thomas, V V Parail, J S Lonnroth, H R Koslowski, C P Perez, F G

Rimini, M F F Nave, P Belo, D C McDonald, Y Andrew, A G Meigs, P Monier Garbet, G D Conway, J Stober, M Kempenaars and contributors to the EFDA-JET workprogramme

- *"pT fusion by RF-heated protons in JET trace tritium discharges"*
  Santala, M. I. K., M. J. Mantsinen, Yu. Baranov, P. Beaumont, P. Belo, L. Bertalot, J. Brzozowski, M. Cecconello, S. Conroy, C. Gowers, M. deBaar, P. deVries, V. Kiptily, J.-M. Noterdaeme, S. Popovichev, A. Salmi, C. Schlatter, S. Sharapov, D. Testa, and JET EFDA collaborators

- *"Transport Analysis of Trace Tritium Experiments on JET using TRANSP Code and Comparison with Theory-Based Transport Models"*
  Voitsekhovitch, D.C. McDonald, K-D Zastrow, Yu Baranov, R. Budny, X. Garbet, D. McCune, J. Ongena, D. Stork, M. Adams, P. Belo, L. Bertalot, G. Bonheure, S. Conroy, J.G. Cordey, L. Garzotti, M von Hellermann, P. Mantica, V. Parail, S Popovichev, M Valovic and JET EFDA Contributors

- *"RF Induced Impurity Transport in the Mode Conversion Regime in a H-D plasma at JET"*
  Weyssow, B., D. Pilipenko, I. Pavlenko, P. Dumortier, D. Van Eester, F. Nave, J. Brzozowski, R. Felton , L. Zabeo, G. Maddison, S. Hacquin, M. Mantsinen, and J.-M. Noterdaeme and contributors to the EFDA-JET Workprogramme

- *"Tritium Transport Experiments on the JET Tokamak"*
  Zastrow, K-D, J.M. Adams, Yu Baranov, P. Belo, L. Bertalot, J.H. Brzozowski, C.D. Challis, S. Conroy, M de Baar, P de Vries, P. Dumortier, J. Ferreira, L. Garzotti, T.C. Hender, E. Joffrin, V. Kiptily, J Mailloux, D.C. McDonald, R. Neu, M.O'Mullane, M.F.F. Nave, J. Ongena, S. Popovichev, M. Stamp, J. Stober, D Stork, I. Voitsekhovitch , M. Valovic, H. Weisen, A.D. Whiteford, A. Zabolotsky and JET EFDA Contributors

- **Theory of Fusion Plasmas Conference, Varenna, Italy, 30 August – 3 September 2004**

- *"Parity and topology of tearing mode perturbations in a cylindrical tokamak"*
  Coelho, R. and E. Lazzaro

- **10th EU-US Transport Task Force Workshop, 6-9 September 2004, Villa Monastero-Varenna, Italy**

- "*Transition from TEM to ITG and consequences on transport properties in ASDEX Upgrade plasmas*"
  Angioni, C., A. G. Peeters, F. Ryter, F. Jenko, G. D. Conway, T. Dannert, H. U. Fahrbach, L. Fattorini, M. Reich, W. Suttrop and the ASDEX Upgrade Team.

- *"On the Energy Transfer Between Flows and Turbulence in the Plasma Boundary of Fusion Devices"*
  Gonçalves, B., C. Hidalgo, E. Sánchez, C. Silva, M.A. Pedrosa, O. Orozco, E. Calderón, G. Falchetto, X. Garbet e M. Hron

- **23rd SOFT, 20-24 September 2004, Venice, Italy**

- *Characterization and stability studies of titanium beryllides*
  Alves, E. L.C. Alves, N. Franco, R. da Silva, A. Paúl, J.B. Hegeman, F. Druyts

- *"ITER-like pam launcher for TORE SUPRA'S LHCD system"*.
  Belo, J. H., Ph. Bibet, J. Achard, B. Beaumont, B. Bertrand, M. Chantant, Ph. Chappuis, L. Doceul, A. Durocher, L. Gargiulo, M. Missirlian, A. Saille, F. Samaille, E. Villedieu

- *"Toward an LHCD system for ITER"*
  Bibet, Ph., B. Beaumont, J. H. Belo, L. Delpech, A. Ekedahl, G. Granucci, F. Kazarian, X. Litaudon, J. Mailloux, F. Mirizzi, V. Pericoli, M. Prou, K. Rantamäki, A. Tuccillo,.

- "*New millimetre-wave access for JET reflectometry and ECE*"
  Cupido, L., E. de la Luna, C. Antonucci, A. Guigon, F.J. van Amerongen, W.A. Bongers, A.J.H. Donné, M.F. Graswinckel, A. Bruschi, S. Cirant, A. Simonetto, C. Sozzi, D. Wagner, M.E. Manso, L. Meneses, F. Silva, P. Varela, N. Balshaw, J.M. Chareau, G. Conway, J. Fessey, S. Hanks, R. Pearce, V. Ricardo, D. Sands, D. Starky, T. Tisconia and JET-EFDA Contributers.

- **12th ICPP, 25-29 October 2004, Nice, France**

- *"On non-zero space average density perturbation effects in tokamak plasma reflectometer signals"*
  Heuraux, S., R. Sabot, F. da Silva, A. Sirinelli, E. Blanco, F. Clairet, P. Hennequin, G. Leclert, L. Vermare

- **WorkShop on the Electric Fields, Structures and Relaxation in Edge Plasmas, 26-27 October 2004, Nice, France**

- *"Emissive Electrode Plasma Biasing Experiments on Tokomak ISTTOK"*
  Figueiredo, H., C. Silva, I.S. Nedzelskiy, C.A.F. Varandas, J.A.C. Cabral e R.M.O. Galvão

- *"Efficiency of plasma biasing by movable localized limiter in tokamak ISTTOK"*
  Nedzelskiy, I.S., C. Silva, H. Figueiredo, C.F.A. Varandas e J.A.C. Cabral

- **20th IAEA Fusion Energy Conference, 1-6 November 2004, Vilamoura, Portugal**

- *"Cross-machine NTM physics studies and implications for ITER"*
  Buttery, R. J., P. Belo, D. P. Brennan, S. Coda, L.-G. Eriksson, B. Gonçalves, J. P. Graves, S. Günter, C. Hegna, T. C. Hender, D. F. Howell, H. R. Koslowski, R. J. La Haye, M. Maraschek, M. L. Mayoral, M. F. F. Nave, O. Sauter, E. Westerhof, C. Windsor, the ASDEX Upgrade and DIII-D teams, and JET-EFDA contributors

- *"Mode Coupling Effects on the Triggering of Neoclassical Tearing Modes and Plasma Momentum Braking"*
  Coelho, R., E. Lazzaro e P. Zanca

- *"On the Momentum Re-distribution Via Turbulence in Fusion Plasmas: Experiments in JET and TJ-II"*
  Gonçalves, B., C. Hidalgo, M.A. Pedrosa, R. O. Orozco, C. Silva, E. Calderón, K. Erents, G. Falchetto, X. Garbet, M. Hron, G. Matthews e E. Sánchez

- *"The "hybrid" scenario in JET: towards its validation for ITER"*
  Joffrin, E., A. C. C. Sips, A. Becoulet, R. Budny, P. Buratti, P. da Silva Aresta Belo, C. D. Challis, F. Crisanti, M. de Baar, P. de Vries, C. Gormezano, C. Giroud, O. Gruber, F. Imbeaux, A. Isayama, X. Litaudon, P. J. Lomas, Y. S. Na, S. D. Pinches, A. Staebler, T. Tala, A. Tuccillo, K.-D. Zastrow and JET-EFDA Contributors to the Work Programme.

- *"Integrated exhaust scenarios with actively controlled ELMs"*
  Lang, P.T., A. Kallenbach, J. Bucalossi, G. D. Conway, A. Degeling, R. Dux, T. Eich, L. Fattorini, O. Gruber, S. Günter, A. Hermann, L. D. Horton, S. Kalvin, G. Kocsis, J. Lister, M. E. Manso, M. Maraschek, Y. Martin, P. J. McCarthy, V. Mertens, R. Neu, J. Neuhauser, I. Nunes, T.Pütterich, W. Schneider, A. C. C. Sips, W. Suttrop, W. Treutterer, H. Zohm and the ASDEX Upgrade Team.

- *"Impurity-seeded ELMy H-modes in JET, with high density and sustainable heat load"*
  Monier-Garbet, P., Ph. Andrew, P. Belo, G. Bonheure, Y. Corre, K. Crombe, P. Dumortier, T. Eich, R. Felton, J. Harling, J. Hogan, A. Huber, S. Jachmich, E. Joffrin, H.R. Koslowski, A. Kreter, G. Maddison, G.F. Matthews, A. Messiaen, M.F. Nave, J. Ongena, V. Parail, M.E. Puiatti, J. Rapp, R. Sartori, J. Stober, M.Z. Tokar, B. Unterberg, M. Valisa, I. Voitsekhovitch, M. von Hellermann, and JET-EFDA contributors.

- *Internal kink Mode Stability in the Presence of ICRH Driven Fast Ions Populations* (Oral presentation)
  Nabais, F., D. Borba, M. Mantsinen, M. F. F. Nave, S. Sharapov e os contributos do JET-EFDA

- *"Density Profile Evolution during Dynamic Processes in ASDEX Upgrade"*
  Nunes, I., J. Santos, F. Salzedas, M. Manso, F. Serra, G. D. Conway, L. D. Horton, J. Neuhauser, W. Suttrop e as equipas do CFN e do ASDEX Upgrade

- *"Study of Runaway Electron Generation Process During Major Disruptions in JET"*
  Plyusnin, V.V., V. Riccardo, R. Jaspers, B. Alper, V.G. Kiptily, J. Mlynar, S. Popovichev, E. de La Luna, P. Helander, F. Andersson e os contributos JET EFDA

- *"Measurements of density profile and density fluctuations in Tore Supra with reflectometry"*
  Sabot, R., F. Clairet, P. Hennequin, S. Heuraux, A. Sirenelli, L. Vermare, J.M. Chareau, J.C. Giaccalone, C. Honoré, G. Leclert, D. Molina, J.L. Ségui, A. Truc, F. da Silva, M.E. Manso

- *"Dimensionless identity experiments in JT-60U and JET"*
  Saibene, G., N. Oyama, Y. Andrew, J.G. Cordey, E. de la Luna, C. Giroud, K. Guenther, T. Hatae, Y. Kamada, MAH Kempenaars, A. Loarte, J. Lönnroth, D. McDonald, A. Meiggs, M.F.F. Nave, V. Parail, R. Sartori, J. Stober, T. Suzuki, M. Takechi, K. Toi

- *"Scaling study of ELMy H-mode global and pedestal confinement at high triangularity in JET"*
  Sartori, R, P Lomas, G Saibene, P R Thomas, O.Sauter, A.Loarte, B Alper, Y Andrew, P Belo, T Bolzonella, I Coffey, C Giroud, K Guenther, D Howell, L C Ingesson, M Kempenaars, H R Koslowski, A Korotkov, H Leggate, E de la Luna, G Maddison, D C McDonald, A Meigs, P Monier Garbet, V Parail, R Pasqualotto, C P Perez, F G Rimini, J Stober K Thomsen

- *"Experimental studies of instabilities and confinement of energetic particles on MAST and JET" (*Oral presentation)
  Sharapov, S., B. Alper, F. Andersson, Y. Baranov, H. Berk, L. Bertalot, D. Borba, C. Boswell, R. Buttery, C. Challis, M. de Baar, P. de Vries, L.-G. Eriksson, A. Fasoli, R. Galvao, V. Goloborodko, N. Hawkes, P. Helander, V. Kiptily, G. Kramer, P. Lomas, J. Mailloux, M. Mantsinen, R. Martin, F. Nabais, F. Nave, R. Nazikian, J.-M. Noterdaeme, S. Pinches, T. Pinfold, S. Popovichev, P. Sandquist, D. Stork, D. Testa, A. Tuccillo, I. Voitsekhovitch, V. Yavorskij, N. Young, F. Zonca , and JET-EFDA contributors.

- *"Comparison of Limiter and Emissive Electrode Bias on the Tokamak ISTTOK"* (Oral presentation)
  Silva, C., I. Nedzelskiy, H. Figueiredo, R.M.O. Galvão, B. Gonçalves, J.A.C. Cabral e C.A.F. Varandas

- *"Small ELM regimes with good connement on JET and comparison to those on ASDEX Upgrade, Alcator C-mod, and JT-60U"*
  Stober, J., P. Lomas, G. Saibene, Y. Andrew, P. Belo, G.D. Conway, L.D. Horton, M. Kempenaars, H.-R. Koslowski, A. Loarte, G.P. Maddison, M. Maraschek,D.C. McDonald, A.G. Meigs, P. Monier-Garbet, D.A. Mossessian, M.F.F. Nave, N. Oyama, V. Parail, Ch.P. Perez, F. Rimini, R. Sartori, A.C.C. Sips, P.R. Thomas, contributors to the EFDA-JET work programme, and the ASDEX Upgrade Team

- *"Overview of Transport, Fast Particle and Heating and Current Drive Physics using Tritium in JET plasmas"*
  Stork, D., Yu. Baranov, P.Belo, L.Bertalot, D.Borba, J.H.Brzozowski, C.D.Challis, D.Ciric, S. Conroy, M.de Baar, P.de Vries, P Dumortier, L.Garzotti, N.C.Hawkes, T.C.Hender, E.Joffrin, T.T.C.Jones, V.Kiptily, P.Lamalle, J.Mailloux, M.Mantsinen, D.C.McDonald, M.F.F.Nave, R.Neu, M. O'Mullane, J.Ongena, R.J.Pearce, S.Popovichev, S.E.Sharapov, M.Stamp, J.Stober, E.Surrey, M.Valovic, I.Voitsekhovitch, H.Weisen, A.D.Whiteford, L.Worth, V.Yavorskij, K-D.Zastrow and JET EFDA contributors.

- *"Studies of the Quiescent H-mode regime in ASDEX Upgrade and JET"*
  Suttrop, W., M. Maraschek, G. D. Conway, H.-U. Fahrbach, P. Gohil, G. Haas, S. Hacquin, L. D. Horton, T. Kurki-Suonio., C. J. Lasnier., A. W. Leonard, P. J. Lomas; G. F. Maddison, C. F. Maggi, H. Meister, A. Mück, M. F. Nave, R. Neu, I. Nunes, R. A. Pitts,Th. P¨utterich, M. Reich, J. Schirmer, S. E. Sharapov, A. C. C. Sips, K.-D. Zastrow the ASDEX Upgrade Team and contributors to the EFDA-JET workprogramme

- *"Anomalous particle and impurity transport in JET"*
  Weisen, H., C. Angioni, A. Bortolon, C. Bourdelle, L. Carraro, I. Coffey, R. Dux,X. Garbet, L. Garzotti, C. Giroud, N. Hawkes, D. Kalupin, H. Leggate, P. Mantica, M. Mattioli, D. Mazon, D.C. McDonald, M.F.F. Nave, R. Neu, V. Parail, M.E. Puiatti, M. Tokar, M. Valisa, M. Valovic, J. Weiland, L. Zabeo, A. Zabolotsky, K.-D. Zastrow and contributors to the JET-EFDA work programme

- *"Edge stability and performance of the ELM-free quiescent H-mode and the quiescent double barrier mode on DIII-D"*
  West, W.P., K.H. Burrell, T.A. Casper, E.J. Doyle, P.B. Snyder, P. Gohil, L.L. Lao, C.J. Lasnier, A.W. Leonard, M.F.F. Nave, T.H. Osborne, D.M. Thomas, G. Wang and L. Zeng.

- **Annual Conference Japanese Society of Plasma Physics and Nuclear Fusion, November 23-26, Shizoka, Japan, 2004**

- *"Microwave refelectometry of turbulence wavenumber spectra in tokamaks"*
  Bruskin, L. G., A. Mase, M. E. Manso, F. Serra, A. Silva, L. Fattorini, G. D. Conway and the ASDEX Upgrade Team.

- **APS - 46th Annual Meeting of the Division of Plasma Physics, Savannah, Georgia, USA**

- *Model odf n=0 energetic particle induced oscillations in JET*
  Berk, H.L., S. Sharapov, MFF Nave, S. D. Pinches and C. Boswell

- *"Poloidal rotation velocity studies on JET"*
  Crombé, K., Y. Andrew, M. Brix, C. Giroud, N.C. Hawkes, A. Murari, M.F.F. Nave, J. Ongena, V. Parail, G. Van Oost, K.-D. Zastrow and contributors to the EFDA-JET work programme

- **U.S./Japan/Europe RF technology workshop, Amsterdam, 2004**

- "*European LHCD antennae test and development*"
  Bibet, Ph., B. Beaumont, J. H. Belo, et al.

- **eLES, e-learning no Ensino Superior, Aveiro, 2004**

- *"O controlo e aquisição de dados de experiências remotas"*
  Fernandes, H., J. Fortunato, J. Pereira

- *"E-escola – um portal de ciências básicas"*
  Fernandes, H., P.A. Santos

- *"Soluções para transmissão de vídeo no ELAB"*
  Fernandes, H., A. Neto, J. Pereira, P. Carvalho

- **Escola de Educação em Física, SPF, Porto, 2004**

- *"ELAB virtual – experiências cooperativas de física na internet"*
  Fernandes, H., A. Neto, S.R.M. Pino

- *"Experiência de Thomson remota – uma implementação no ELAB"*
  Fernandes, H., A. Neto, I. Carvalho

15.2. CENTRO DE FÍSICA DOS PLASMAS

15.2.1. Ph.D thesis

- *"LIDARLAB: lidar bi-comprimento-de-onda e multi-direccional para detecção remota de aerossóis"*
  José A. Rodrigues, 2004
  Universidade Técnica de Lisboa

- *"Quantum theory of photon acceleration and quantum effects in non-stationary optical media"*
  Ariel Guerreiro, 2004
  Universidade Técnica de Lisboa

15.2.2. Master thesis

- *"Caracterização da fase spectral de impulses laser ultra-curtos"*
  João Wemans, 2004
  Universidade Técnica de Lisboa

- *"Estudo de um plasma de grandes dimensões produzido por ondas de superfície"*
  Alexandre Alves Martins, 2004
  Universidade Técnica de Lisboa

15.2.3. Articles in scientific journals

- *"Fluid description of the energy absorption in microwave discharges: a new perspective"*
  Alves, L.L.
  Eur. Phys. J. Appl. Phys. 26 (DOI 10.1051), 195-201, 2004.

- *"Neutrino plasma coupling in dense astrophysical plasmas"*
  Bingham, R., L. O. Silva, J. T. Mendonça, P. K. Shukla, W. B. Mori, and A. Serbeto
  Plasma Physics and Controlled Fusion 46 B327-B334, 2004

- *"On the generation of Totem Pole emissions"*
  Brinca, A.L., F.J. Romeiras, L. Gomberoff and M.H. Marçal, J. Geophys. Res.,109, 6201, doi:10.1029/2004JA010388, 2004.

- *"Bandwidth increase by controlled angular dispersion of signal beam in optical parametric amplification"*
  Cardoso, L., G. Figueira
  Optics Express 12, 108, 2004

- *"Alfvén limit in fast ignition"*
  Davies, J. R.
  Physical Review E 69, 065402(R), 2004

- *"Local diagnostics in gas discharges: free electrons, field probes and antennas"*
  Dias, F. M., Tsv. K. Popov, M. Dimitrova
  Vacuum 76, 381-388, 2004

- *"Excited Species in a Large-Scale N_2-O_2 Microwave Plasma Source"*
  Ferreira, C.M., E. Tatarova, F.M. Dias and A. Ricard
  Vacuum 76, 347-350, 2004

- "*A Large-Volume N_2-Ar Microwave Plasma Source Based on Surface Waves"*
  Ferreira, C.M., E. Tatarova, J. Henriques and F.M. Dias
  Vacuum 76, 343-346, 2004

- *"Effect of a large-amplitude circularly polarized wave on linear beam-plasma electromagnetic instabilities"*
  Gomberoff, L., J. Hoyos and A.L. Brinca,
  J. Geophys. Res., 108, 1472, doi:10.1029/2003JA010144, 2004.

- *"Behavior of linear beam-plasma instabilities in presence of finite amplitude circularly polarized waves"*
  Gomberoff, L., J. Hoyos and A. L. Brinca, *Braz. J. Phys., 34,* 1547, 2004.

- *"Electrostatic instabilities induced by large amplitude left-hand polarized waves"*
  Gomberoff, L., J. Hoyos, A.L. Brinca and R. Ferrer,
  J. Geophys. Res., 109, 7108, doi:10.1029/2004JA010466, 2004.

- *"Ion acoustic instability triggered by finite amplitude polarized waves in th solar wind"*
  Gomberoff, L., J. Hoyos and A.L. Brinca,
  J. Geophys. Res., accepted for publication, 2004.

- "*Dynamical Monte Carlo simulation of surface atomic recombination, Plasma"*
  Guerra, V. and J. Loureiro,
  Sources Sci. and Technol. 13, 85, 2004.

- "*Self-Consistent Modeling of DC and Microwave Nitrogen Discharges and Their Afterglows"*
  Guerra, V.
  in L. Had ievski, T. Grozdanov e N. Bibi (editores), The Physics of Ionized Gases, American Institute of Physics, AIP Conference Proceedings - Volume 740, Melville, Nova Iorque, E.U.A., 2004.

- *"Kinetic modeling of nitrogen discharges and post-discharges*"
  Guerra, V., P. A. Sá and J. Loureiro e N. Sadeghi,
  Eur. Phys.J. Appl. Phys. 28, 125, 2004.

- *"Ion acceleration from the shock front induced by hole boring in ultraintense laser-plasma interactions"*
  Habara, H., K. L. Lancaster, S. Karsch, C. D. Murphy, P. A. Norreys, R. G. Evans, M. Borghesi, L. Romagnani, M. Zepf, T. Norimatsu, Y. Toyama, R. Kodama, J. A. King, R. Snavely, K. Akli, B. Zhang, R. Freeman, S. Hatchett, A. J. MacKinnon, P.Patel, M. H. Key, C. Stoeckl, R. B. Stephens, R. A. Fonseca, and L. O. Silva
  Physical Review E 70, 046414, 2004

- *"Laser pulse frequency upshifts by relativistic ionization fronts"*
  Lopes, N.C., G. Figueira, J. M. Dias, L. O. Silva, J. T. Mendonça, P. Balcou, C. Stenz, , *Europhysics Letters* 66, 371, 2004

- *"Creation and expansion of a magnetized plasma bubble"*
  Loureiro, J., J.T. Mendonça, A.L. Brinca, R. Fonseca, L.O. Silva and I. Vieira, *J. Atmos. Solar Terr. Phys.,* submitted, 2005.

- *"Capacitively coupled hydrogen discharges: modelling vs. experiment"*
  Marques, L., J. Jolly, G. Gousset and L.L. Alves
  J. High Temp. Mat. Proc. 8, 499-518, 2004.

- *"Double Sheaths in RF Discharges"*
  Marques, L., G. Gousset and L.L. Alves
  to be published in IEEE Trans.Plasma Sci. - Special Issue on Images In Plasma Science, 2005.

- *"Pulse compression and frequency up-shift with nonlinear plasma waves"*
  Martins, S.F., J. P. Santos, R. A. Fonseca, L. O. Silva, Physica Scripta T113, 118, 2004

- *"Micrometeoroid flight in the upper atmosphere: electron emission and charging"*
  Mendis, M. Rosenberg, Wai-Ho Wong, G. Sorasio, Accepted for publication in Journal of Atmospheric and Solar-Terrestrial Physics, 2004

- *"Physical problems of artificial magnetospheric propulsion"*
  Mendonça, J.T., A.L. Brinca, R. Fonseca, J.Loureiro, L.O. Silva and I. Vieira,
  J. Plasma Phys., submitted, 2004.

- *"Some remarks about variable mass systems*"
  Pinheiro, M. J.,
  Eur. J. Phys. 25, L5-L7, 2004.

- *"Determination of the electron density in current-less argon plasma using Langmuir probe measurements"*
  Popov, Tsv. K. , M. Dimitrova, F. M. Dias
  Vacuum 76, 417-420, 2004

- *"Global model for laser-driven MeV electrons in fast ignition"*
  Ren, C., M. Tzoufras, F. S. Tsung, W. B. Mori, S. Amorini, R. A. Fonseca, L. O. Silva, J. C. Adam, A. Héron
  Physical Review Letters 93, 185004, 2004

- *"Self consistent theory of melting dynamics of grains in plasma sheaths"*
  Resendes, D.P., G. Sorasio and P. K. Shukla,

Phys. Plasmas 11, 2394, 2004

- *"Self-consistent kinetic model of the short-lived afterglow in flowing nitrogen*"
  Sá, P. A., V. Guerra, J. Loureiro e N. Sadeghi,
  J. Phys. D: Appl. Phys. 37, 221, 2004

- *"Systematic characterization of low-pressure capacitively coupled hydrogen discharges"*
  Salabas, A., L. Marques, J. Jolly, G. Gousset and L.L. Alves
  J. Appl. Phys. **95**, 4605-4620 (2004).

- *"Neutrino-Beam-Plasma Interactions"*
  Silva, L.O., R. Bingham, J. T. Mendonça, W. B. Mori, and P. K. Shukla,
  Physica Scripta T107, 9, 2004

- *"Proton shock acceleration in laser-plasma interactions"*
  Silva, L.O., M. Marti, J. R. Davies, R. A. Fonseca, C. Ren, F. Tsung and W. B. Mori, Physical Review Letters 92, 015002 (2004); also in Virtual Journal of Ultrafast Science 3, issue 2, 2004

- *"Origin of ELF/ULF Waves triggered by positive cloud to ground lightning above mesoscale convective systems"*
  Sorasio, G., P.K.Shukla, D. P. Resendes and J. T. Mendonça
  Geophysical Research Letters 31, L12110, 2004; Correction exists: Geophysical Research Letters 31, L14112, 2004

- *"Drift-wave instability excited by field-aligned ion flow velocity shear in the absence of electron current"*
  Sorasio, G., P. K. Shukla and L. Stenflo,
  Comment on Physical Review Letters 92, 69501, 2004

- *"Instability and threshold of ULF waves triggered by positive cloud to ground lightning"*
  Sorasio, G., P.K. Shukla and G.L. Delzanno
  Physica Scripta TIW 30, 65, 2004

- *"Molecular Dissociation in N_2-H_2 Microwave Discharge"*
  Tatarova, E., F. M. Dias, B. Gordiets and C. M. Ferreira
  Plasma Sources and Science Technology 13, 19-31, 2004.

- "*A Large scale Ar Plasma Source Excited by a TM33 mode"*
  Tatarova, E., F. M. Dias, J Henriques and C. M. Ferreira
  IEEE Transactions on Plasma Science, 33, 866-875, 2005.

- *"Near-GeV-energy laser-wakefield acceleration of self-injected electrons in a cm-scale plasma channel"*
  Tsung, F.S., R. Narang, W. B. Mori, C. Joshi, R. A. Fonseca, L. O. Silva
  Physical Review Letters 93, 185002, 2004

- *"An update of argon inelastic cross-sections for plasma discharges"*
  Yanguas, A., J. Cotrino and L.L. Alves
  to be published in J. Phys. D: Appl. Phys., 2005.

- *"A high-intensity highly coherent soft X-ray femtosecond laser seeded by a high harmonic beam"*
  Zeitoun, Ph., G. Faivre, S. Sebban, T. Mocek, M. Fajardo, S. Hallou, Ph. Balcou, F. Burgy, D. Douillet, T. Lefrou, P. Mercère, A. S. Morlens, J. P. Rousseau, and C. Valentin, S. Kazamias, D. Aubert, G. de Lachèze-Murel, S. le Pape
  Nature 431, 426–429, 2004

- *"Recent developments in X-UV Optics and X-UV Diagnostics"*
  Zeitoun, Ph., Ph. Balcou , S. Bucourt, F. Delmotte,G. Dovillaire, D.Douillet, J. Dunn, G. Faivre, M. Fajardo,K.A. Goldberg, S.Hubert, J.R. Hunter, M. Idir, S. Jacquemot, S. Kazamias, S. lePape, X. Levecq, C.L.S. Lewis, R.Marmoret, P. Mercère , A.S. Morlens, P.P. Naulleau , M. F. Ravet , C. Remond,J. J. Rocca , R.F. Smith, P. Troussel, C. Valentin and L. Vanbostal, Applied Physics B 78, 983, 2004

15.2.4. Papers in international conferences

- **31th IEEE, ICOPS, Baltimore, Maryland, USA, 2004**

- *"Wave driven Ar- N_2-O_2 discharges as sources of active species"*
  J. Henriques, E. Tatarova, C. M. Ferreira and A. Ricard

- **XVth International Conference on Gas Discharges and their Applications, Toulouse, France, 2004**

- *"Experimental investigation of a large-scale microwave plasma source in N_2-O_2 and N_2–Ar"*
  Dias, F. M., E. Tatarova and C. M. Ferreira

- **31st EPS Plasma Physics, London, June 2004**

- *"Photon acceleration by counter-propagating relativistic mirrors"*
  Dias, J.M., N.C. Lopes, L. O. Silva, D. A. Jaroszynski, J. T. Mendonça

- *"Relativistic mirrors for THz radiation sources induced by ionization fronts"*
  Dias, J. M., N. C. Lopes, L. O. Silva, D. A. Jaroszynski, J. T. Mendonça

- *"Photon acceleration of X-rays in a waveguide"*
  Fajardo, M., T. Mendonça, J.M. Dias

- *"On the role of the electromagnetic counter-streaming instability in GBRs"*
  Fiore, M., R. A. Fonseca, L. O. Silva, C. Ren, M. A. Tzoufras, W. B. Mori,

- *"Electron beams for fast ignition"*
  Fonseca, R. A., J. R. Davies, L. O. Silva,

- *"Large scale hybrid simulations of interacting plasmas in space"*
  Gargaté, L., R. Bingham, R. A. Fonseca, L. O. Silva, J. T. Mendonça, P.K.Shukla

- *"A laser triggered plasma channel for GeV plasma accelerators"*
  Lopes, N.C., G. Figueira, J. M. Dias, J. Vieira, R. A. Fonseca, L. O. Silva, J. T. Mendonça

- *"Collisionless shocks driven by ultra-intense lasers"*
  Marti, M., J. R. Davies, R. A. Fonseca, L. O. Silva, J. Fahlen, M. A. Tzoufras, C. Ren, F. S. Tsung, W. B. Mori

- *"Tunneling ionization in OSIRIS"*
  Martins, S. F., R. A. Fonseca, L. O. Silva, S. Deng, T. Katsouleas, F. Tsung, W. B. Mori,

- *"A self-consistent study for the laser-induced coulomb explosion of large deuterium clusters"*
  Peano, F., R. A. Fonseca, M. Marti, S. Martins, L. O. Silva,

- *"Wigner description of laser driven instabilities at arbitrary intensities"*
  Santos, J. P., L. O. Silva, R. Bingham

- *"Taming ultra intense fields in plasmas for particle acceleration"*
  Silva, L. O.

- *"A quasi-particle approach to the modulational instability of broadband drift mode turbulence coupled to zonal flows"*
  Trines, R.M.G.M., R. L. Bingham, L. O. Silva, J. T. Mendonça, P. K. Shukla, W. B. Mori,

- *"A photon-in-cell code for laser wakefield accelerators"*
  Trines, R. M. G. M., R. L. Bingham, L. O. Silva, J. T. Mendonça, P. K. Shukla, W. B. Mori, R. A.Cairns, A. Reitsma,

- *"Blowout regime for laser wakefield in plasma channels"*
  Vieira, J. F., R. A. Fonseca, L. O. Silva, F. Tsung, W. B. Mori,

- **ICTP: Workshop on Theoretical Plasma Physics, 5-16 July, Trieste, Italy, 2004**
- *"Laser heated plasma fronts for thrust generation"*
  Resendes, D.P. G. Sorasio, S. Mota, J.T. Mendonça, P.K. Shukla

- *"Instability and threshold of ULF waves triggered by positive cloud to ground lightning"*
  Sorasio, G.

- **22nd SPIG (Summer School and International Symposium on the Physics of Ionized Gases), Servia and Montenegro, August, 2004**
- *Self-consistent modeling of DC and microwave nitrogen discharges and their afterglows*
  Guerra,V., P. A. Sá e J. Loureiro

- **XV International Symposium on Gas Flow and Chemical Lasers & High Power Laser Conference, Prague, Aug-Sep 2004**
- *"Bandwidth increase by controlled angular dispersion of signal beam in optical parametric amplification"*
  Cardoso, L., G. Figueira, N. Lopes, J. Wemans, J. T. Mendonça

- *"Performance and characterization of a 2.8 TW Ti:sapphire-Nd:glass chirped pulse amplification laser system"*
  Figueira, G., N. Lopes, L. Cardoso, J. Wemans, J. M. Dias, M. Fajardo, C. Leitão, J. T. Mendonça

- *"Characterisation and optimisation of a multiterawatt CPA laser system using SPIDER"*
  Wemans, J., G. Figueira, N. Lopes, L. Cardoso

- **ESCAMPIG 17 (17th European Conference on Atomic & Molecular Physics of Ionized Gases), Constanta, Romenia, September, 2004**
- *"Theoretical investigation of the dependence of the probability of atomic surface recombination with the wall temperature"*
  Guerra, V.

- *"Self-consistent modeling of nitrogen discharges: influence of the cross sections for transitions between vibrational levels"*
  Guerra,V., A. A. Mihajlov, J. Loureiro and Z. Lj. Petrovi

- *"Time-afterglow of an N_2-O_2 microwave discharge used for plasma sterilization*"
  Pintassilgo, C. D., J. Loureiro e V. Guerra

- *"On the possibility of electron mediated V-E energy transfer processes in the nitrogen afterglow*"
  Sá,P. A., V. Guerra e J. Loureiro

- *Marques, L., J. Jolly, G. Gousset and L.L. Alves*
  Proceed. 17th ESCAMPIG (V. Ciupina, G. Musa and R. Vladoiu, eds.), Constanta, Rumania 2004, pp. 113-114.

- *Letout, S., L.L. Alves, C. Boisse-Laporte and P. Leprince*
  Proceed. 17th ESCAMPIG (V. Ciupina, G. Musa and R. Vladoiu, eds.), Constanta, Rumania 2004, pp. 191-192.

- **46th APS DPP 2004, Savannah, Georgia, Nov. 2004**
- *"Remote visualization for large data sets from plasma simulations"*
  Abreu, P. T., R. A. Fonseca, M. Marti, L. O. Silva

- *"Relativistic mirrors for THz radiation"*
  Dias, J. M., N. C. Lopes, L. O. Silva, J. T. Mendonça, D. A. Jaroszynski

- *"Baryon loading and the Weibel instability in GRBs"*
  Fiore, M., R. A. Fonseca, L. O. Silva, C. Ren, M. Tzoufras, W. B. Mori

- *"Electron Beams for Fast Ignition"*
  Fonseca, R. A., J. R. Davies, L. O. Silva

- *"Tunneling ionization and Wigner transform diagnostics in OSIRIS"*
  Fonseca, A., L. O. Silva, S. Deng, T. Katsouleas, F. Tsung, W. B. Mori,

- *"dHybrid: a three dimensional hybrid code for large scale simulations of interacting plasmas in space"*
  Gargaté, L., R. Bingham, R. A. Fonseca, L. O. Silva

- *"Collisionless shocks and the role of collisions"*
  Marti, M., J. R. Davies, R. A. Fonseca, L. O. Silva, J. Fahlen, M. Tzoufras, C. Ren, W. B. Mori

- *"Tunneling ionization and Wigner transform diagnostics in OSIRIS"*
  Martins, S., R. A. Fonseca, L. O. Silva, S. Deng, T. Katsouleas, F. Tsung, W. B. Mori

- *"Towards the theory of nonlinear Weibel turbulence"*
  Medvedev, M., L. O. Silva

- *"Electron acceleration from total reflection in ultra intense laser pulses"*
  Mendonça, J. T., L. O. Silva, R. Bingham

- *"Particle-in-cell simulation of LWFA using 50 fs pulses in guided and unguided plasmas"*
  Mori, W. B., F. S. Tsung, M. Tzoufras, C. Joshi, R. A. Fonseca, L. O. Silva

- *"Shock shells in the Coulomb explosions of very large cluster"*
  Peano, F., R. A. Fonseca, L. O. Silva,

- *"Laser driven instabilities at arbitrary intensities and broadband effects using the Wigner-Moyal formalism"*
  Santos, J., L. O. Silva, R. Bingham

- *"ULF waves triggered by cloud to ground lightning above mesoscale convective systems"*
  Sorasio , G.

- *"Photon-in-cell code for laser wakefield accelerators"*
  Trines, R., R. Bingham, L. O. Silva, J. T. Mendonça, P. K. Shukla, W.. B. Mori, R. Cairns, A. Reitsma

- *"Blowout, wavebreaking and self-injection in laser wakefield in plasma channels"*
  Vieira, J., R. A. Fonseca, L. O. Silva, F. Tsung, W. B. Mori

- **The European Material Conference, E-MRS Spring Meeting, Strasbourg, France, 2004**

- *"Capacitively coupled hydrogen discharges: modeling vs. experiment"* (Invited paper)
  Marques, L., J. Jolly, G. Gousset and L.L. Alves

- **57th Gaseous Electronics Conference, Bunratty, Ireland 2004;**

- Yanguas-Gil, A., J. Cotrino and Alves
  Proceed. Bull. Am. Phys. Soc. 49, 22 (2004).

- Letout, S. C. Boisse-Laporte, A. Yanguas-Gil and L.L. Alves
  Proceed. Bull. Am. Phys. Soc. 49, 23 (2004).

- Alves, L.L. and J. Cotrino
  Proceed. Bull. Am. Phys. Soc. 49, 23 (2004).

- **11 Advanced Accelerator Concepts workshop - AAC'04, Stony Brook, New York (USA)**

- *"Plasma waveguides for laser accelerators: simulations and experiments"*
  Lopes, N. C.

- *"Plasma waveguides for laser accelerators: Simulations and experiments"*
  Mendonça, J. T.

- *"Standard problems in advanced acceleration"*
  Fonseca, R.

- **International Meeting on Quantum Information Science - Foundations of Quantum Information, Camerino (Italy)**

- *"Particle statistics in quantum information processing"*
  Y. Omar

- **Workshop on Quantum Entanglement in Physical and Information Sciences, Pisa (Italy)**

- *"Quantum walk on a line with two particles"*
  Y. Omar, N. Paunkovic, L. Sheridan, S. Bose

- **1st Workshop of ELAN, 4-6 May, Frascati (Italy)**

- *"Theory,simulations and experiments on second-generation plasma based accelerators at GoLP-IST"*
  Lopes, N. C.